

Supporting Information (SI)

Acceleration of the Arbuzov-type reaction via double activation of imine and H-phosphonate

Nikita Sidlyaruk,^a Andrey Smolobochkin,^{*,a} Almir Gazizov,^a Tanzilya Rizbayeva,^a Daria Gerasimova,^a Valeriy Shirokov,^b Airat Garifzyanov,^b Alexander Burilov,^a Michail Pudovik^a

^a Arbuzov Institute of Organic and Physical Chemistry, FRC Kazan Scientific Center, Russian Academy of Sciences,

8 Arbuzova str., Kazan, Russian Federation. E-mail: smolobochkin@iopc.ru

^b Kazan Federal University, 18 Kremlyovskaya str., Kazan, Russian Federation

*Correspondence: smolobochkin@iopc.ru

Contents

Crystallographic Data.....	S2–S4
Copies of ¹ H, ¹³ C, ³¹ P NMR spectra.....	S5–S58
Quantum chemical calculations.....	S59–S61

Crystallographic Data

Single-crystal X-ray diffraction. X-ray diffraction study of the single crystals **3bb-CF₃COO⁻**, **3bc** and **3be** were obtained on a Bruker D8 QUEST three-circle diffractometer (Bruker, Germany) with a PHOTON III area detector and an I μ S DIAMOND microfocus X-ray tube (Incoatec, Germany) at a temperature of 150(2) K: graphite monochromator, $\lambda(\text{MoK}\alpha) = 0.71073 \text{ \AA}$, ω/φ scanning mode with a step of 0.5°. Data collection and indexing, determination, and refinement of unit cell parameters were carried out using the *APEX4* software package (v2021.10–0, Bruker AXS). Numerical absorption correction based on the crystal shape, additional spherical absorption correction, and systematic error correction were performed using the *SADABS–2016/2* software [Krause L., Herbst-Irmer R., Sheldrick G.M., Stalke D. Comparison of silver and molybdenum microfocus X-ray sources for single-crystal structure determination. *J. Appl. Crystallogr.*, 2015. – V. 48, Pt. 1. – P. 3–10]. Using *Olex2* [Dolomanov O.V., Bourhis L.J., Gildea R.J., Howard J.A.K., Puschmann H. OLEX2: A Complete Structure Solution, Refinement and Analysis Program. *J. Appl. Crystallogr.*, 2009. – V. 42, № 42. – P. 339–341], structures were solved by direct methods using the *SHELXT–2018/2* program [Sheldrick G.M. SHELXT – Integrated space-group and crystal-structure determination. *Acta Crystallogr., Sect. A: Found. Adv.*, 2015. – V. 71, Pt. 1. – P. 3–8] and refined by full-matrix least-squares on F^2 using the *SHELXL–2019/1* program [Sheldrick G.M. Crystal Structure Refinement with SHELXL. *Acta Crystallogr., Sect. C: Struct. Chem.*, 2015. – V. 71, Pt. 1. – P. 3–8]. Nonhydrogen atoms were refined anisotropically. Positions of H(N/O) hydrogen atoms for crystals **3bb-CF₃COO⁻**, **3bc** and **3be** were determined from difference electron density maps and refined isotropically. The positions of hydrogen atoms of methyl groups were inserted using the rotation of the group with idealized bond angles. The remaining hydrogen atoms were refined using a riding model. The figures were drawn using the *Mercury* [Macrae C.F., Sovago I., Cottrell S.J., Galek P.T.A., McCabe P., Pidcock E., Platings M., Shields G.P., Stevens J.S., Towler M., Wood P.A. Mercury 4.0: from visualization to analysis, design and prediction. *J. Appl. Crystallogr.*, 2020. – V. 53, Pt. 1. – P. 226–235] program. The crystallographic data for the structures **3bb-CF₃COO⁻**, **3bc** and **3be** reported in this article have been deposited with the Cambridge Crystallographic Data Center and are freely available on request on the website www.ccdc.cam.ac.uk/data_request/cif. The most important characteristics of the experiments, structure refinement, and the reference numbers are given in Table S1.

Table S1. Crystallographic data and X-ray structural experiment parameters for the single crystals **3bb-CF₃COO⁻**, **3bc** and **3be**.

Compound	3bb-CF₃COO⁻	3bc	3be
Empirical formula	C ₁₇ H ₁₇ ClNO ₂ P	C ₁₇ H ₁₈ BrNO ₂ P ⁺ , Cl ⁻ , 0.5(H ₂ O)	C ₁₈ H ₂₁ NO ₃ P ⁺ , Cl ⁻ , H ₂ O
Formula weight	333.73	423.66	383.79
Crystal system	monoclinic	triclinic	monoclinic
Space group	<i>P2₁/n</i> (No. 14)	<i>P</i> $\bar{1}$ (No. 2)	<i>Pc</i> (No. 7)
Unit cell dimensions:	12.043(2),	6.6018(4),	6.337(4),

$a, b, c, \text{Å};$ $\alpha, \beta, \gamma ^\circ$	5.5867(9), 27.643(4); 90, 94.199(4), 90	16.2369(9), 16.8101(9); 93.138(2), 100.567(2), 93.351(2)	16.965(10), 9.393(5); 90, 104.174(12), 90
Volume, Å^3	1854.8(5)	1764.40(17)	979.0(10)
Z and Z'	4 and 1	4 and 2	2 and 1
Calculated density, g cm^{-3}	1.195	1.595	1.302
Absorption coefficient, mm^{-1}	0.297	2.584	0.298
$F(000)$	696	860	404
Crystal size, mm^3	$0.230 \times 0.097 \times 0.067$	$0.487 \times 0.180 \times 0.078$	$0.409 \times 0.256 \times 0.122$
θ range for data collection, $^\circ$	2.690 to 26.991	2.471 to 26.997	2.401 to 26.989
Index ranges	$-15 \leq h \leq 15,$ $-7 \leq k \leq 7,$ $-35 \leq l \leq 35$	$-8 \leq h \leq 8,$ $-20 \leq k \leq 20,$ $-21 \leq l \leq 21$	$-8 \leq h \leq 8,$ $-21 \leq k \leq 20,$ $-11 \leq l \leq 11$
Reflections collected	30594	72687	8828
Independent reflections	4026	7719	3706
R_{int}	0.0525	0.0655	0.0695
R_σ	0.0311	0.0333	0.0967
Observed Data [$I > 2\sigma(I)$]	3853	6497	3009
Completeness to $\theta = 25.242^\circ$, %	99.9	99.9	99.8
Max. and min. transmission	0.7460 and 0.6260	0.7460 and 0.6347	0.7460 and 0.5509
Data / restraints / parameters	4026 / 0 / 207	7719 / 4 / 456	3706 / 3 / 219
Goodness-of-fit on F^2	1.289	1.050	1.133
Final R indices [$I > 2\sigma(I)$]	$R1 = 0.1009, wR2 = 0.1927$	$R1 = 0.0343, wR2 = 0.0770$	$R1 = 0.0944, wR2 = 0.2041$
R indices (all data)	$R1 = 0.1035, wR2 = 0.1937$	$R1 = 0.0448, wR2 = 0.0810$	$R1 = 0.1137, wR2 = 0.2140$
Largest diff. peak and hole, $e \text{Å}^{-3}$	0.664 and -0.607	0.758 and -0.454	0.994 and -0.758
CCDC number	2440417	2440418	2440419

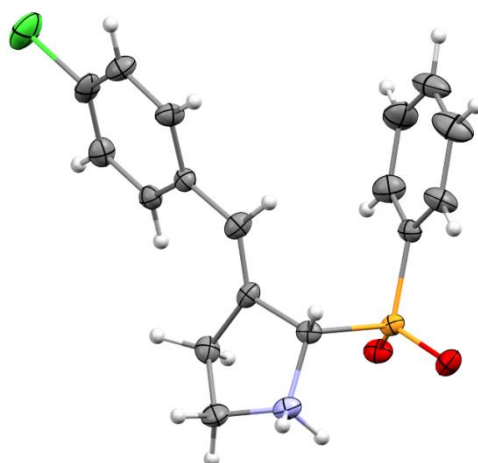


Figure S1. Molecular geometry in the crystal **3bb-CF₃COO⁻**. Thermal ellipsoids for non-H atoms are set at the 50% probability level.

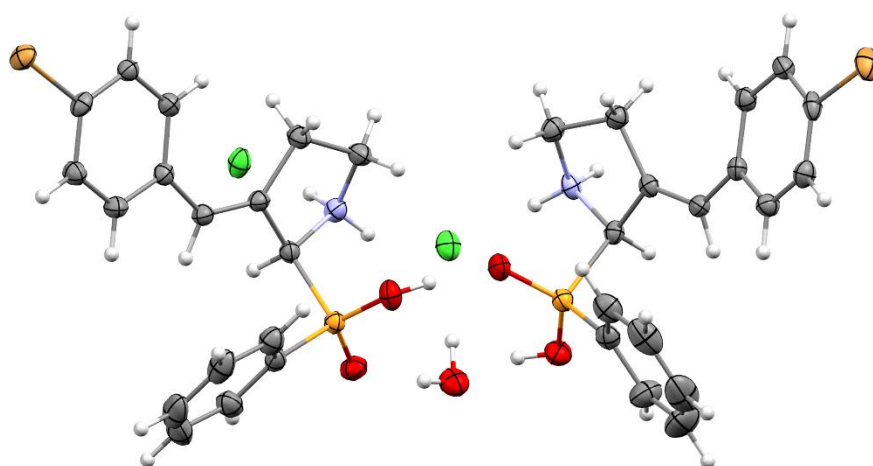


Figure S2. Molecular geometry in the crystal **3bc**. Thermal ellipsoids for non-H atoms are set at the 50% probability level.

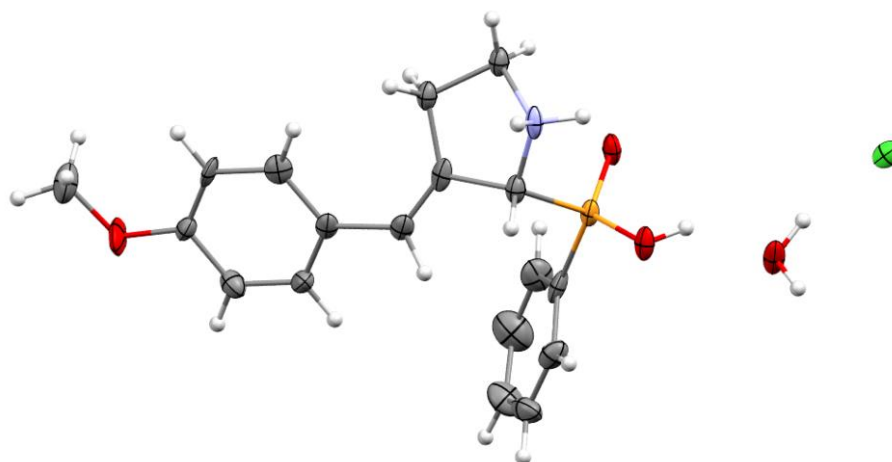


Figure S3. Molecular geometry in the crystal **3be**. Thermal ellipsoids for non-H atoms are set at the 50% probability level.

Copies of ^1H , ^{13}C , ^{31}P NMR spectra

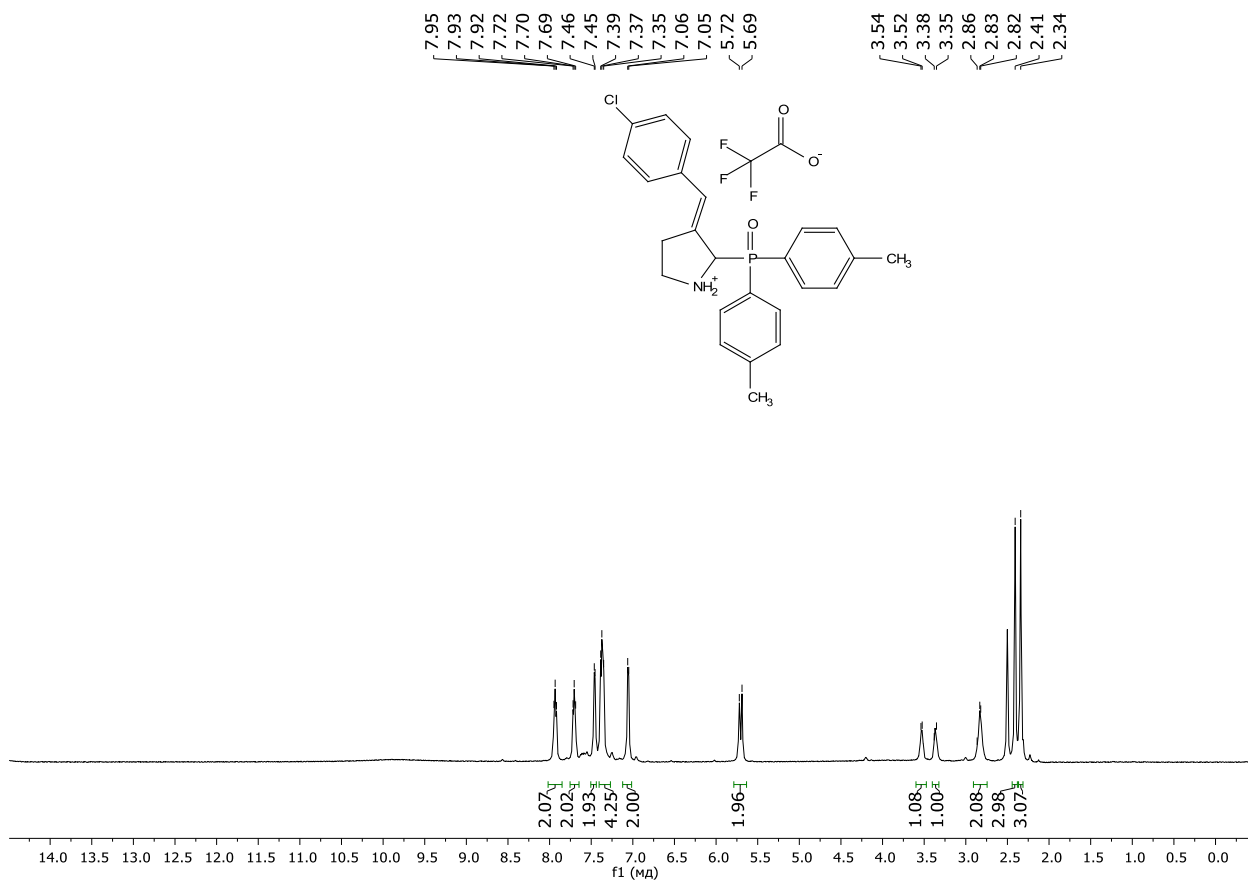


Figure S4. ^1H NMR (DMSO- d_6 , 600 MHz) spectrum of the compound 3aa

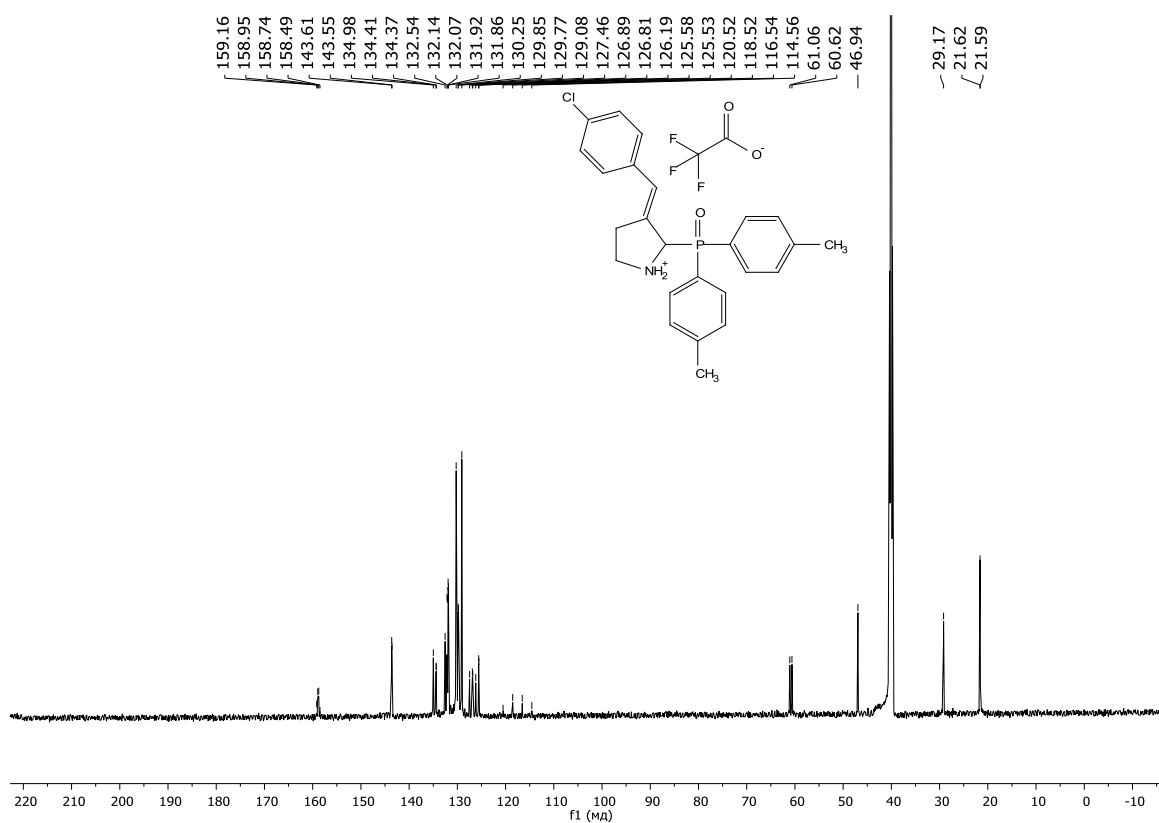


Figure S5. $^{13}\text{C}\{^1\text{H}\}$ NMR (DMSO- d_6 , 150 MHz) spectrum of the compound 3aa

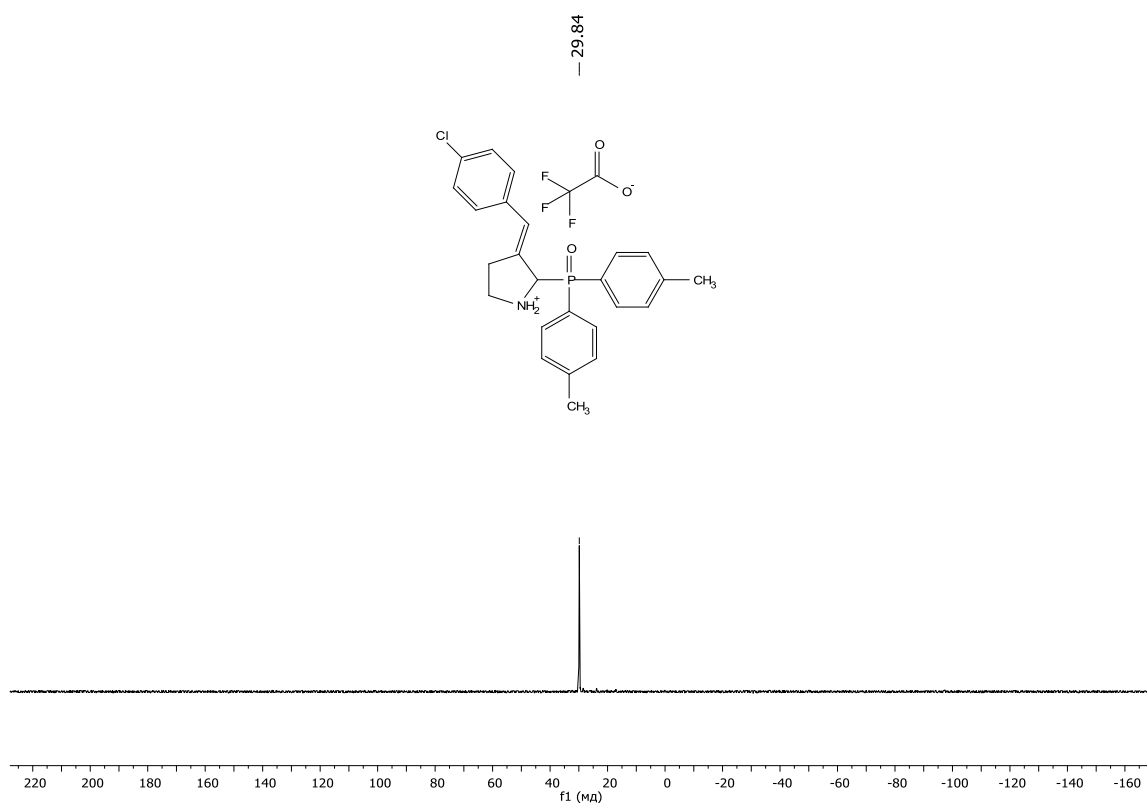


Figure S6. $^{31}\text{P}\{^1\text{H}\}$ NMR (DMSO- d_6 , 161 MHz) spectrum of the compound **3aa**

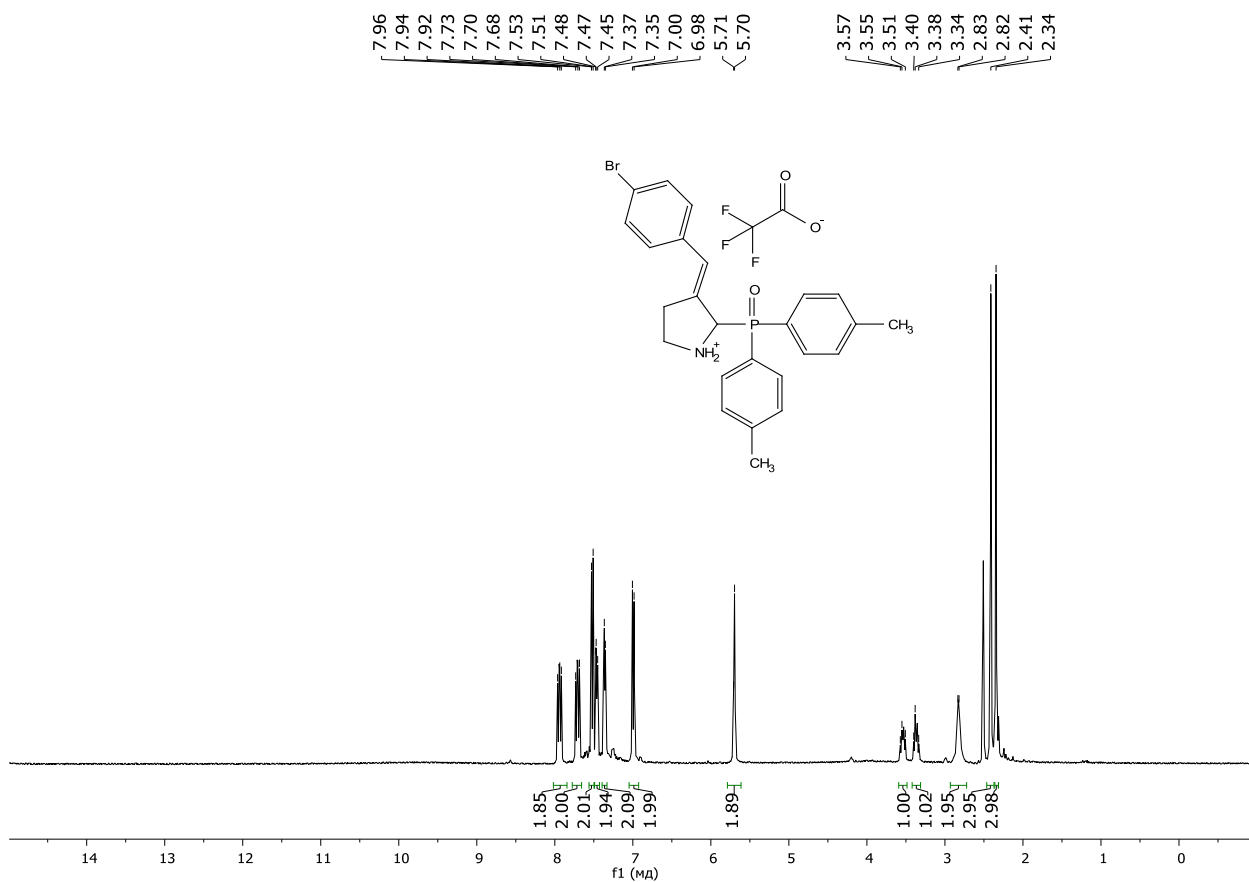


Figure S7. ^1H NMR (DMSO- d_6 , 600 MHz) spectrum of the compound **3ab**

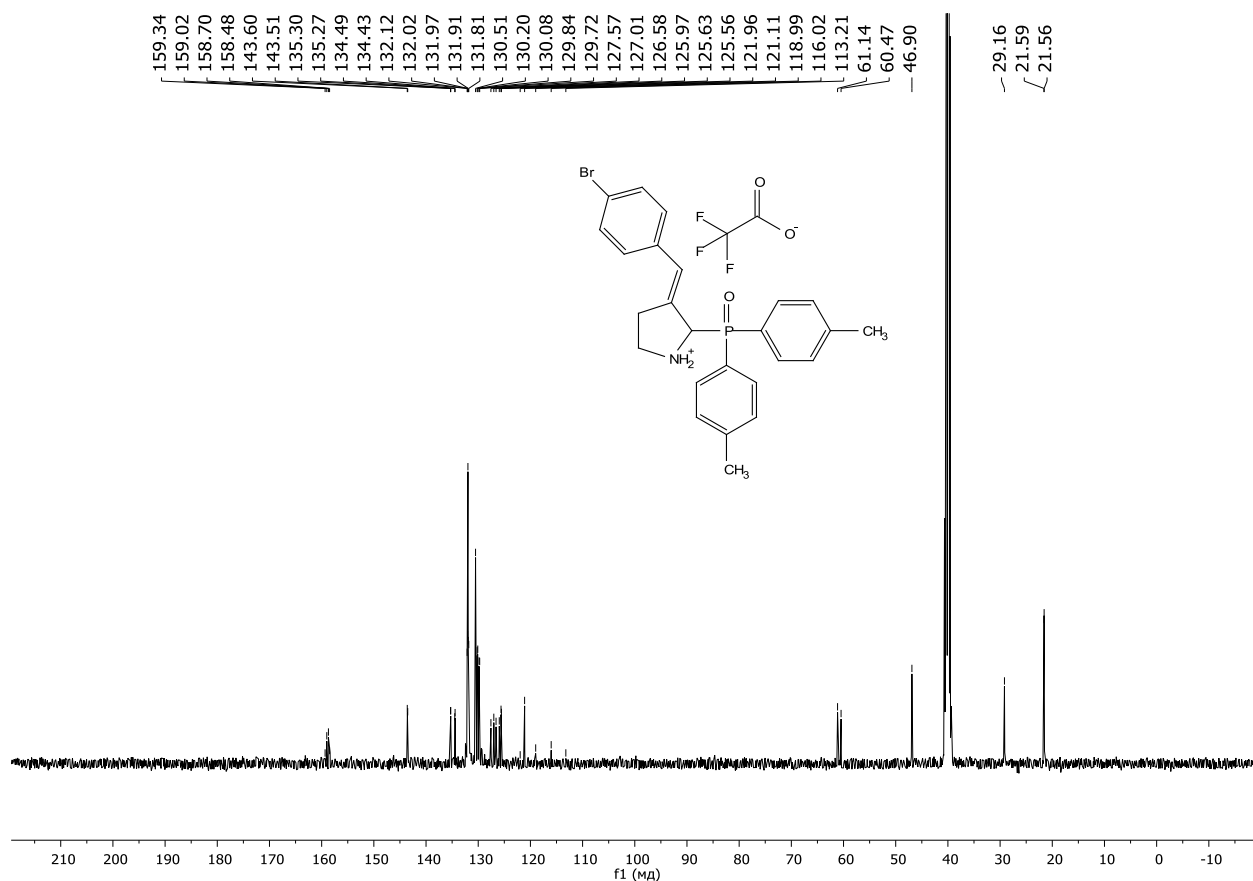


Figure S8. $^{13}\text{C}\{^1\text{H}\}$ NMR ($\text{DMSO-}d_6$, 150 MHz) spectrum of the compound **3ab**

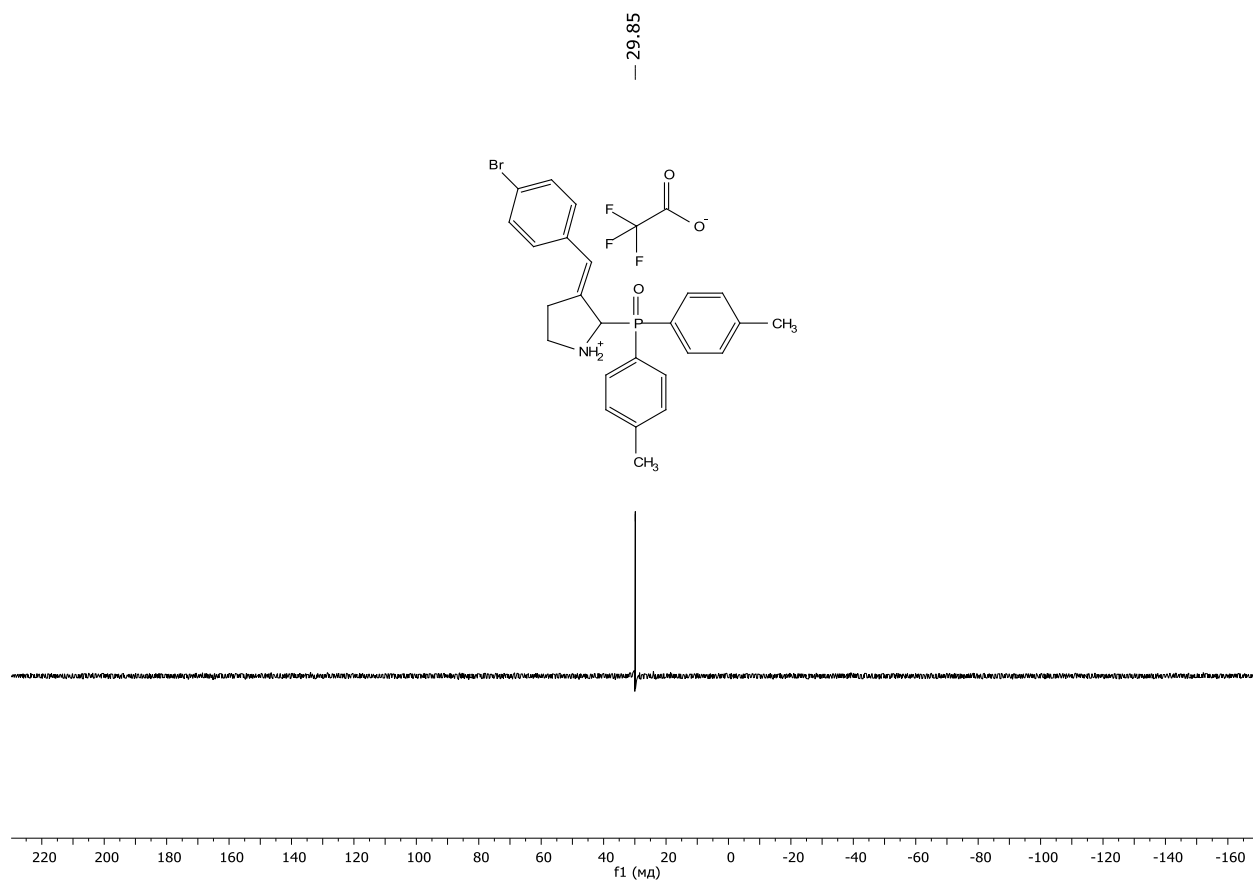


Figure S9. $^{31}\text{P}\{^1\text{H}\}$ NMR ($\text{DMSO-}d_6$, 161 MHz) spectrum of the compound **3ab**

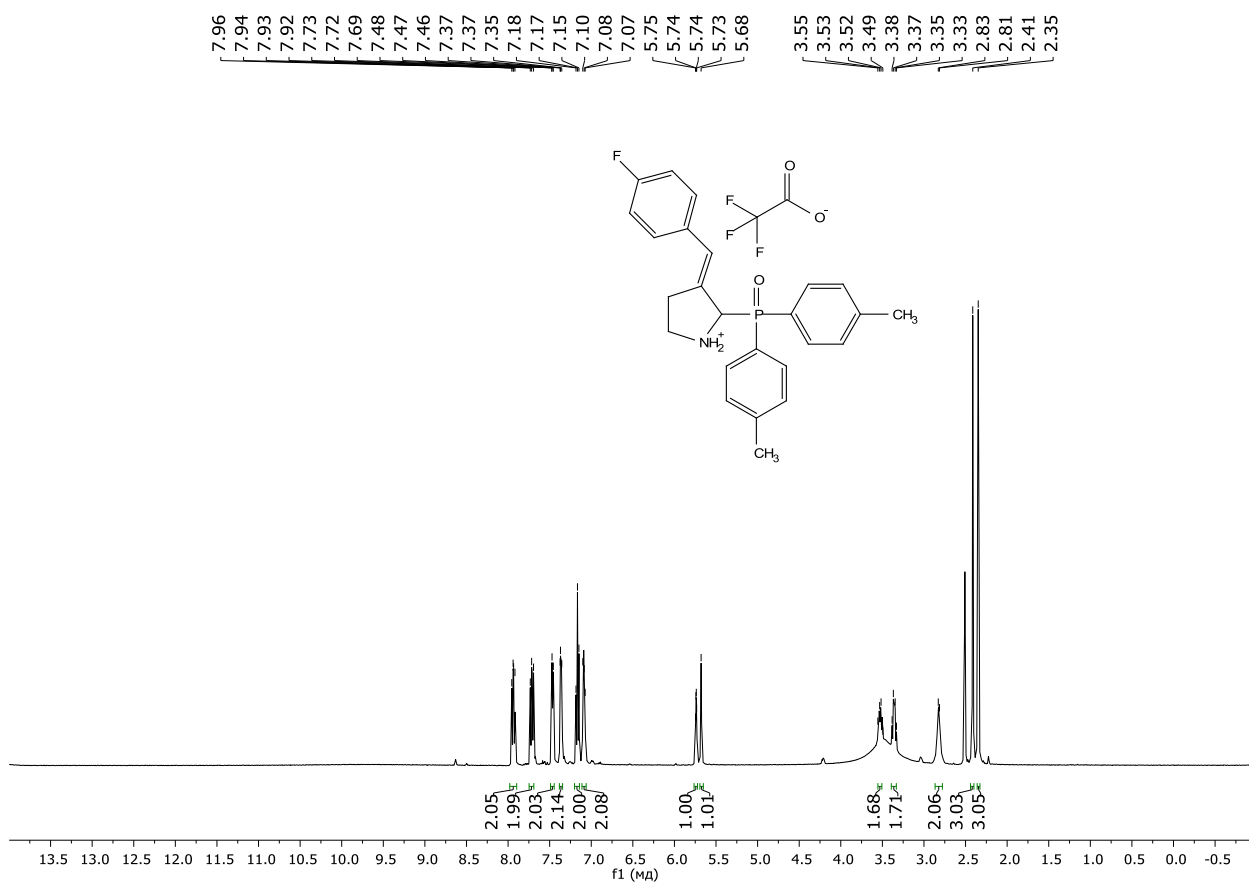


Figure S10. ¹H NMR (DMSO-d₆, 600 MHz) spectrum of the compound 3ac

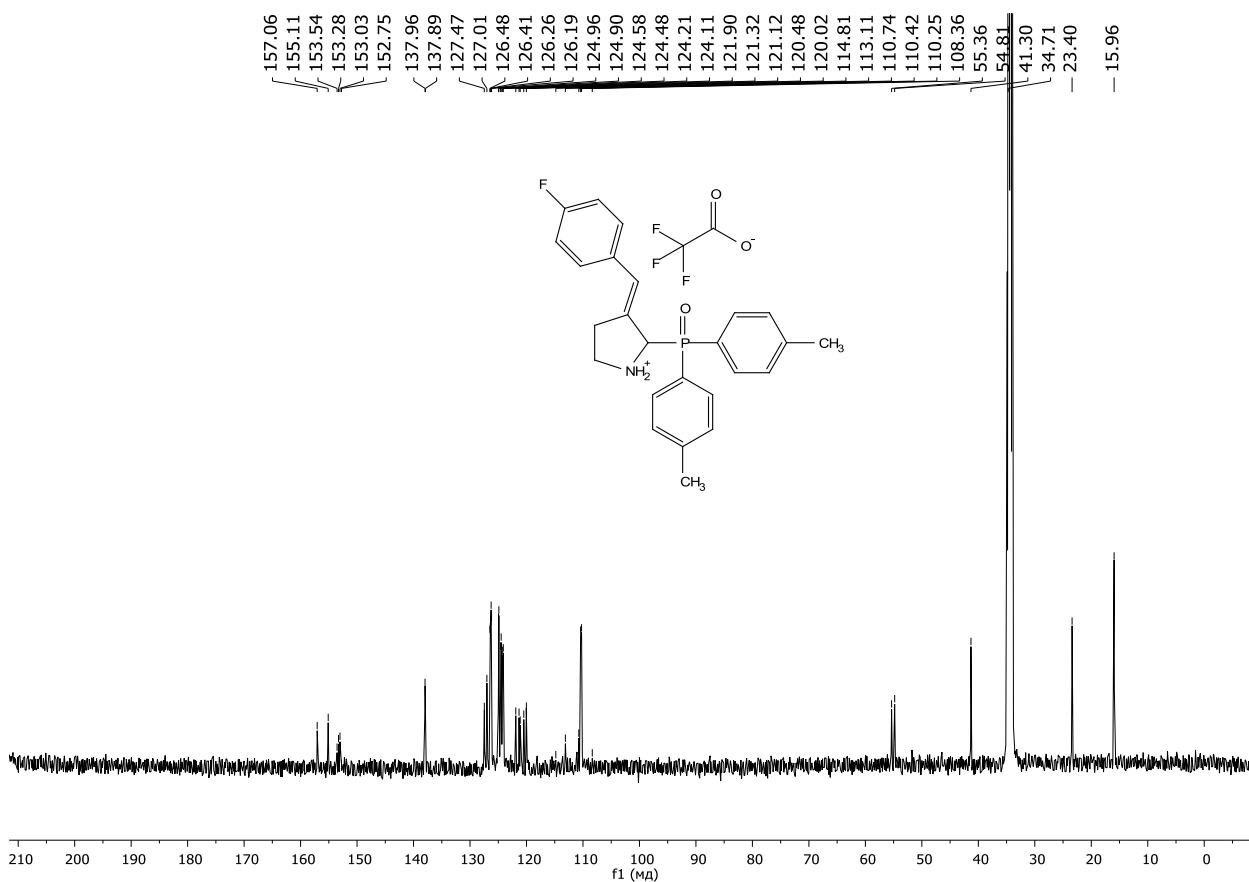


Figure S11. ¹³C{¹H} NMR (DMSO-d₆, 150 MHz) spectrum of the compound 3ac

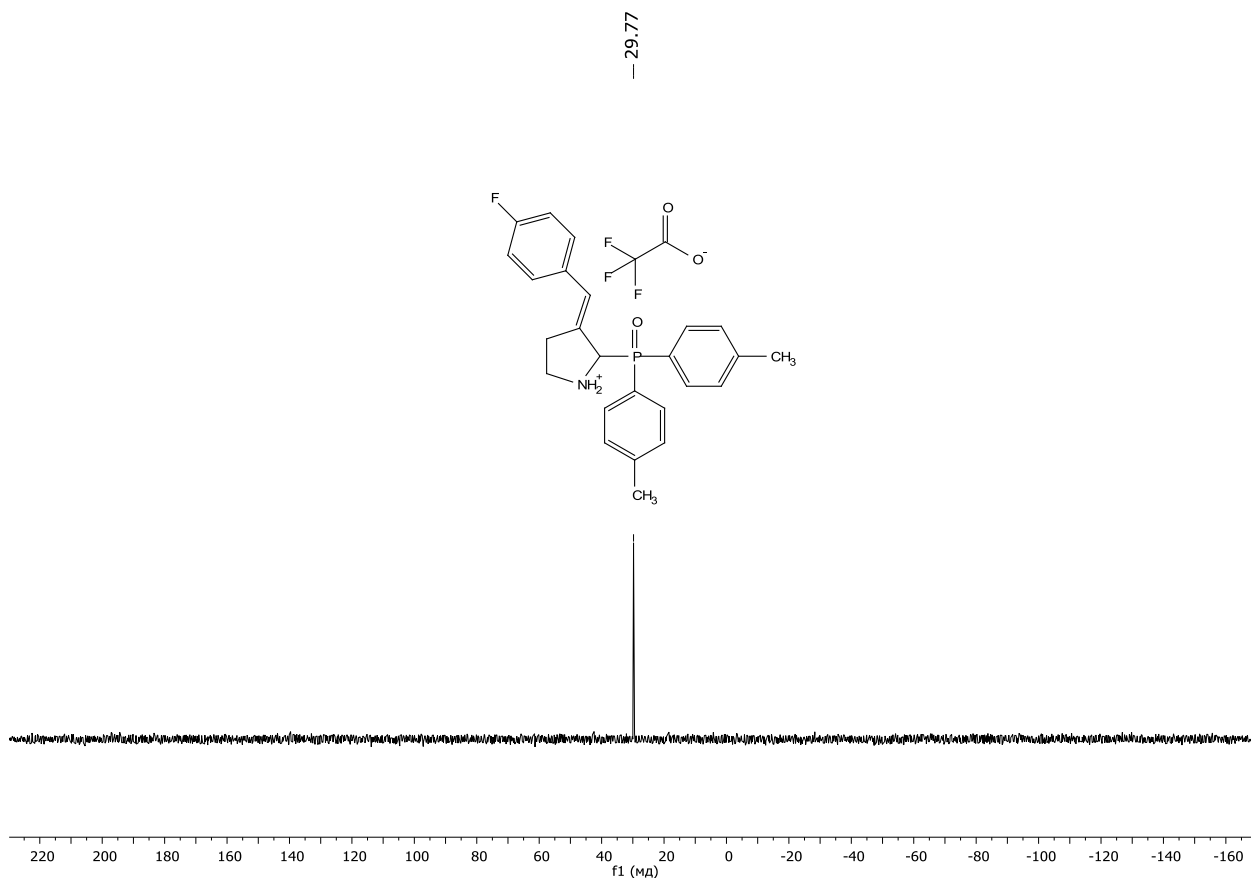


Figure S12. $^{31}\text{P}\{^1\text{H}\}$ NMR ($\text{DMSO-}d_6$, 161 MHz) spectrum of the compound **3ac**

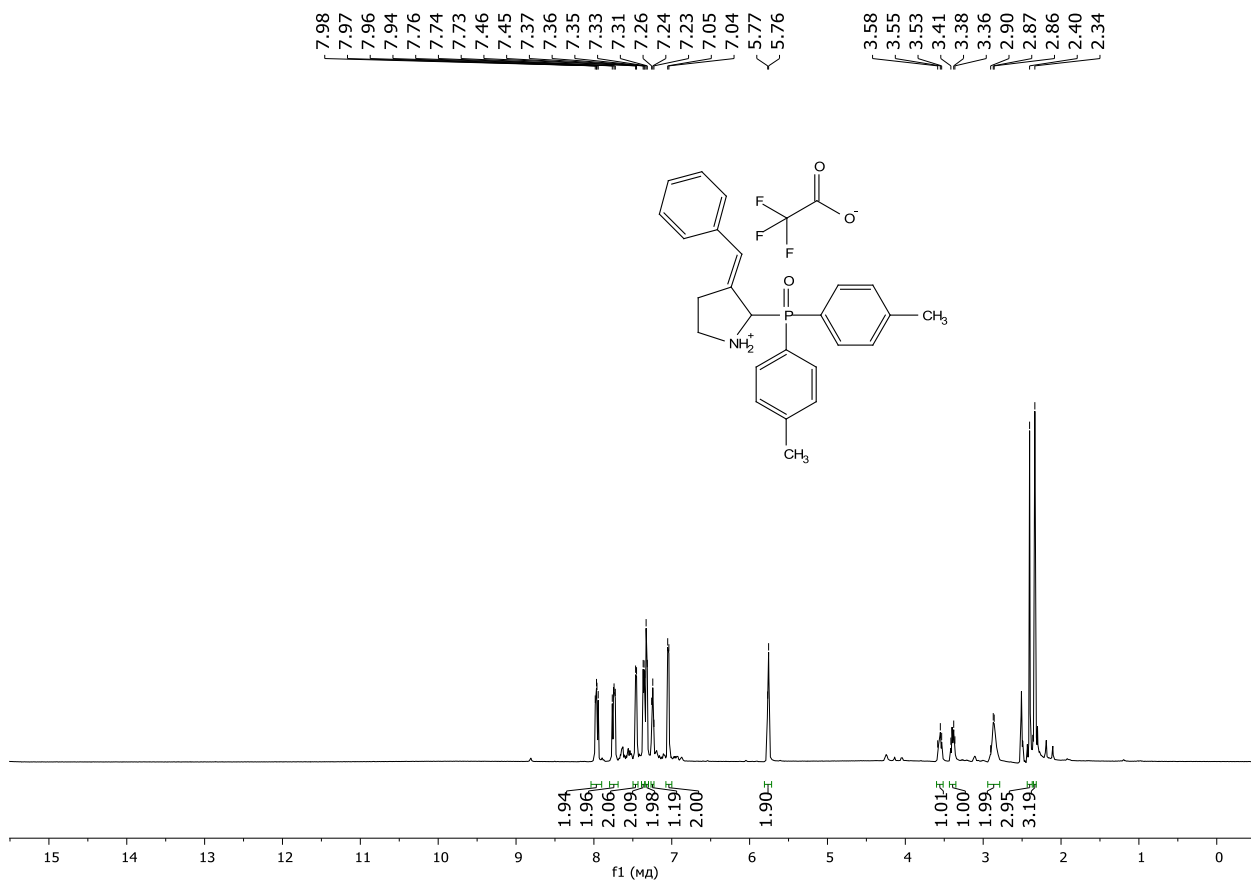


Figure S13. ^1H NMR ($\text{DMSO-}d_6$, 600 MHz) spectrum of the compound **3ad**

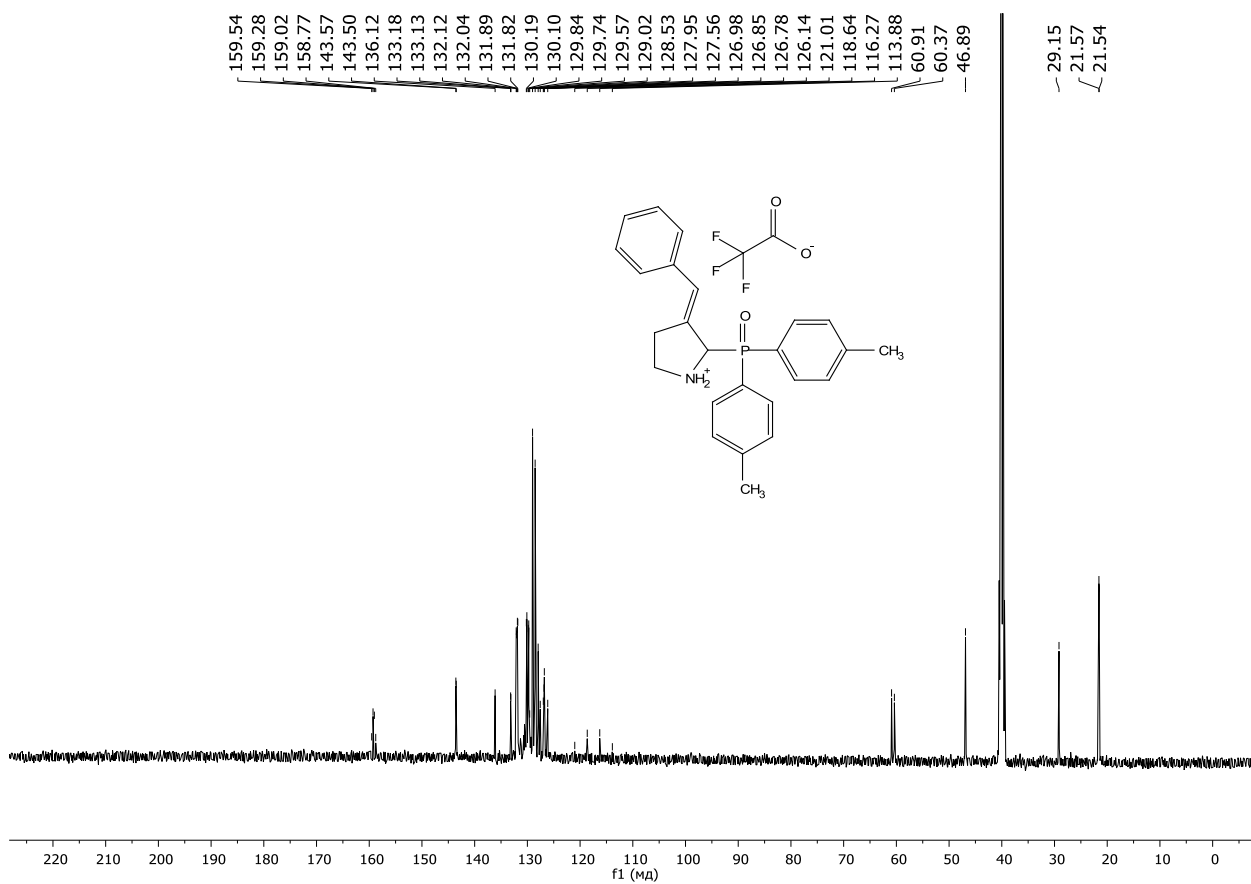


Figure S14. $^{13}\text{C}\{^1\text{H}\}$ NMR (DMSO- d_6 , 150 MHz) spectrum of the compound **3ad**

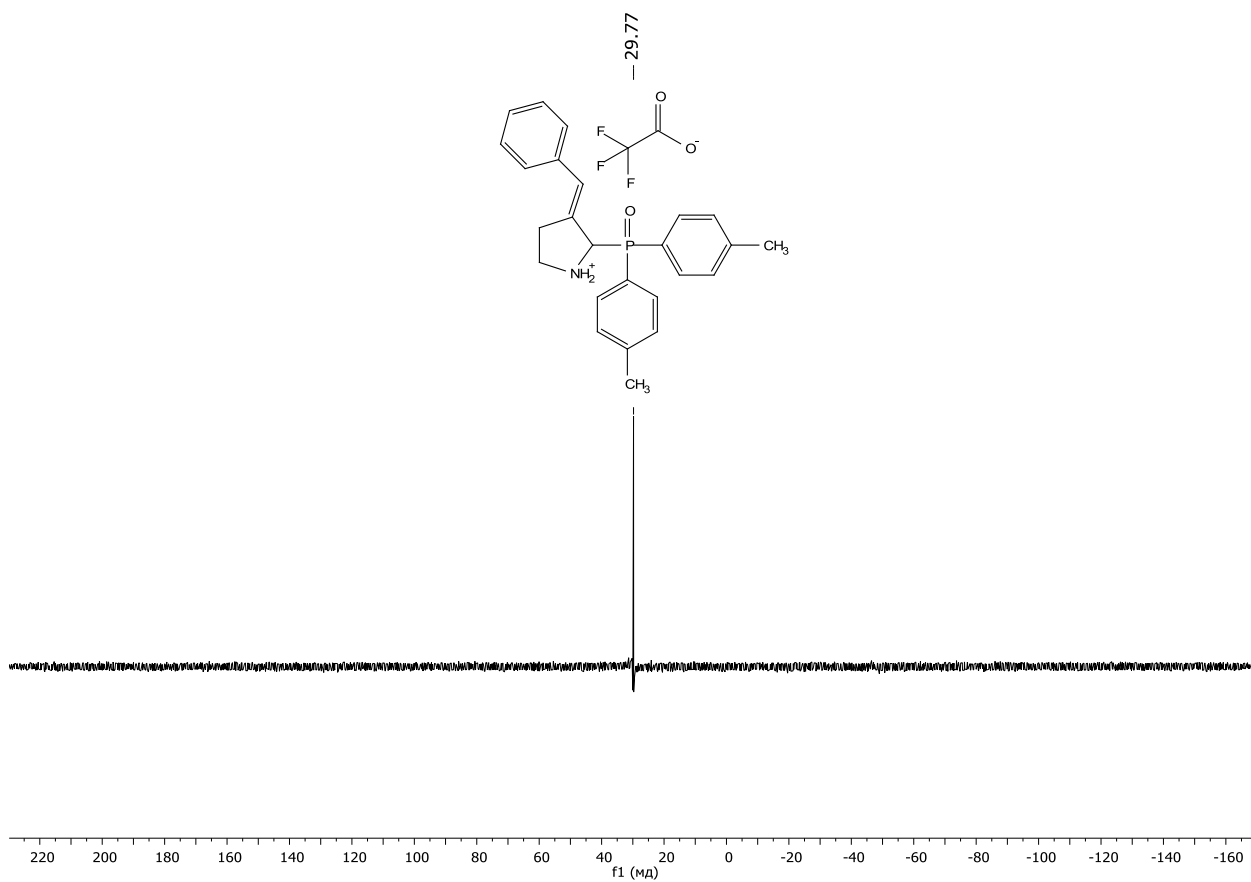


Figure S15. $^{31}\text{P}\{^1\text{H}\}$ NMR (DMSO- d_6 , 161 MHz) spectrum of the compound **3ad**

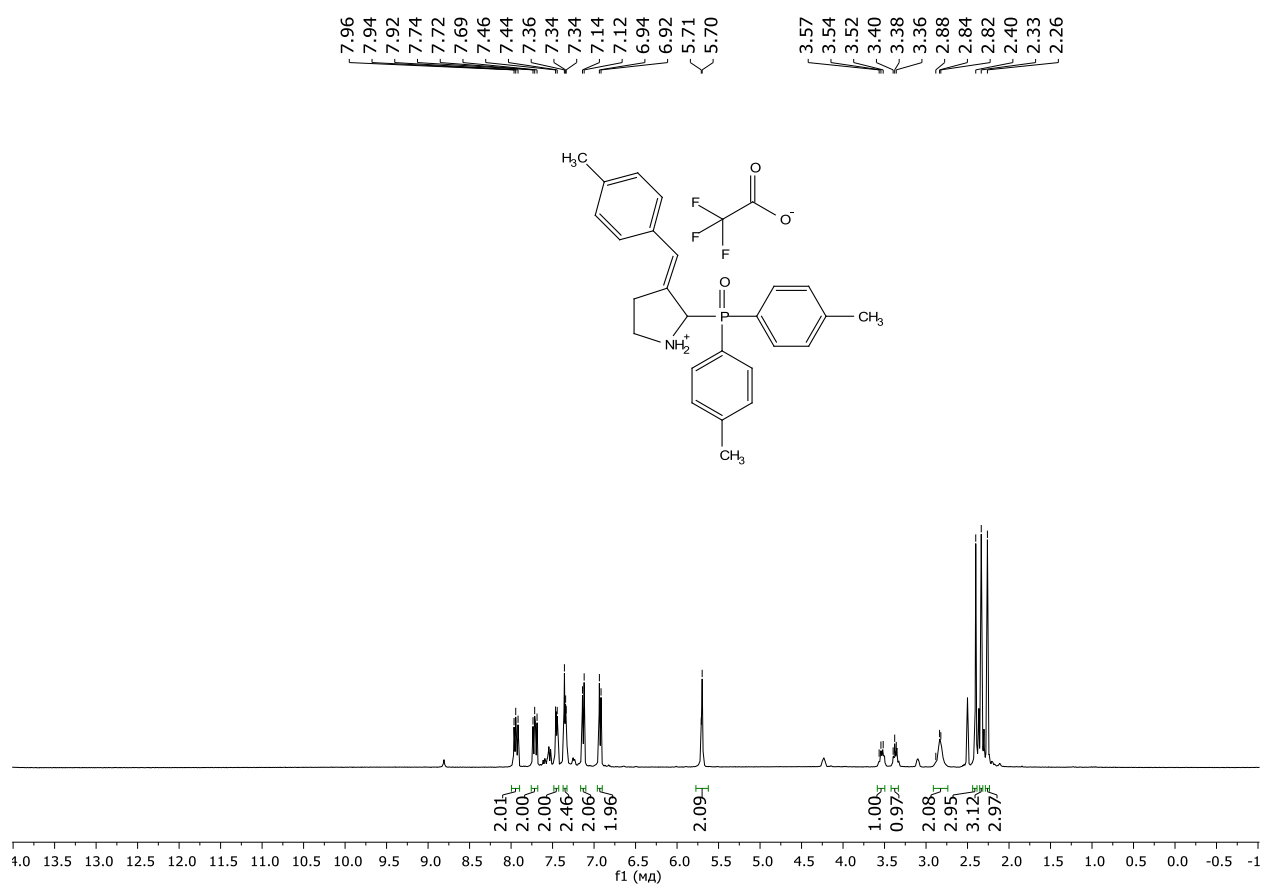


Figure S16. $^1\text{H NMR}$ (DMSO- d_6 , 600 MHz) spectrum of the compound 3ae

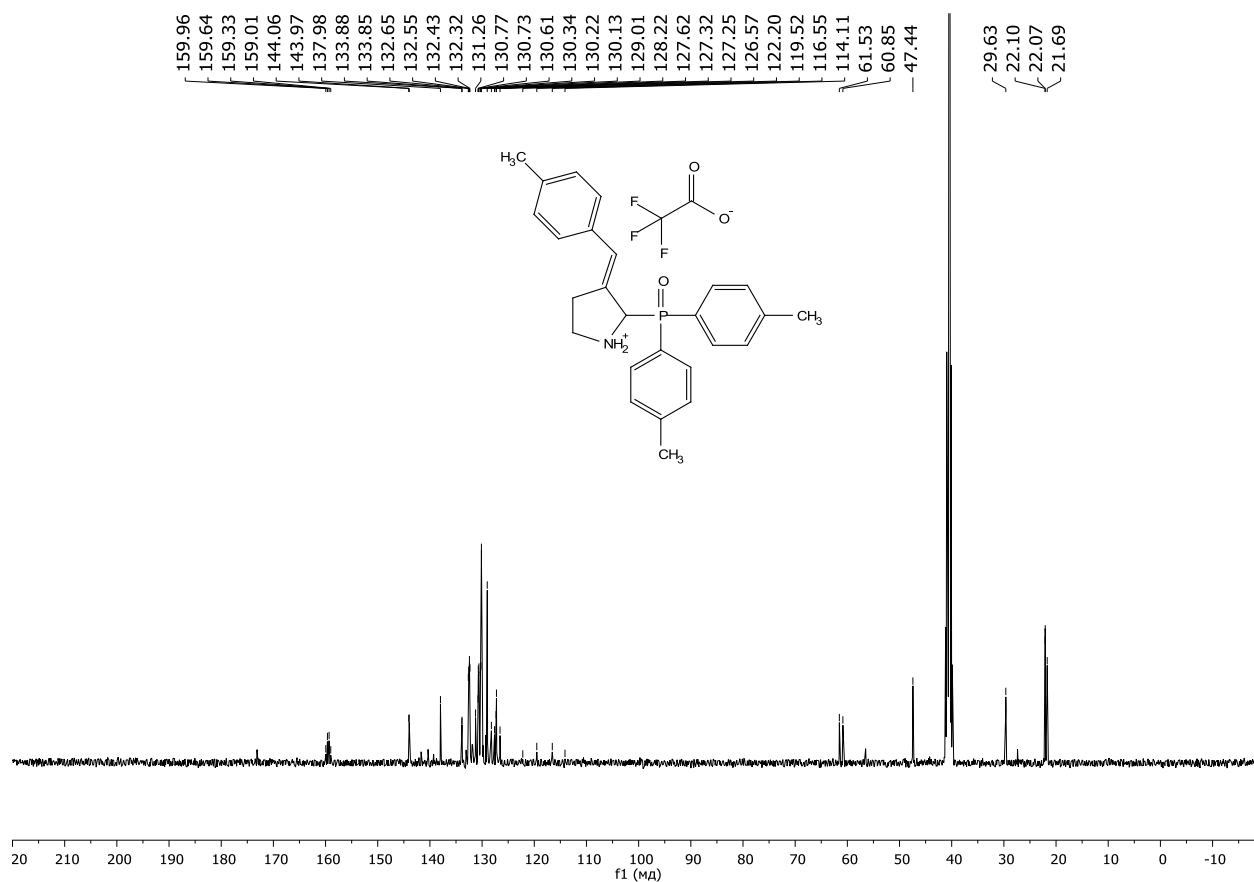


Figure S17. $^{13}\text{C}\{^1\text{H}\}$ NMR (DMSO- d_6 , 150 MHz) spectrum of the compound 3ae

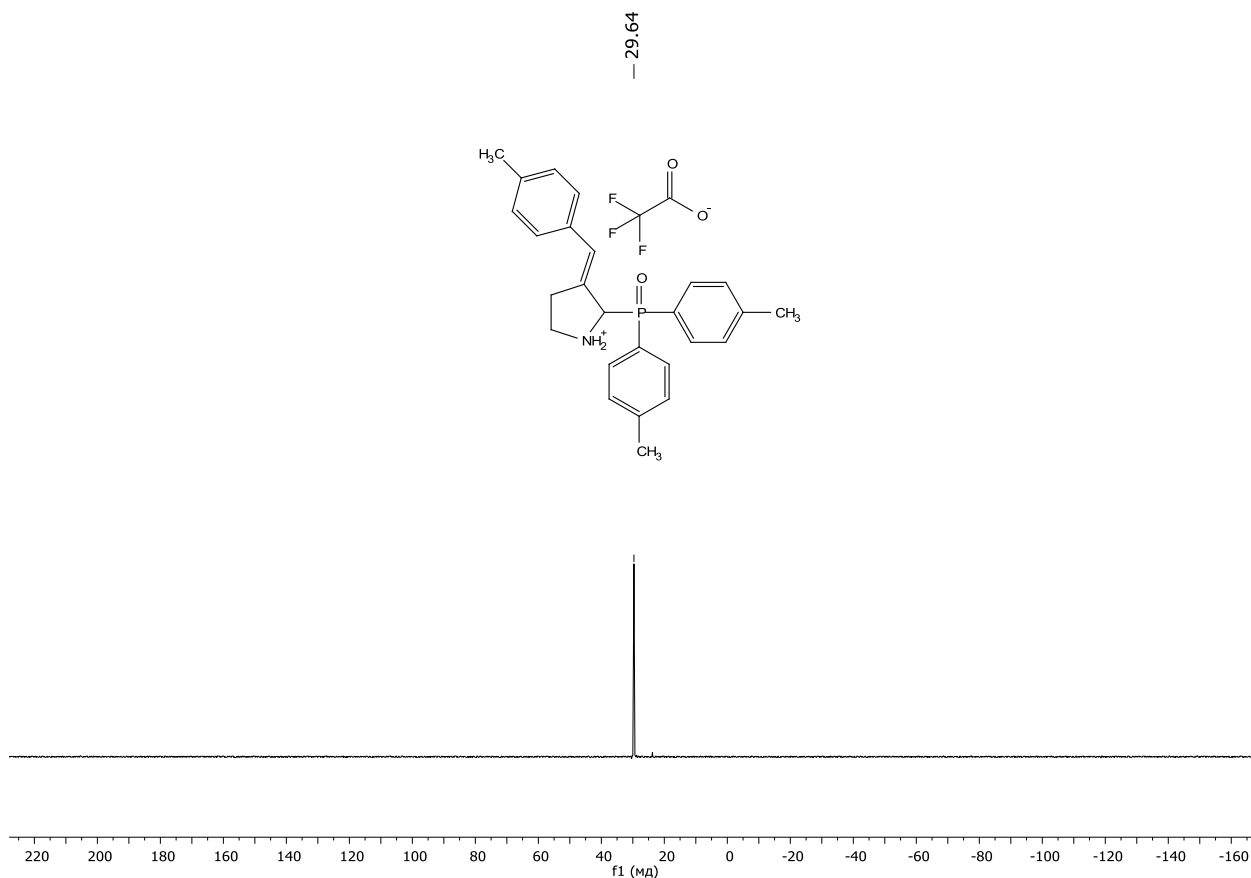


Figure S18. $^{31}\text{P}\{^1\text{H}\}$ NMR (DMSO- d_6 , 161 MHz) spectrum of the compound **3ae**

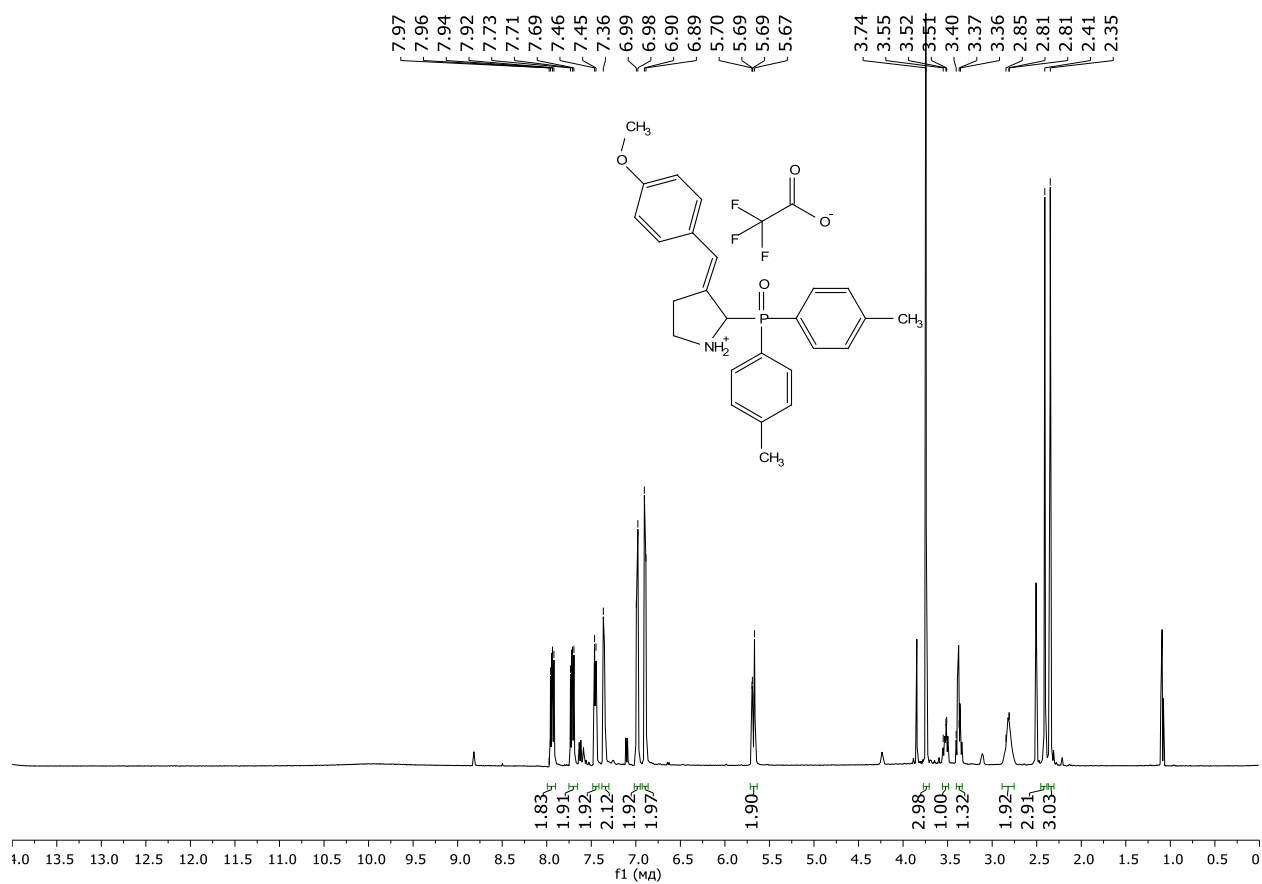


Figure S19. ^1H NMR (DMSO- d_6 , 600 MHz) spectrum of the compound **3af**

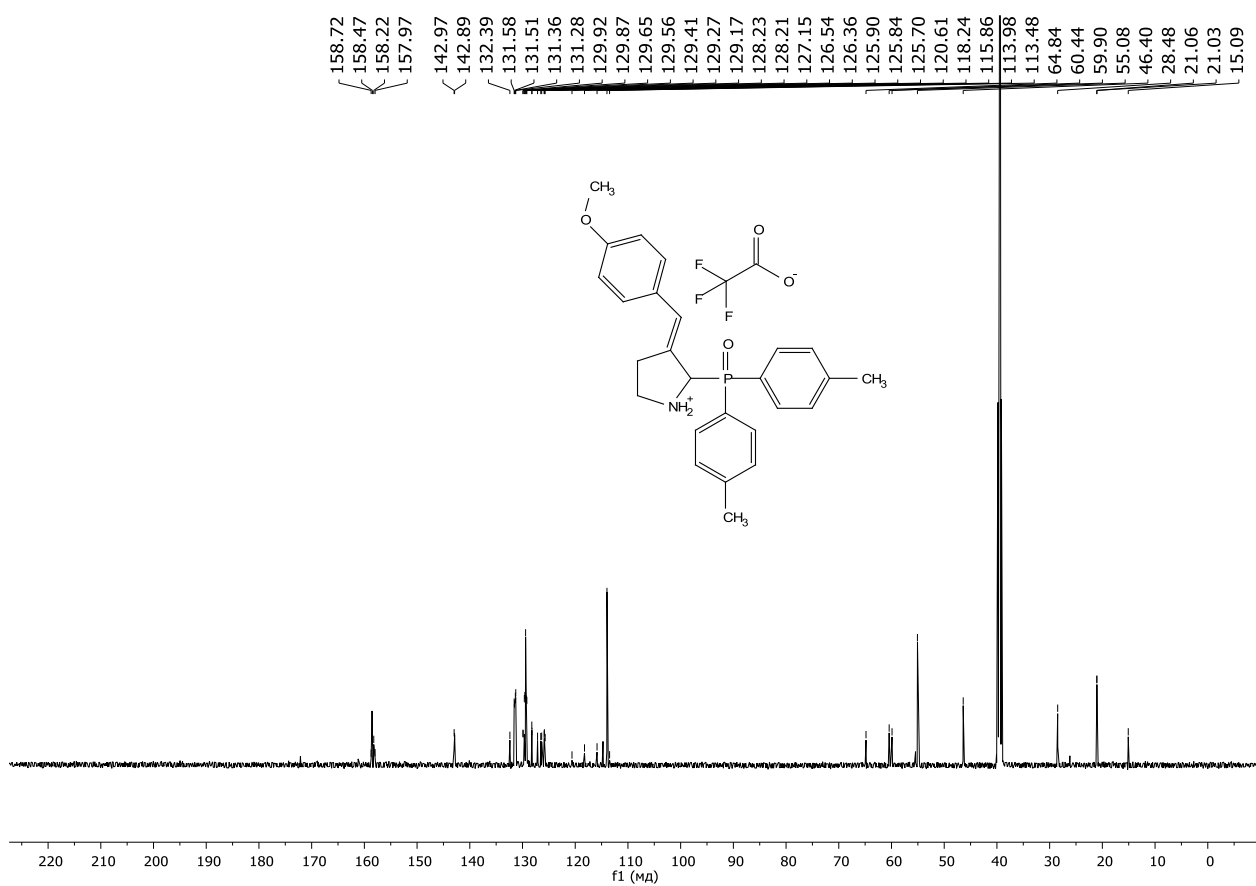


Figure S20. $^{13}\text{C}\{^1\text{H}\}$ NMR (DMSO- d_6 , 150 MHz) spectrum of the compound **3af**

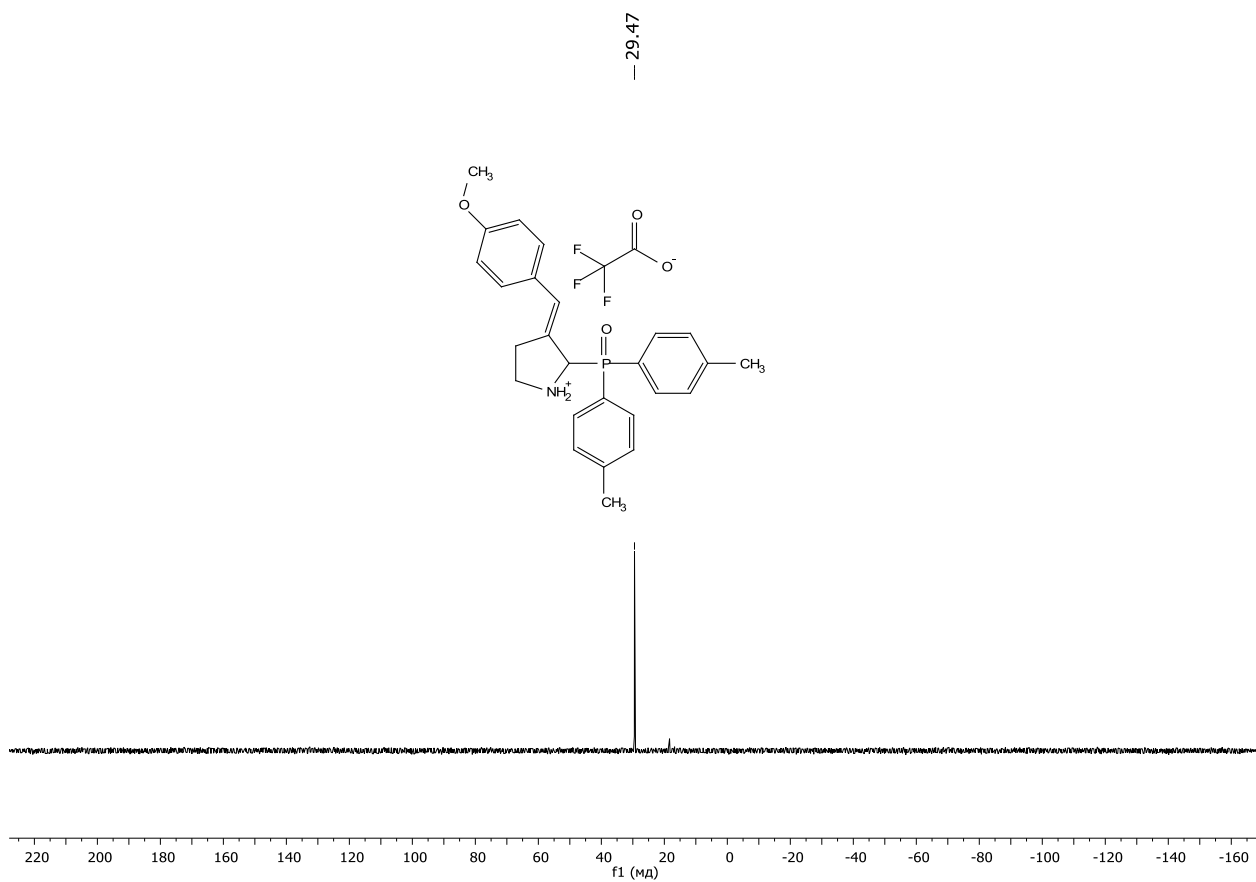


Figure S21. $^{31}\text{P}\{^1\text{H}\}$ NMR (DMSO- d_6 , 161 MHz) spectrum of the compound **3af**

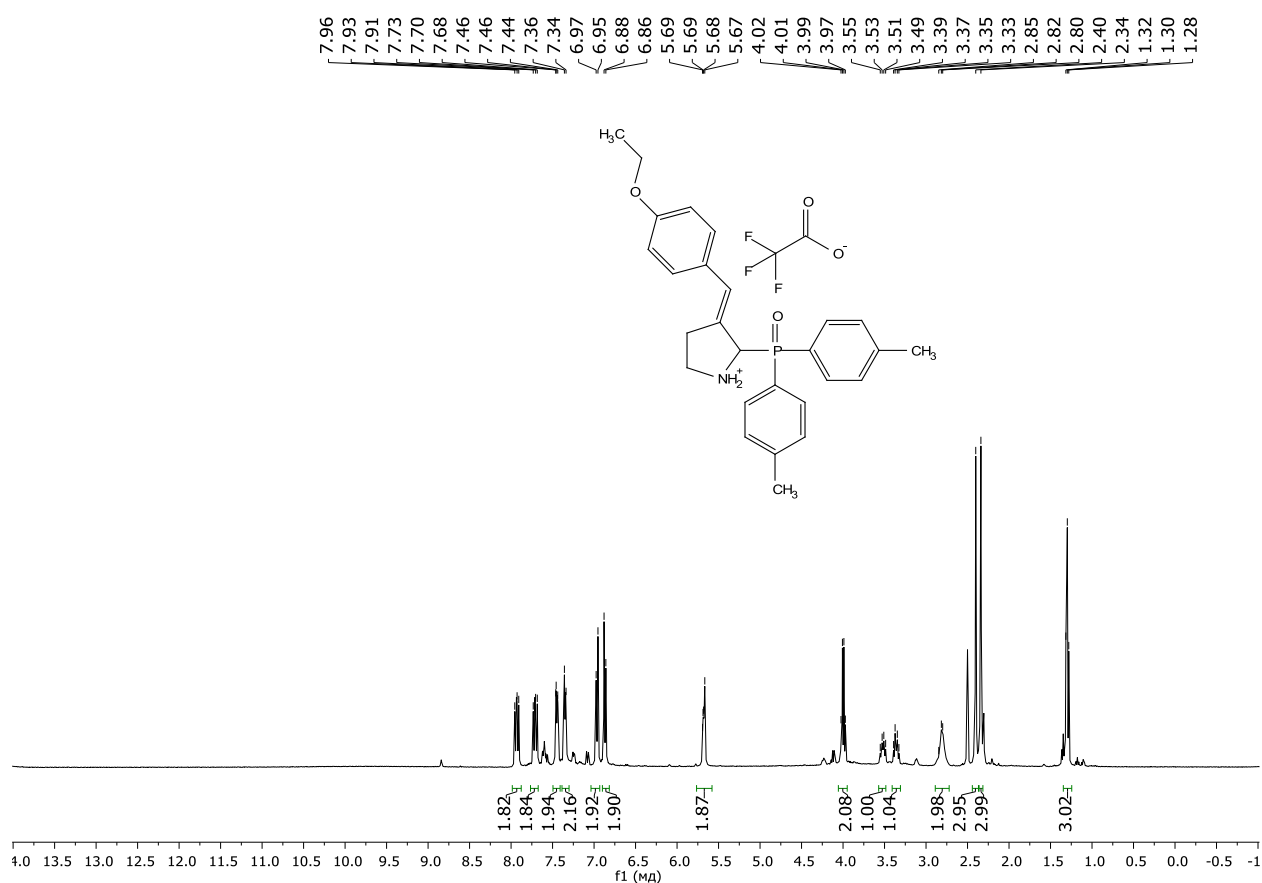


Figure S22. ¹H NMR (DMSO-d₆, 600 MHz) spectrum of the compound 3ag

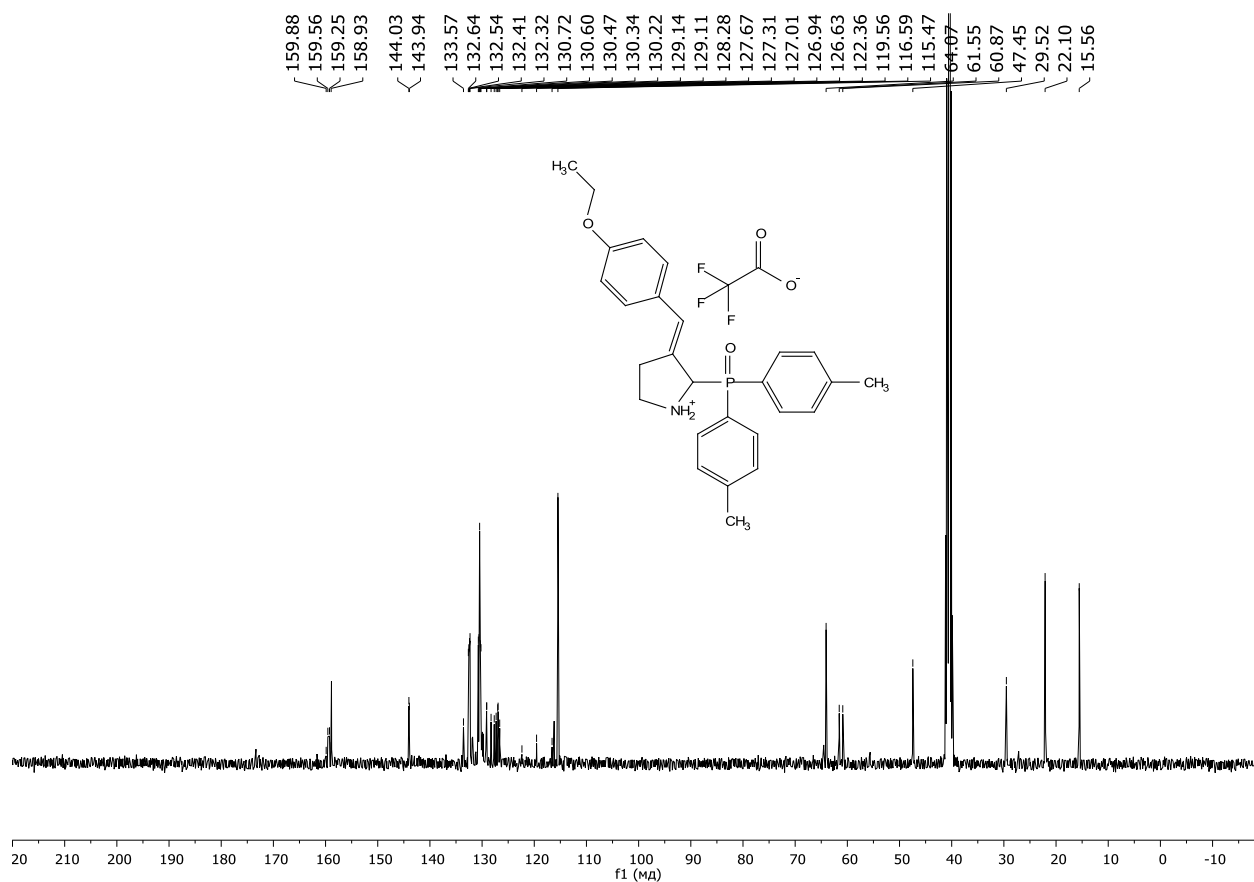


Figure S23. ¹³C{¹H} NMR (DMSO-d₆, 150 MHz) spectrum of the compound 3ag

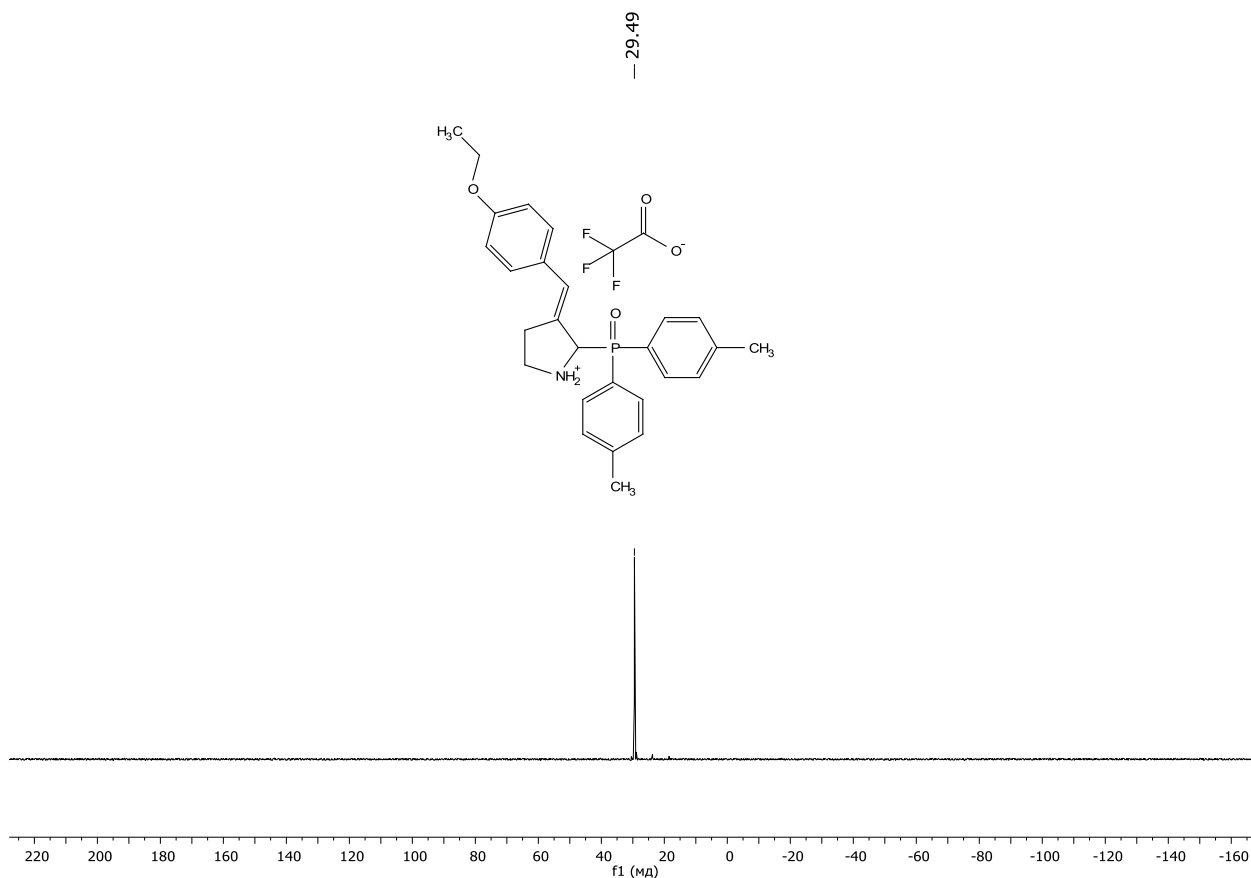


Figure S24. $^{31}\text{P}\{^1\text{H}\}$ NMR ($\text{DMSO-}d_6$, 161 MHz) spectrum of the compound **3ag**

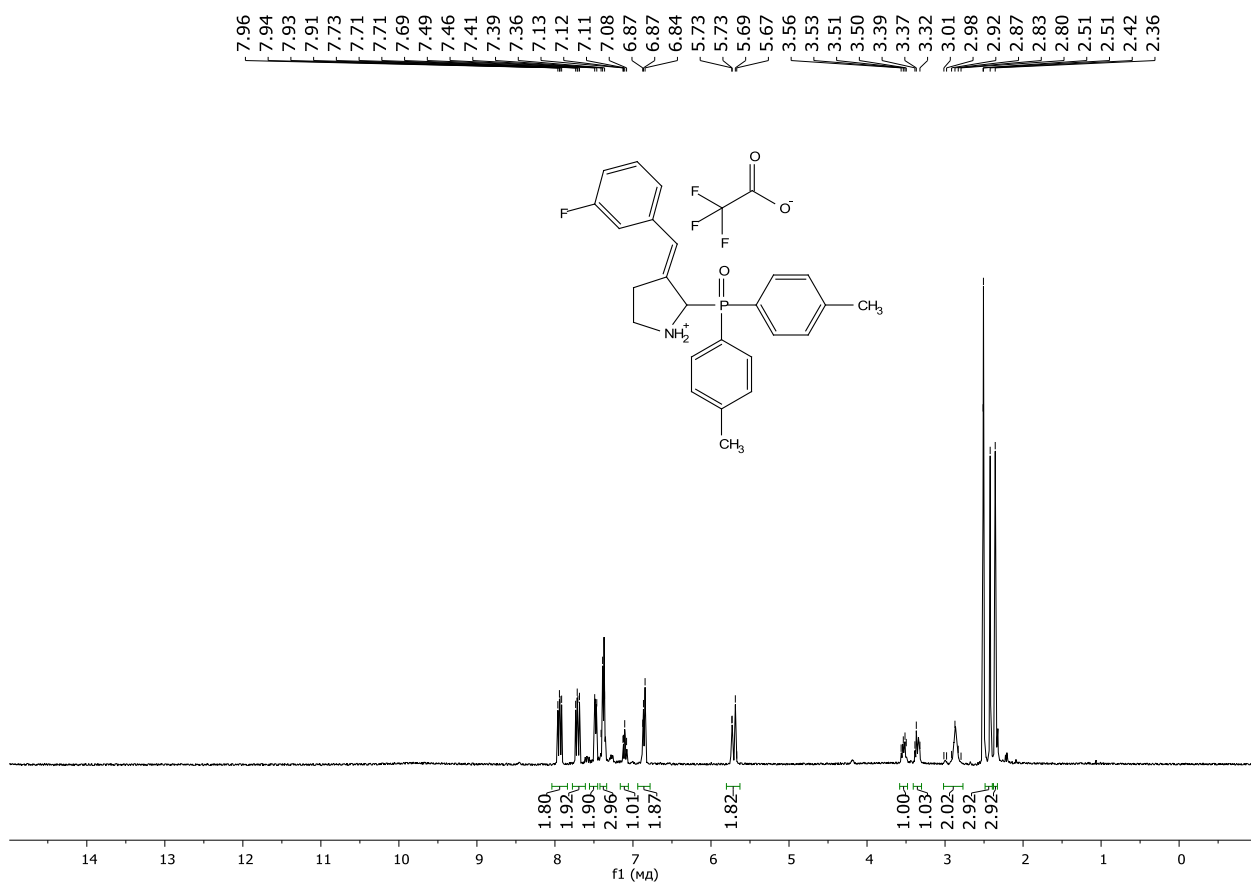


Figure S25. ^1H NMR ($\text{DMSO-}d_6$, 600 MHz) spectrum of the compound **3ah**

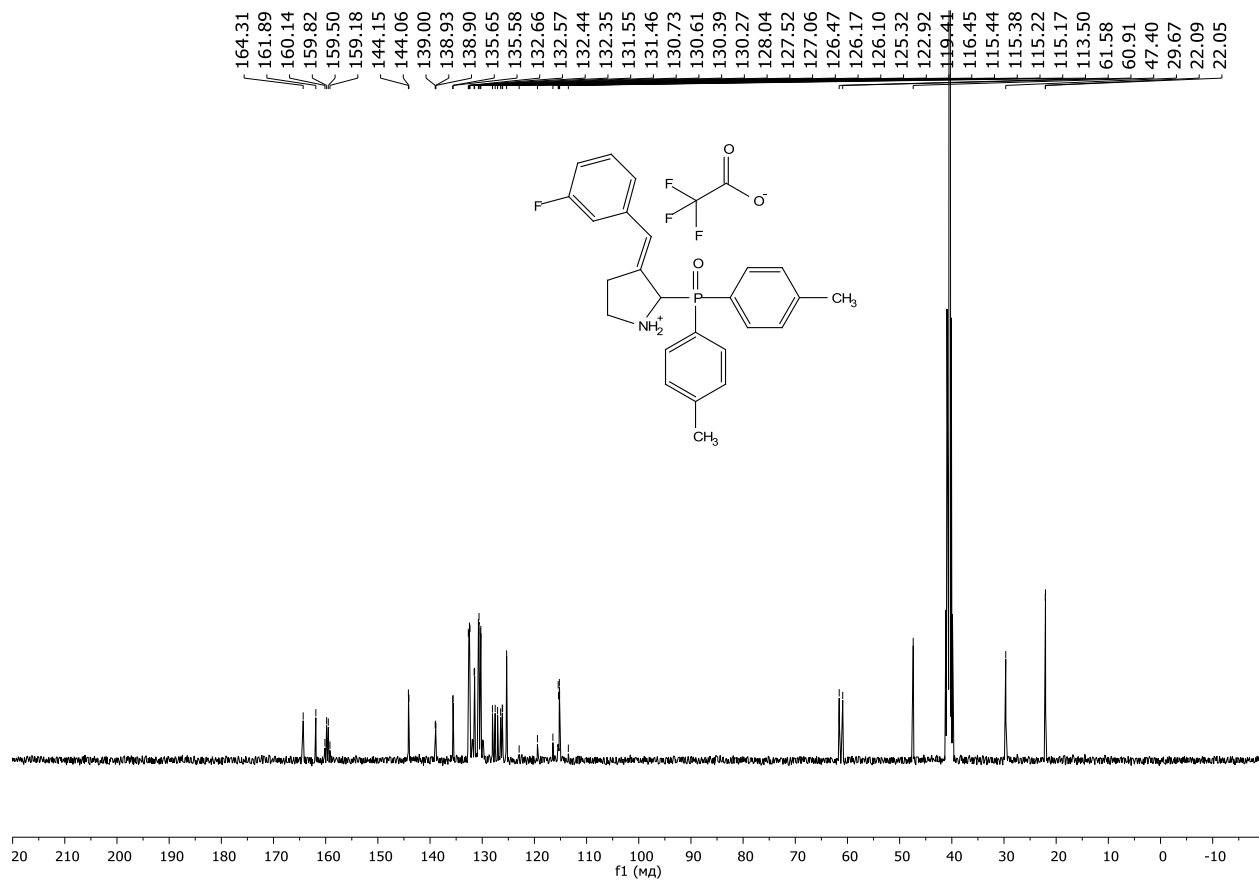


Figure S26. $^{13}\text{C}\{^1\text{H}\}$ NMR ($\text{DMSO-}d_6$, 150 MHz) spectrum of the compound 3ah

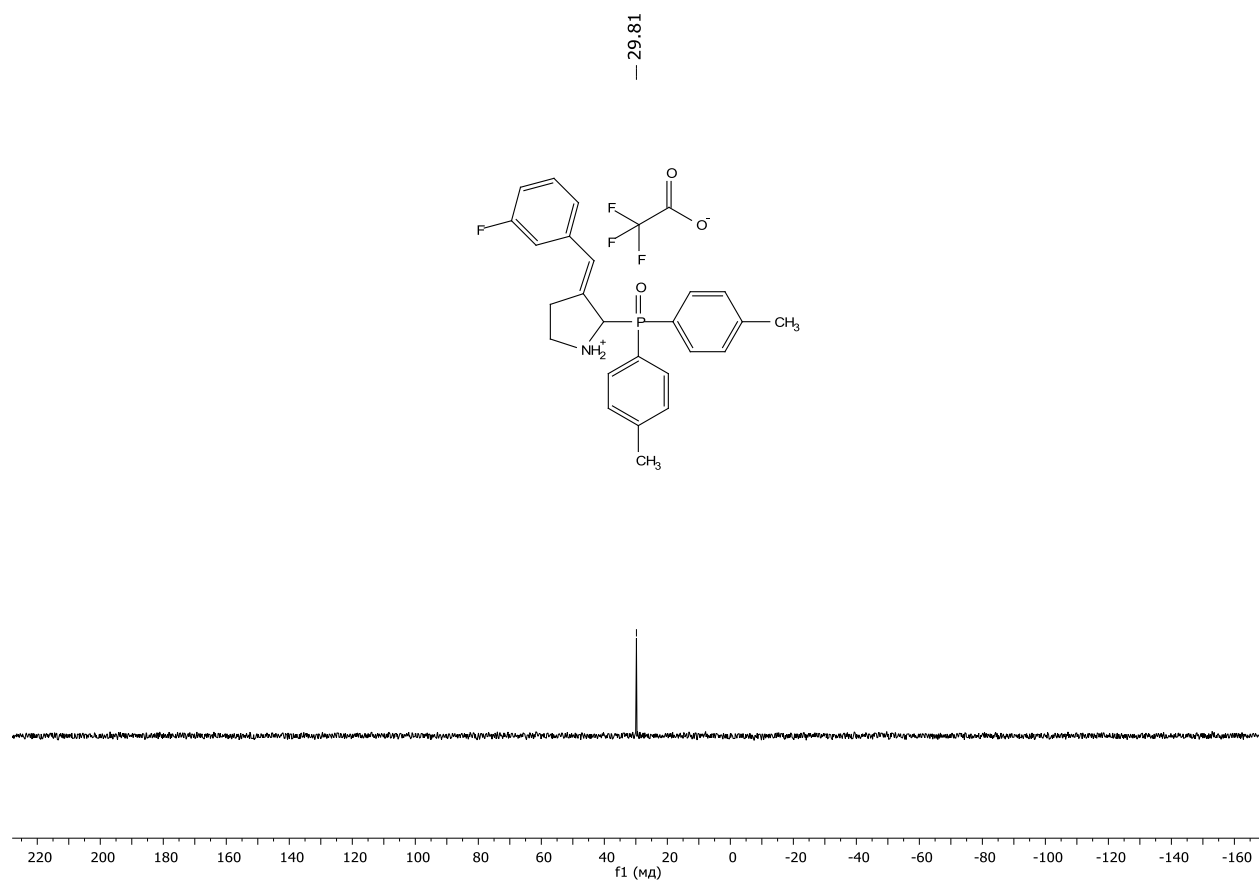


Figure S27. $^{31}\text{P}\{^1\text{H}\}$ NMR ($\text{DMSO-}d_6$, 161 MHz) spectrum of the compound 3ah

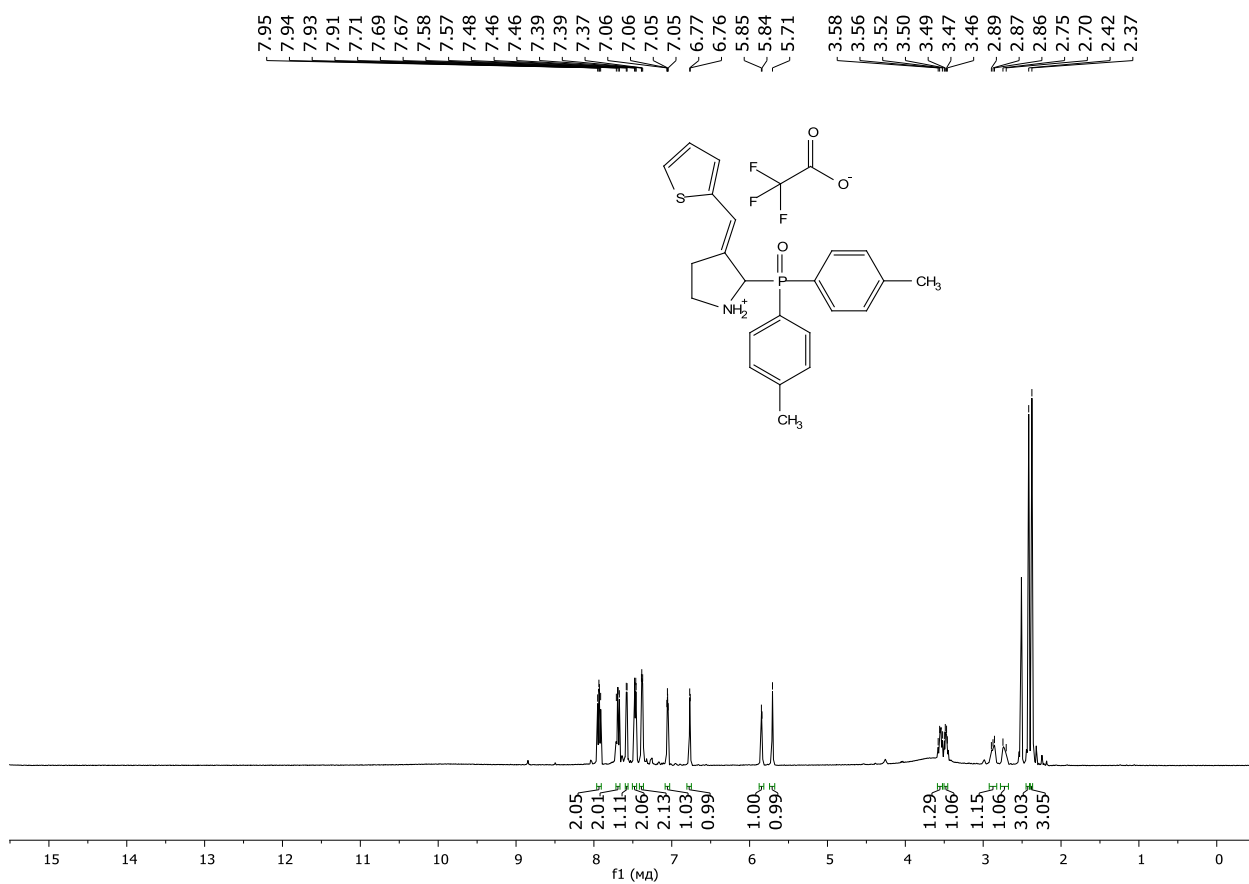


Figure S28. ¹H NMR (DMSO-*d*₆, 600 MHz) spectrum of the compound 3ai

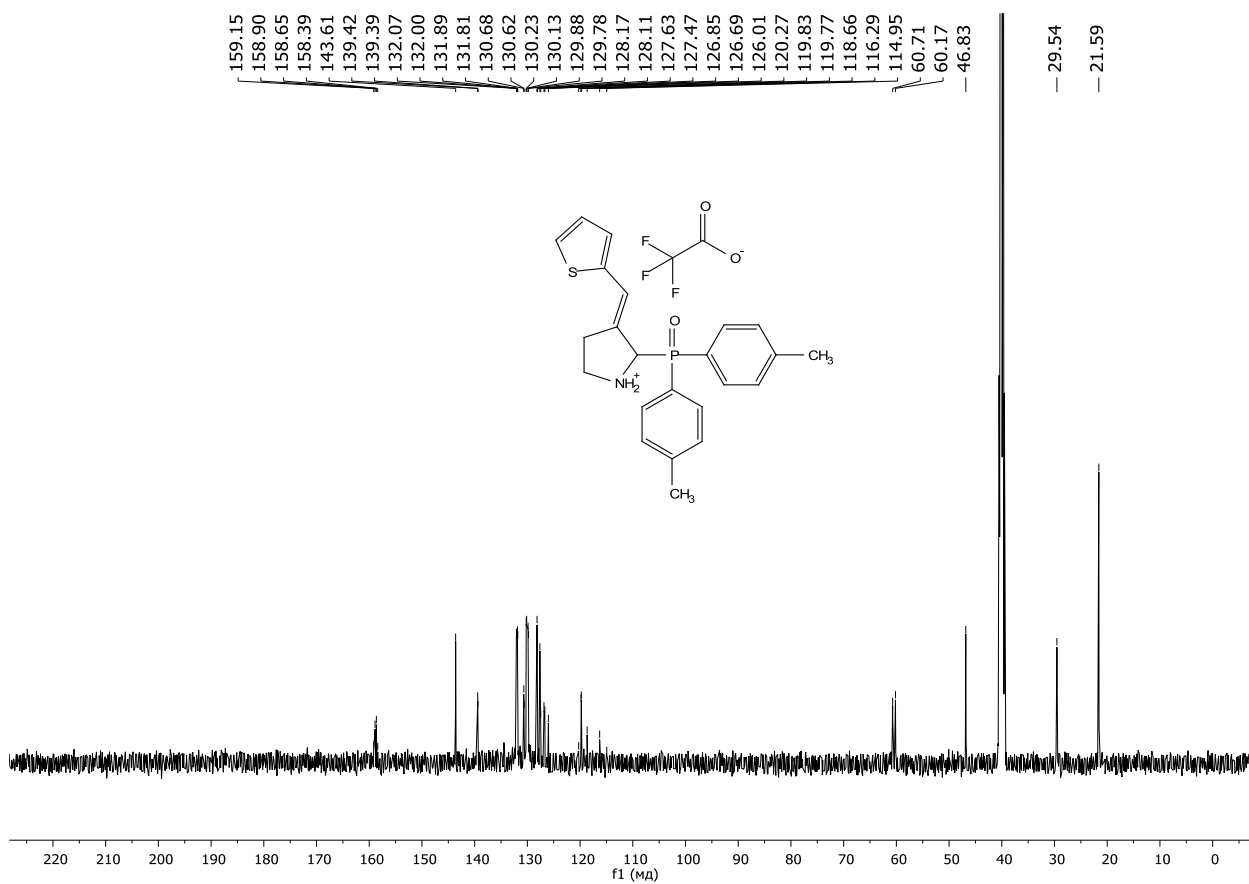


Figure S29. ¹³C{¹H} NMR (DMSO-*d*₆, 150 MHz) spectrum of the compound 3ai

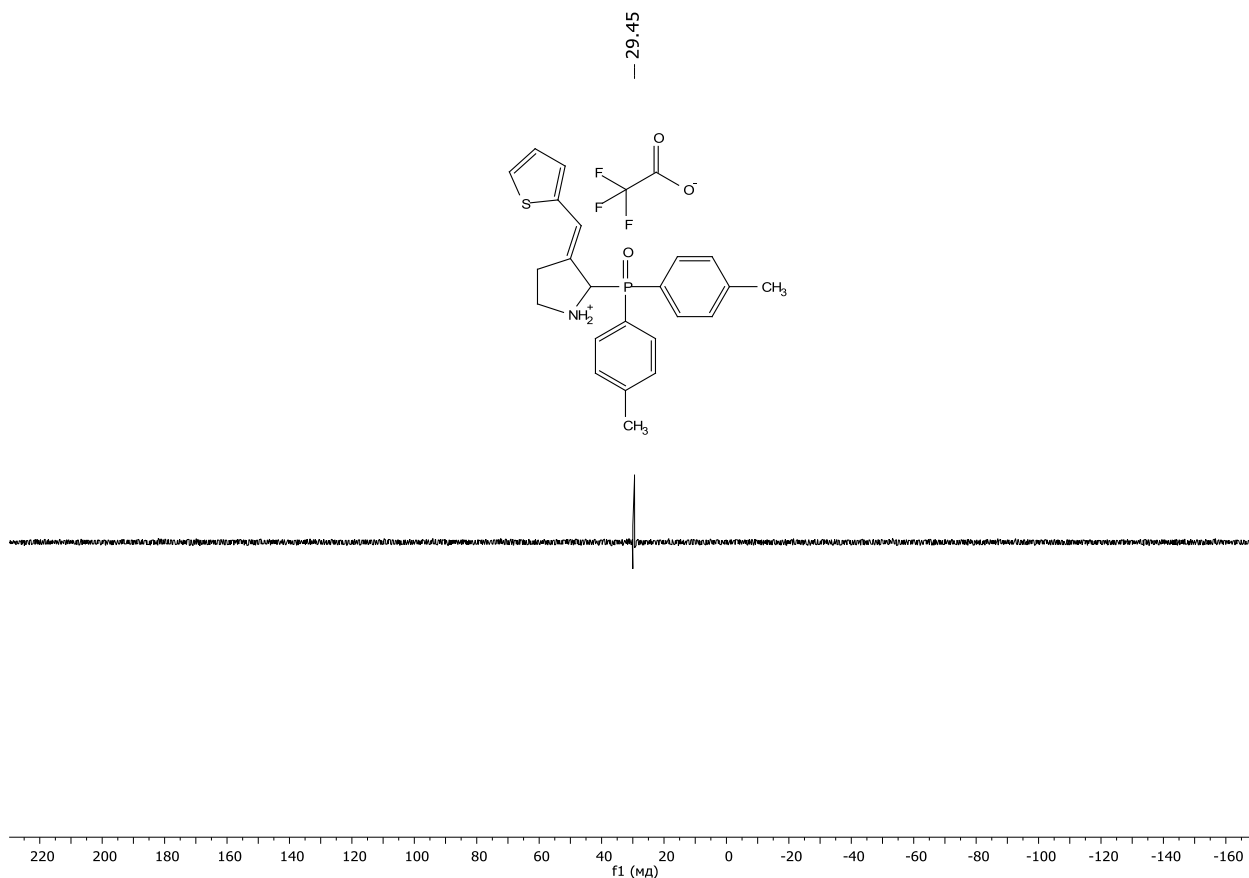


Figure S30. $^{31}\text{P}\{^1\text{H}\}$ NMR ($\text{DMSO-}d_6$, 161 MHz) spectrum of the compound **3ai**

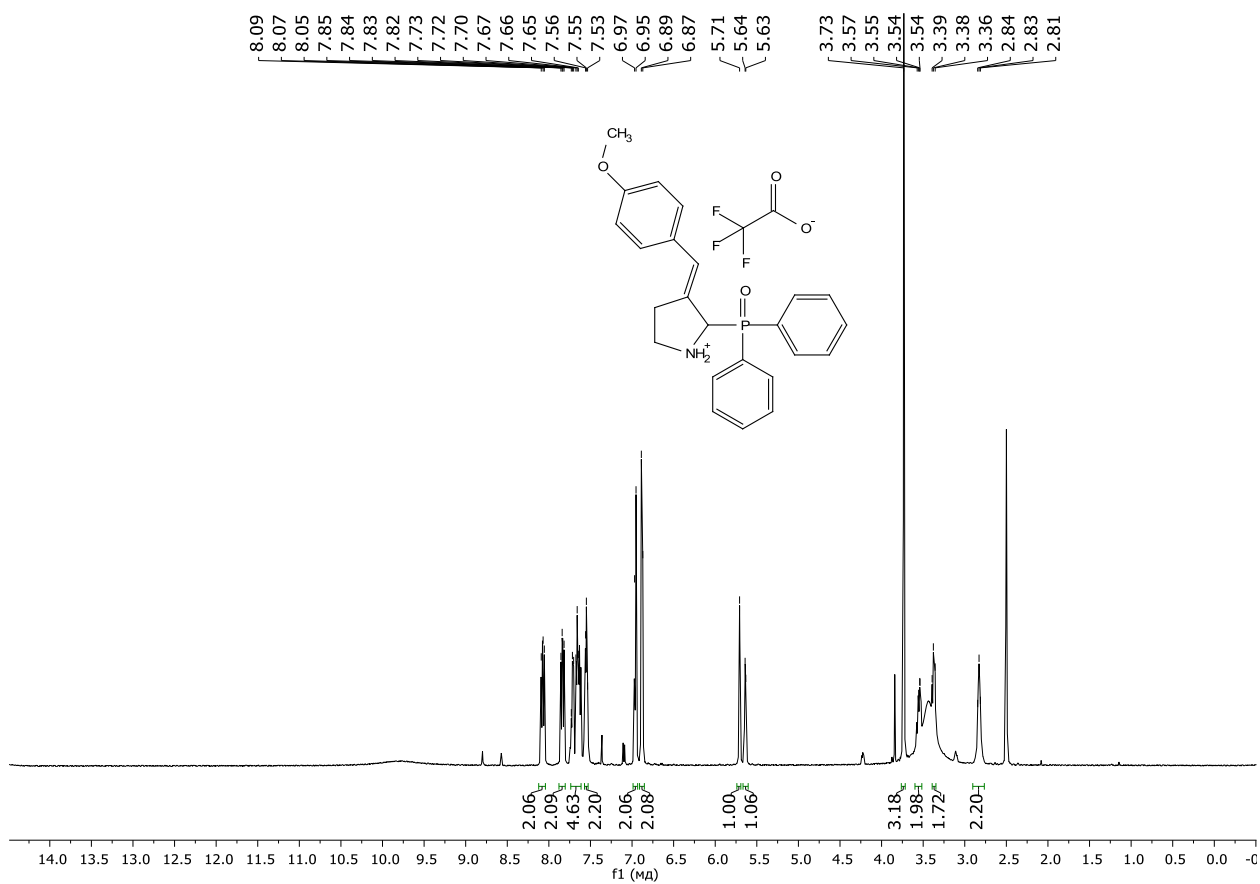


Figure S31. ^1H NMR ($\text{DMSO-}d_6$, 600 MHz) spectrum of the compound **3aj**

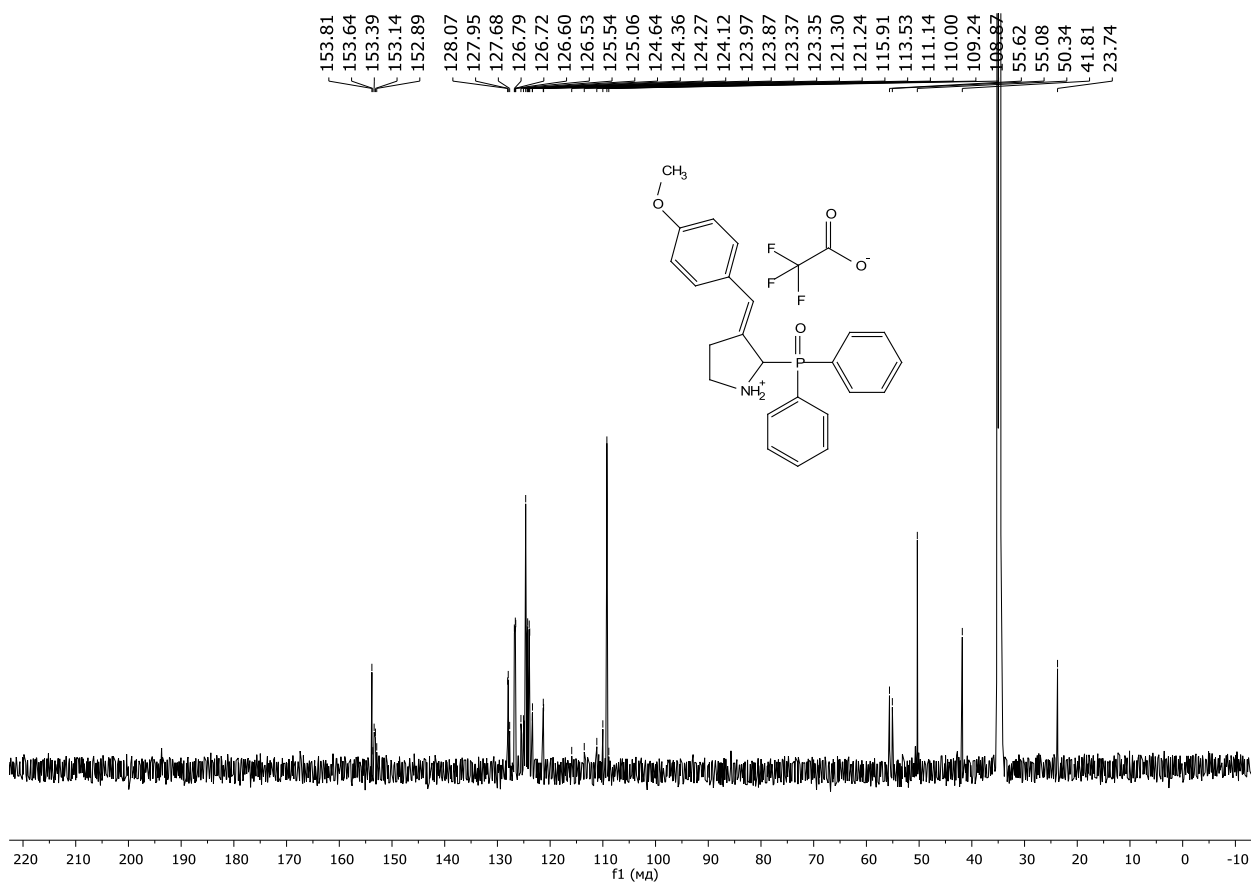


Figure S32. $^{13}\text{C}\{^1\text{H}\}$ NMR (DMSO- d_6 , 150 MHz) spectrum of the compound 3aj

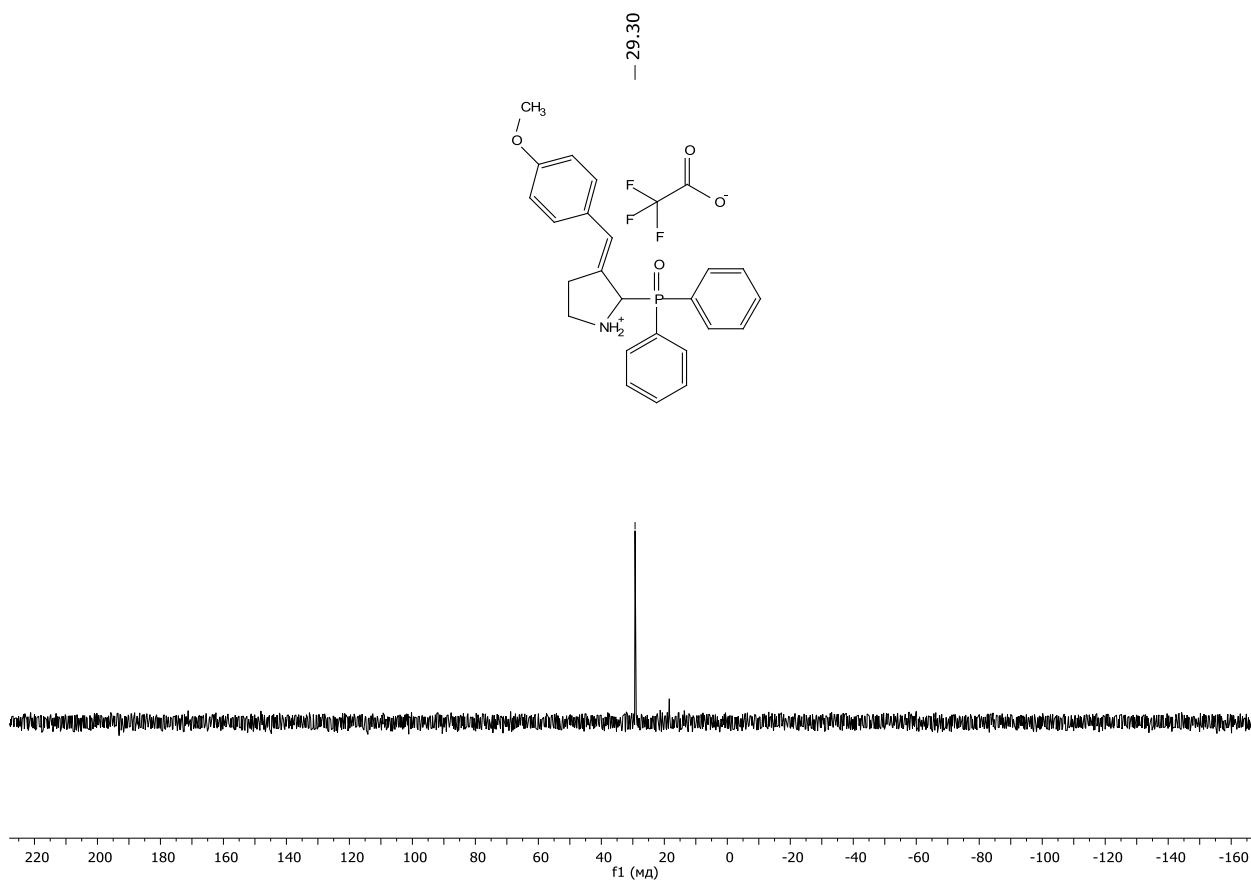
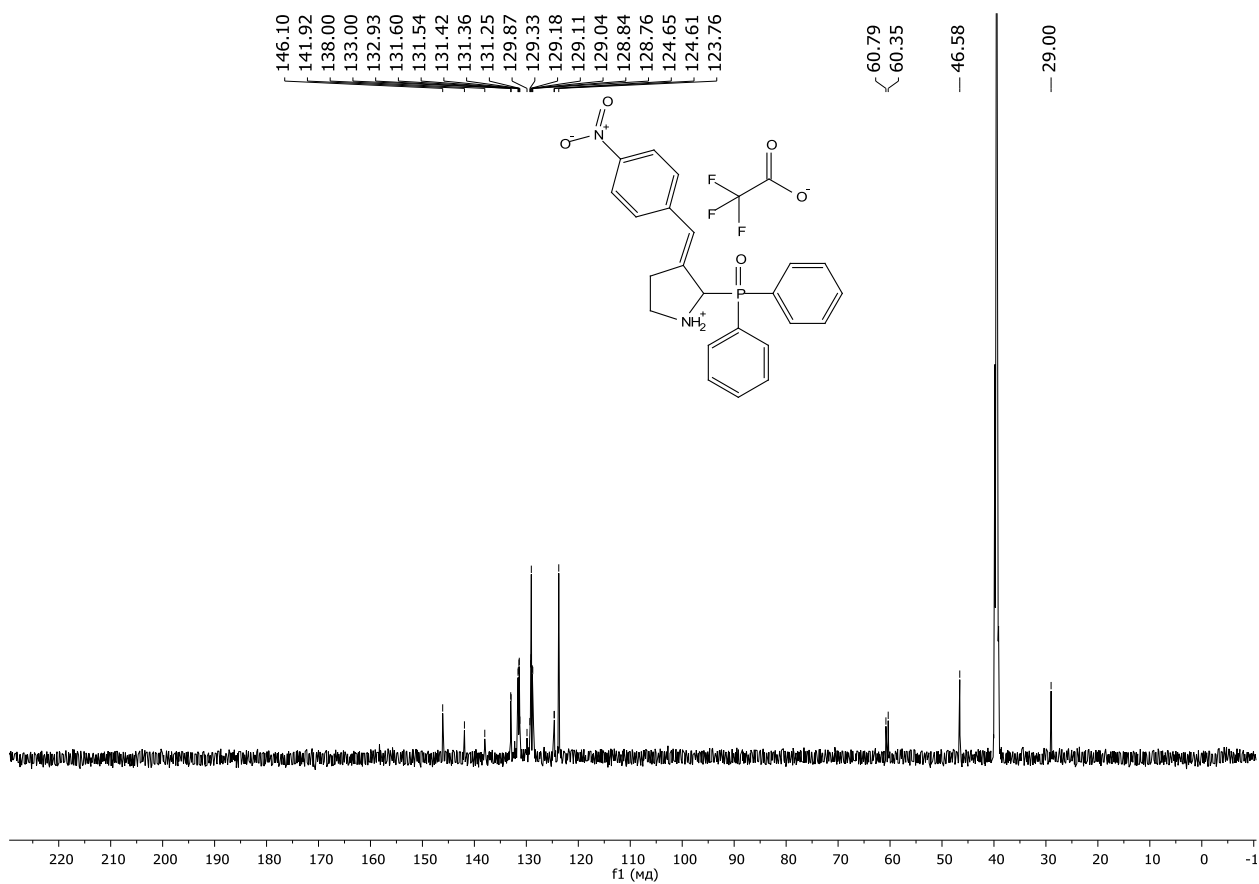
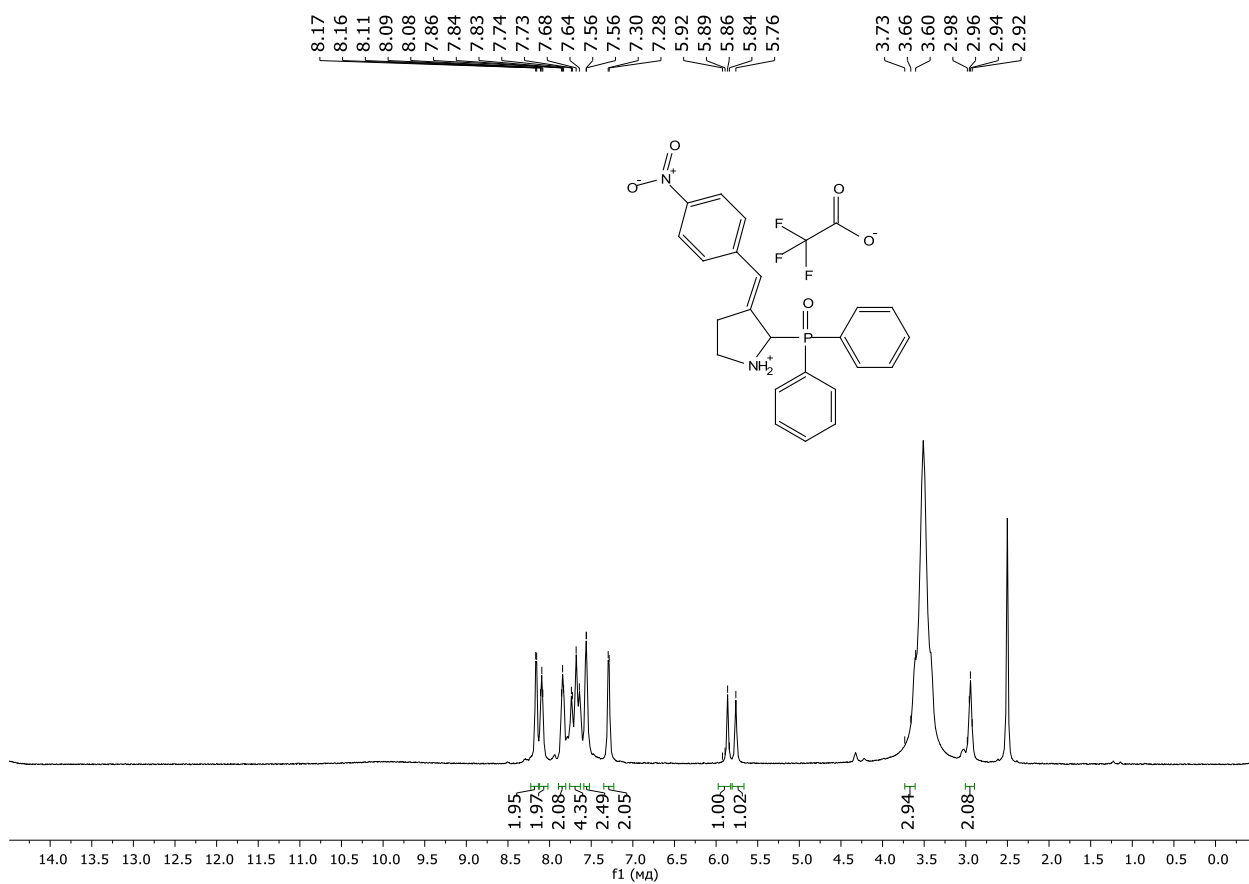


Figure S33. $^{31}\text{P}\{^1\text{H}\}$ NMR (DMSO- d_6 , 161 MHz) spectrum of the compound 3aj



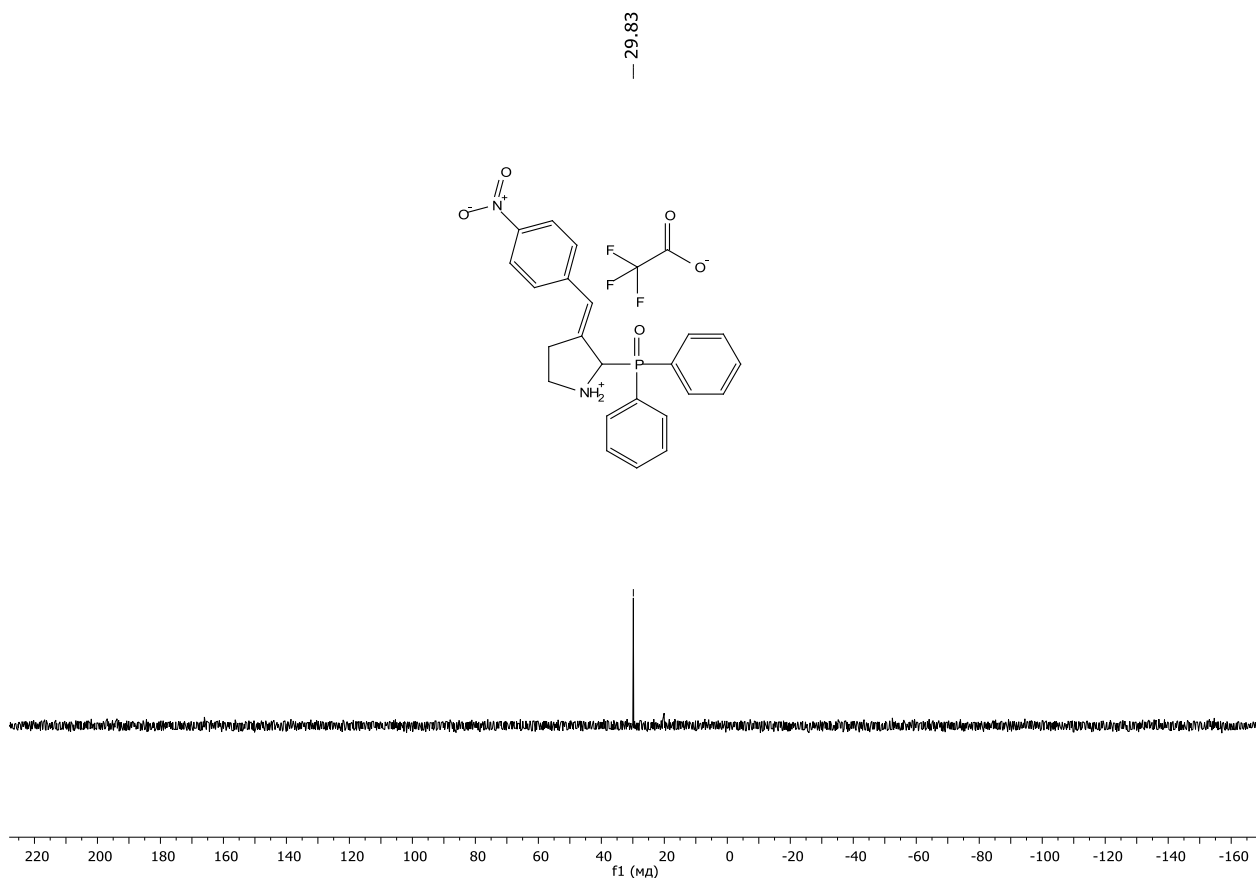


Figure S36. $^{31}\text{P}\{^1\text{H}\}$ NMR ($\text{DMSO-}d_6$, 161 MHz) spectrum of the compound **3ak**

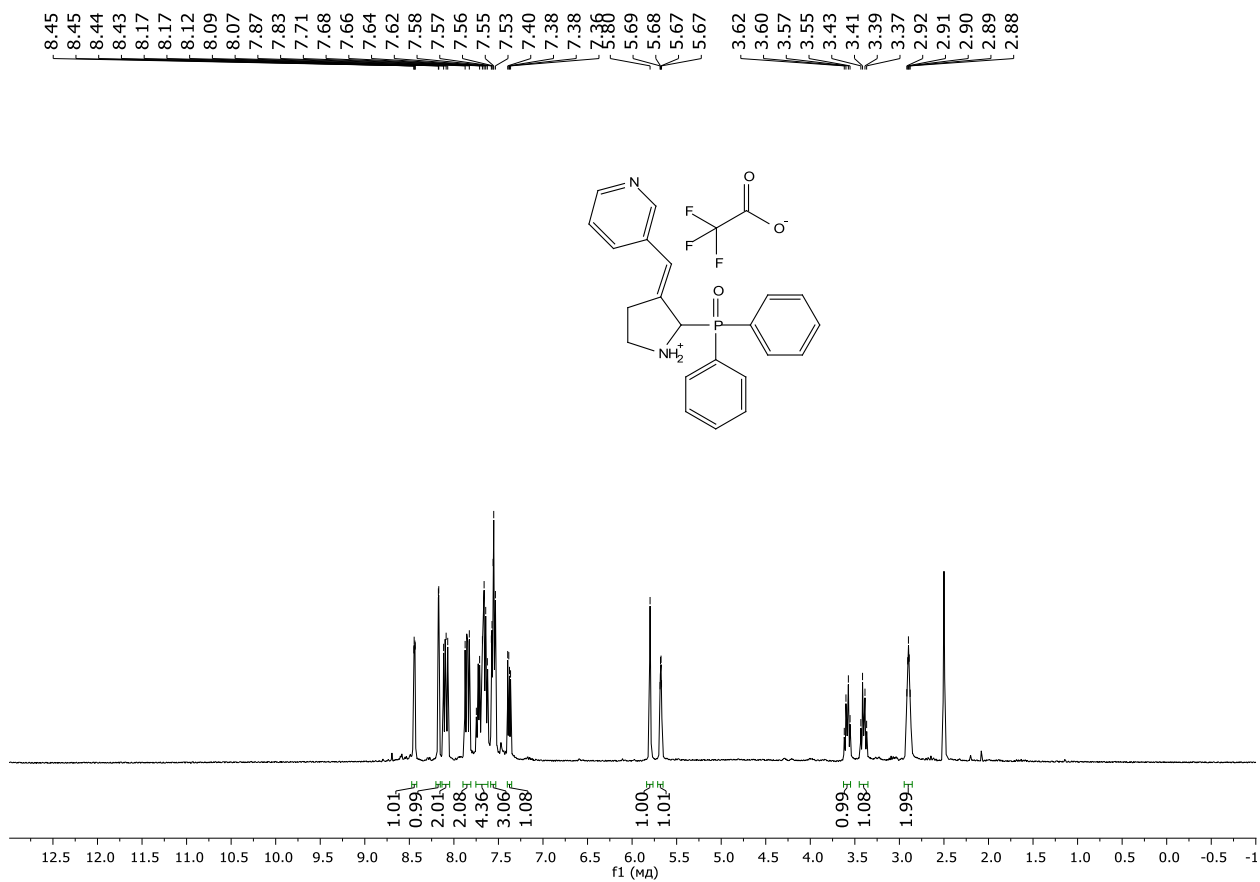


Figure S37. ^1H NMR ($\text{DMSO-}d_6$, 600 MHz) spectrum of the compound **3al**

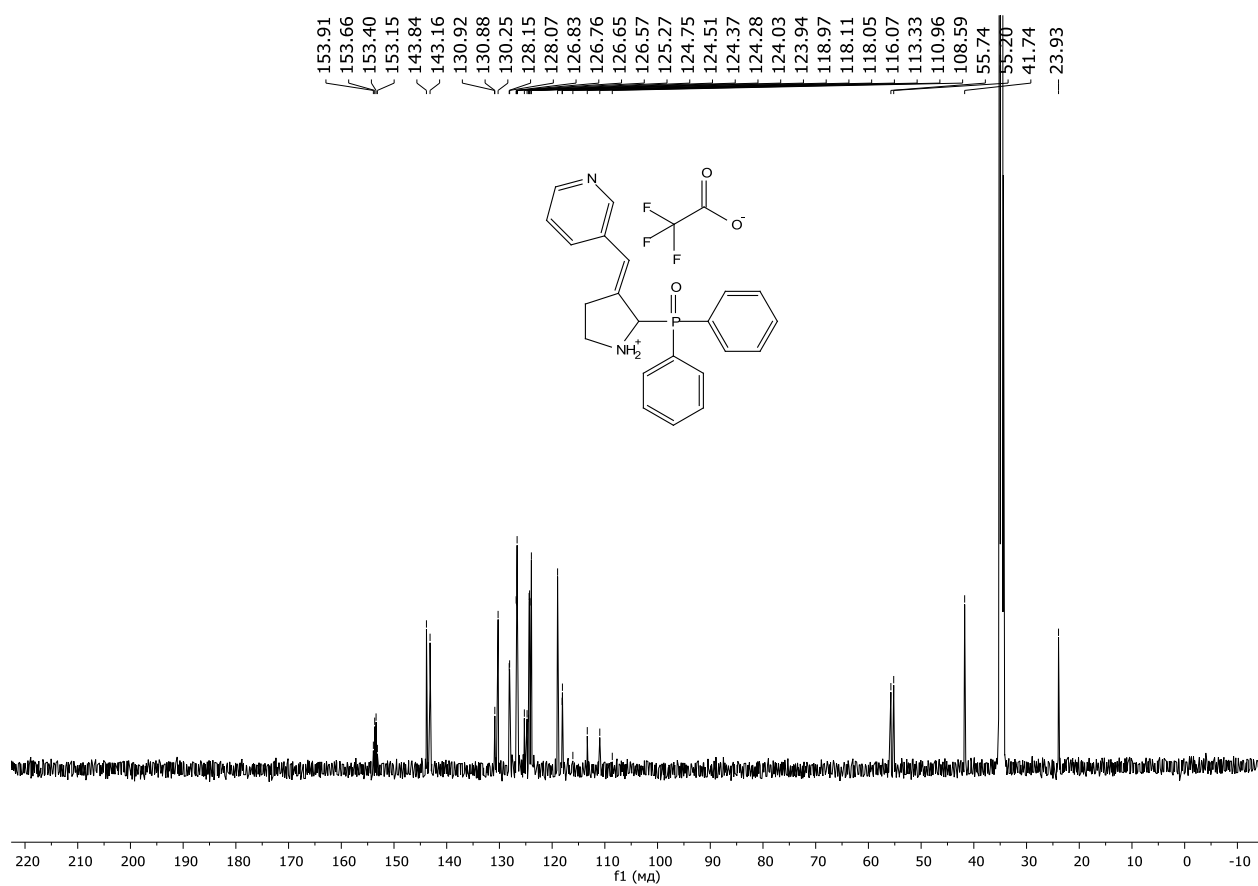


Figure S38. $^{13}\text{C}\{^1\text{H}\}$ NMR (DMSO- d_6 , 150 MHz) spectrum of the compound 3aI

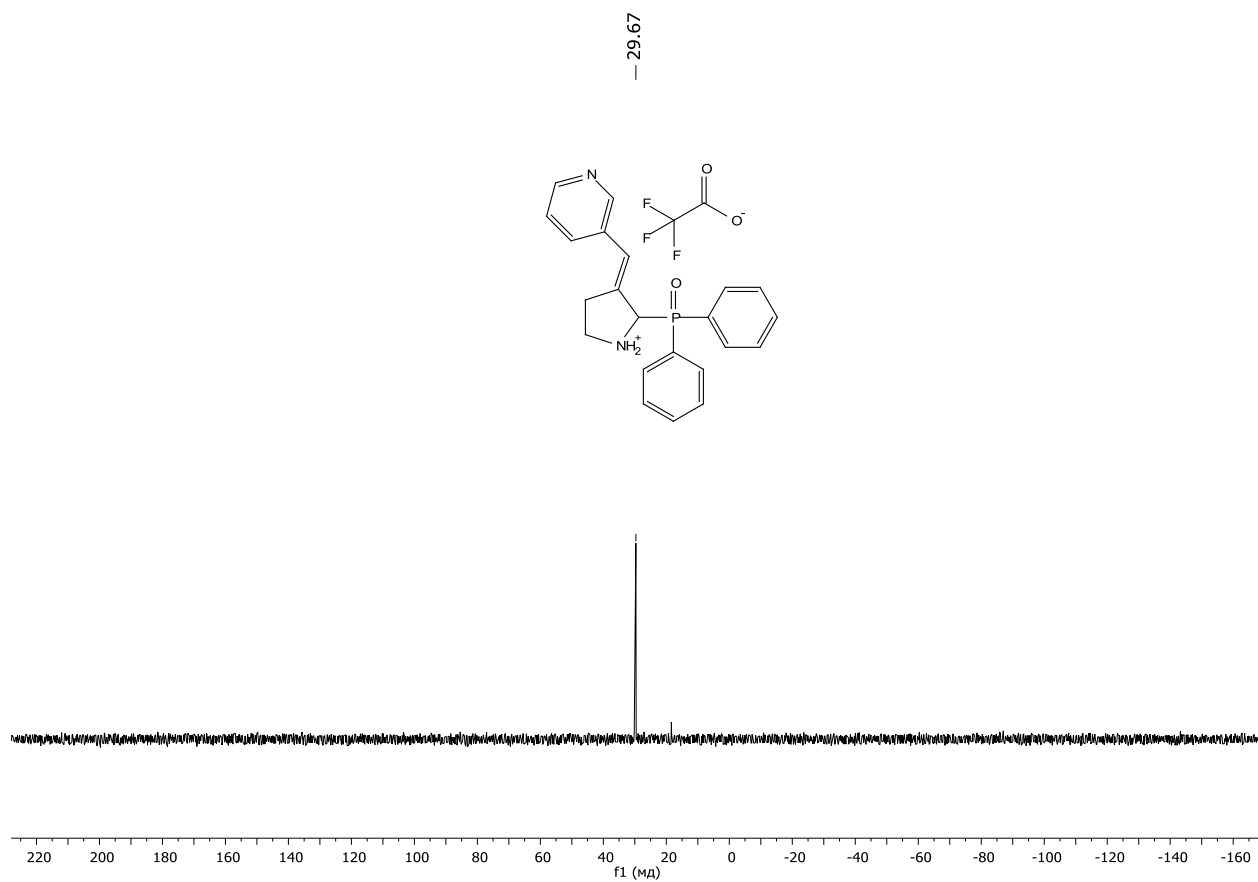


Figure S39. $^{31}\text{P}\{^1\text{H}\}$ NMR (DMSO- d_6 , 161 MHz) spectrum of the compound 3aI

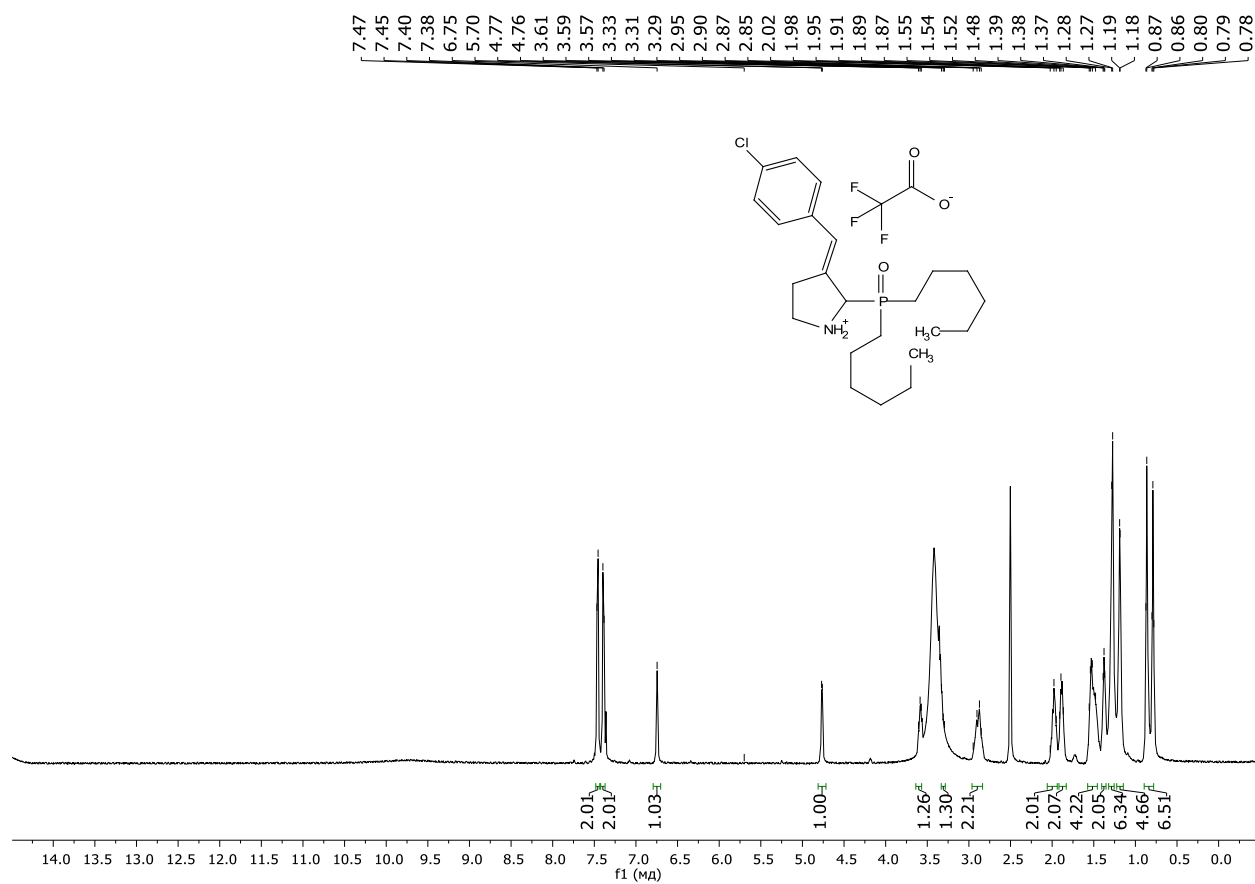


Figure S40. ¹H NMR (DMSO-*d*₆, 600 MHz) spectrum of the compound **3am**

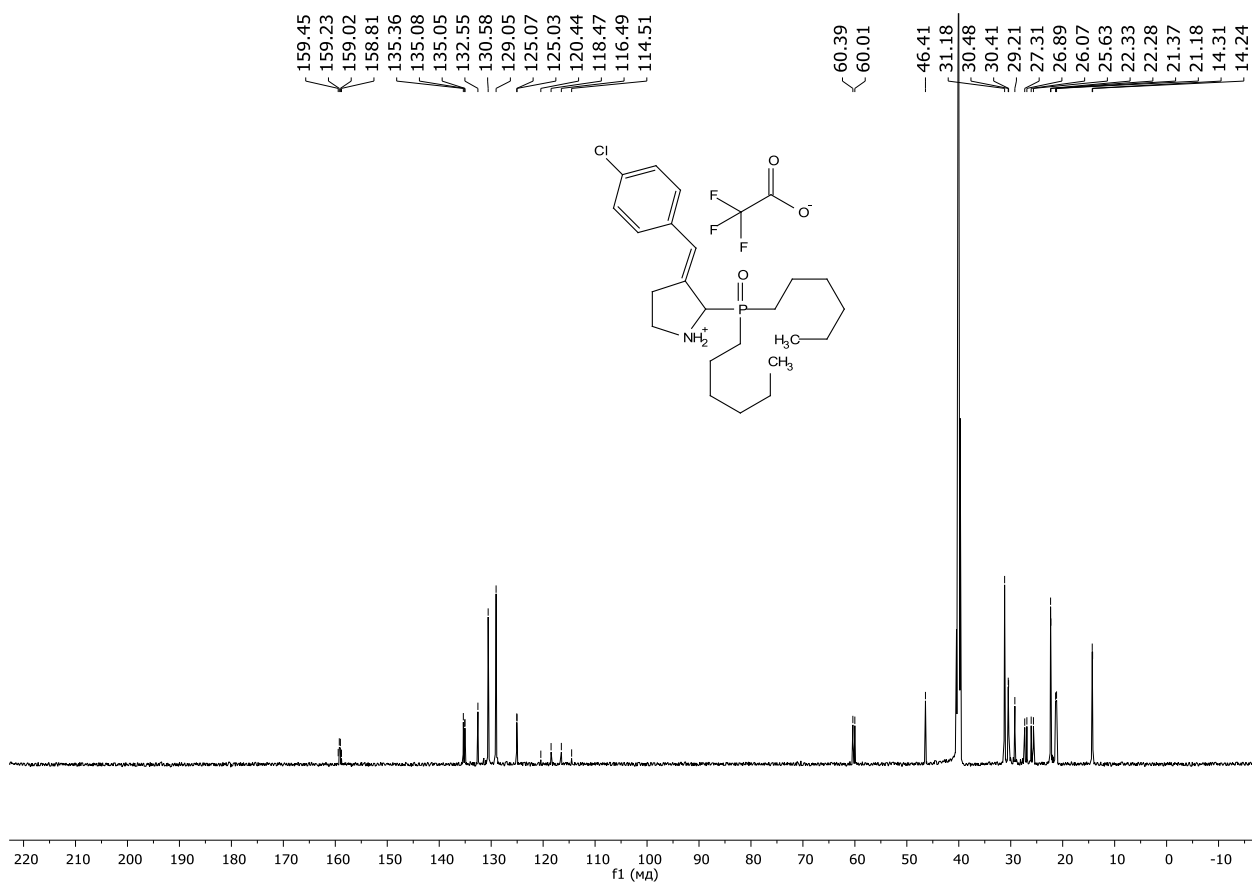


Figure S41. ¹³C{¹H} NMR (DMSO-*d*₆, 150 MHz) spectrum of the compound **3am**

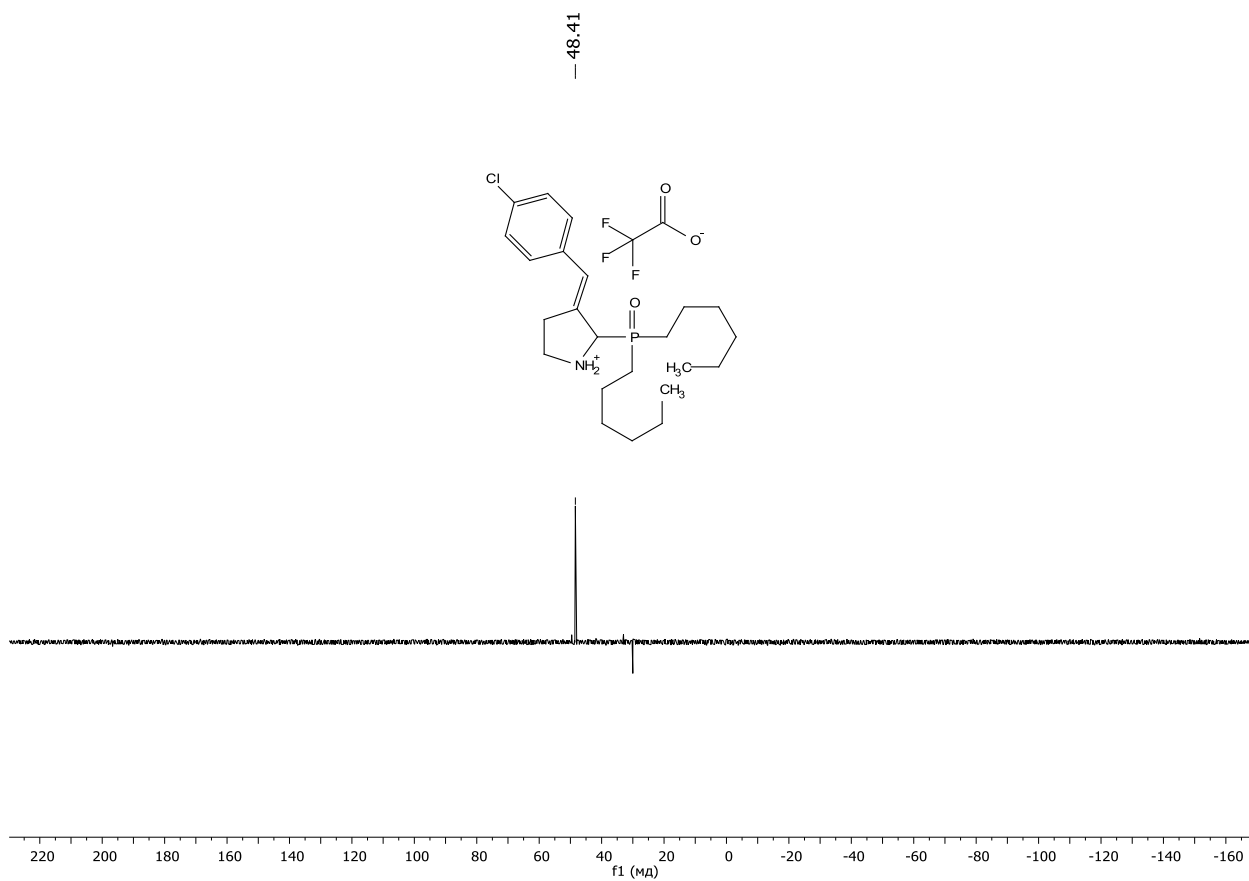


Figure S42. $^{31}\text{P}\{^1\text{H}\}$ NMR (DMSO- d_6 , 161 MHz) spectrum of the compound **3am**

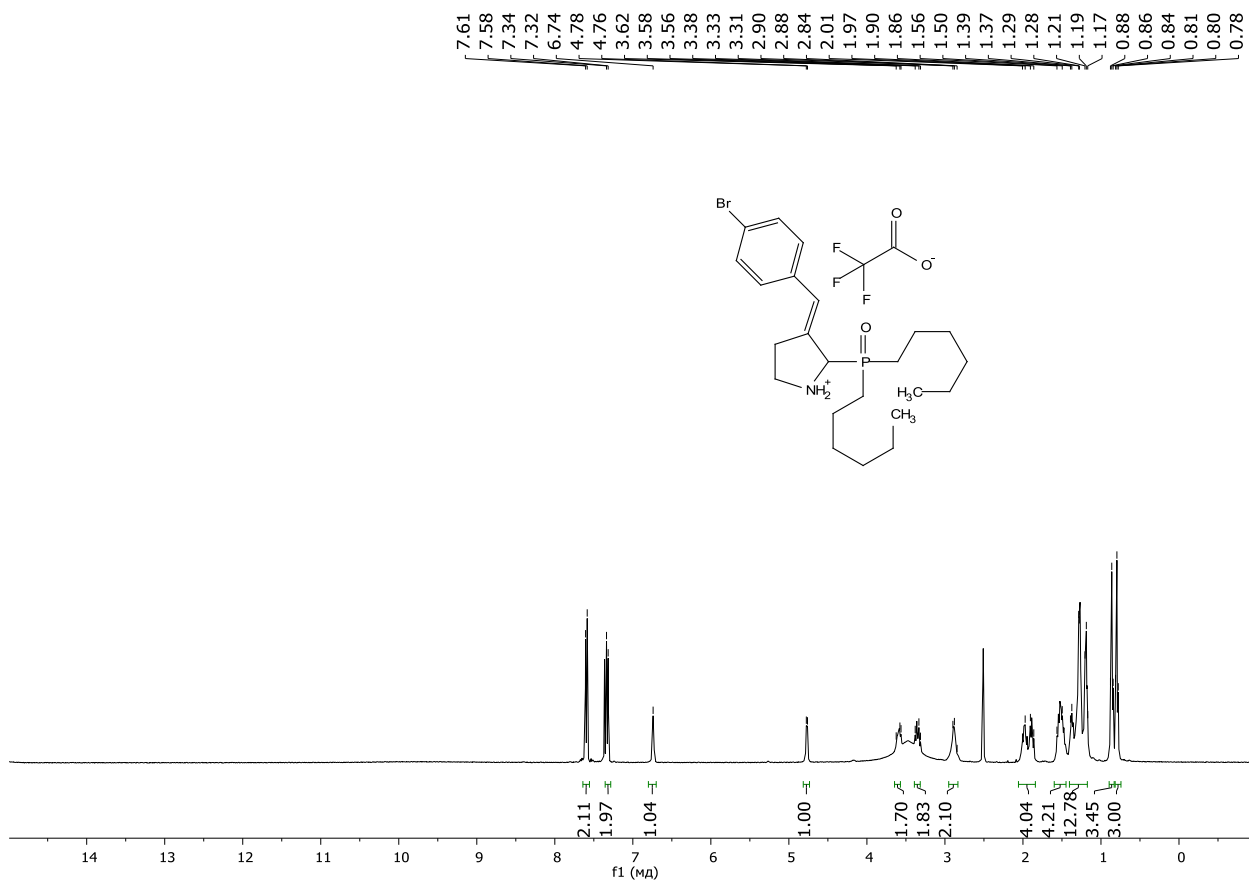


Figure S43. ^1H NMR (DMSO- d_6 , 600 MHz) spectrum of the compound **3an**

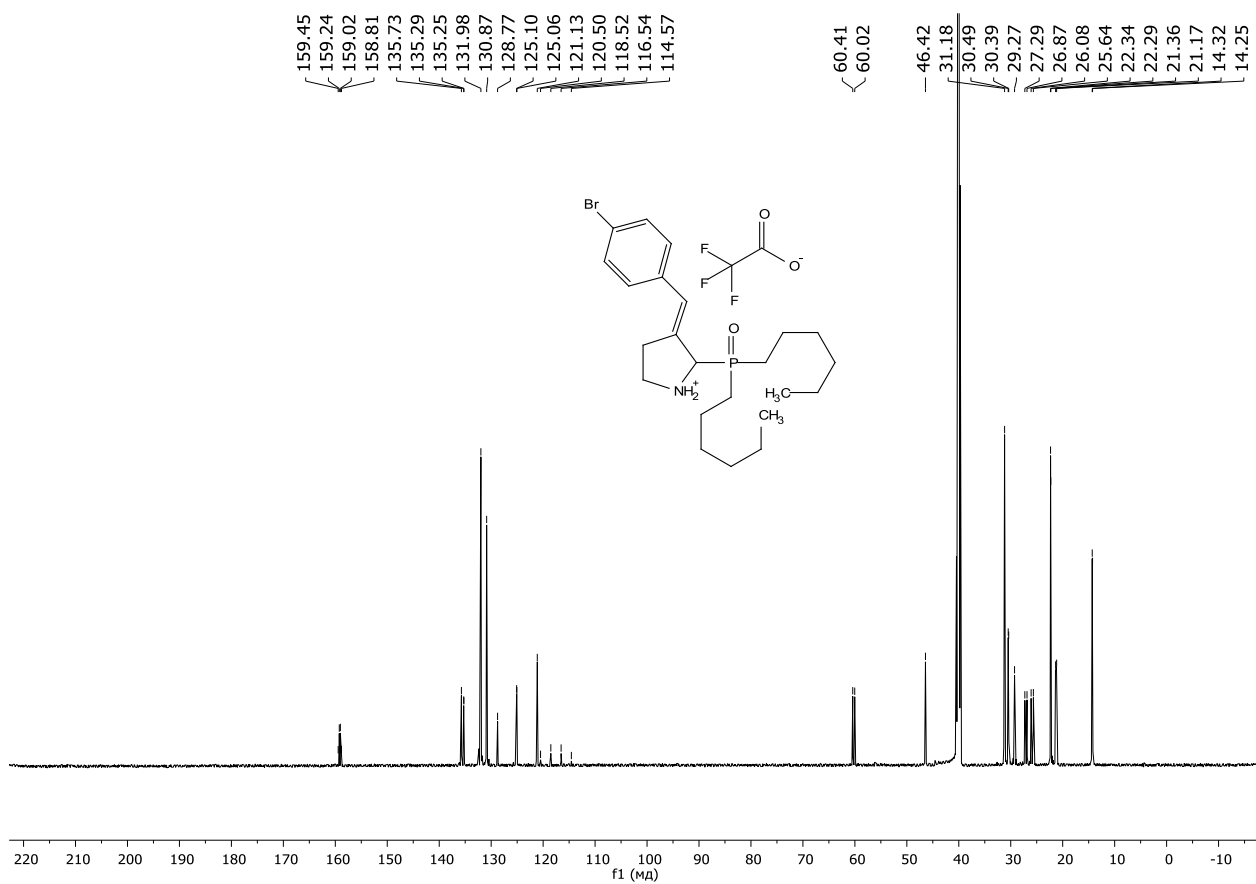


Figure S44. $^{13}\text{C}\{^1\text{H}\}$ NMR (DMSO- d_6 , 150 MHz) spectrum of the compound **3an**

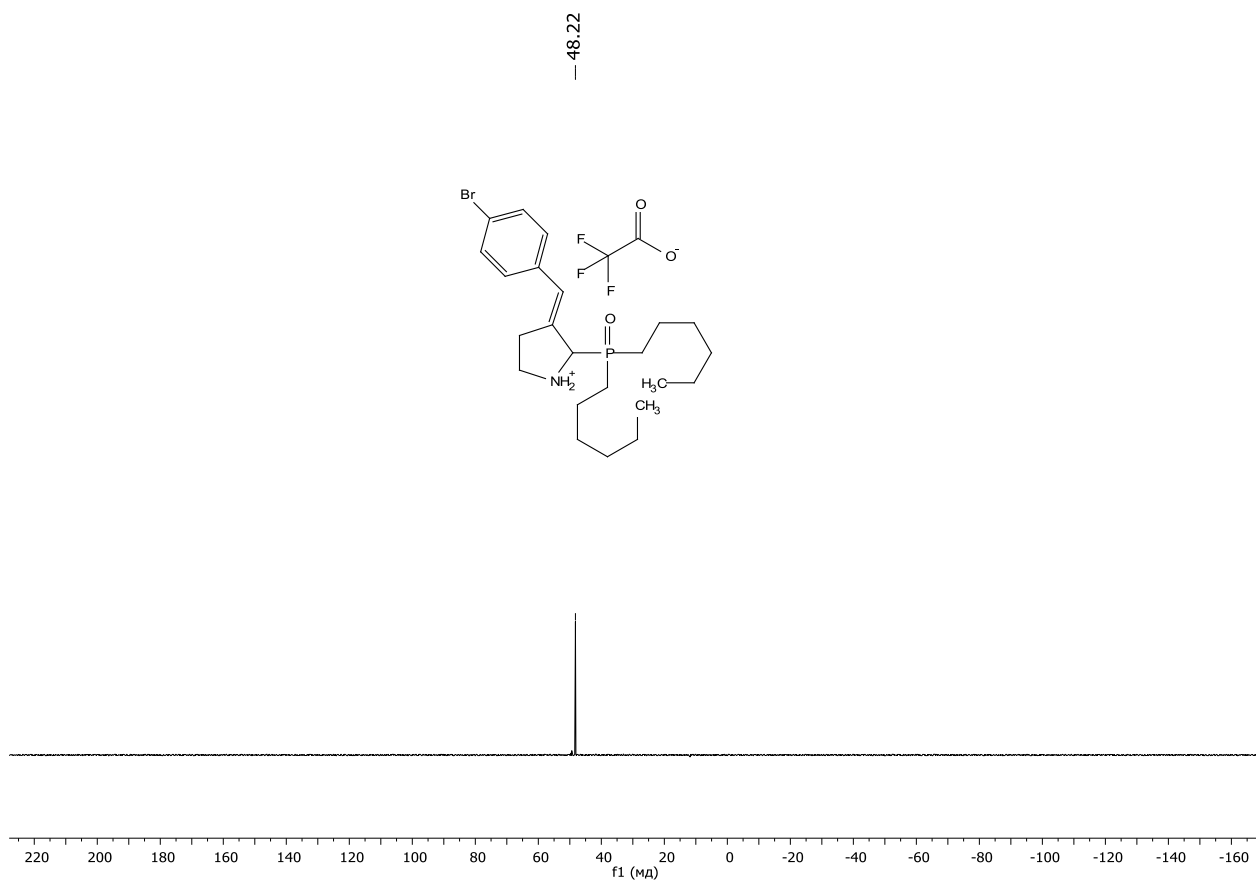


Figure S45. $^{31}\text{P}\{^1\text{H}\}$ NMR (DMSO- d_6 , 161 MHz) spectrum of the compound **3an**

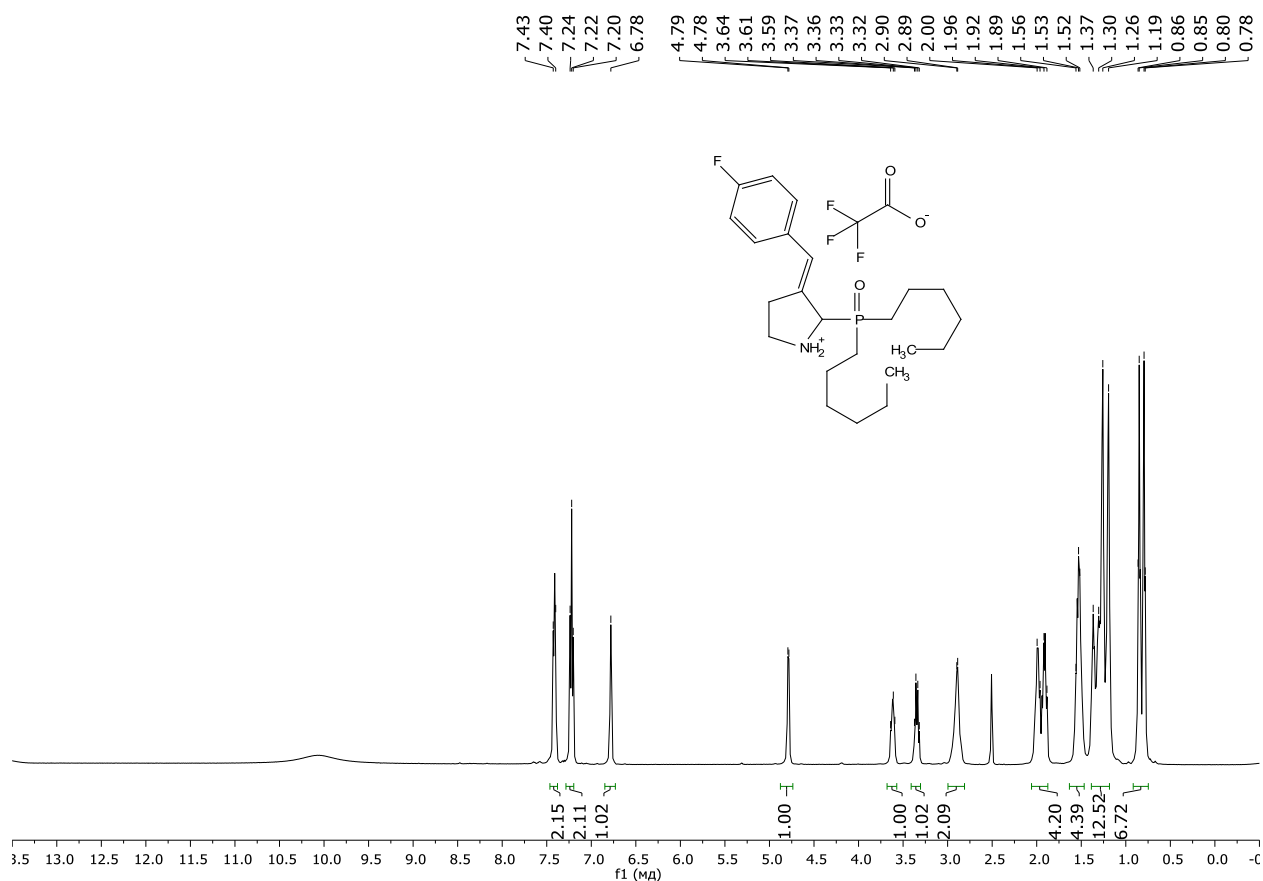


Figure S46. ^1H NMR (DMSO- d_6 , 600 MHz) spectrum of the compound 3ao

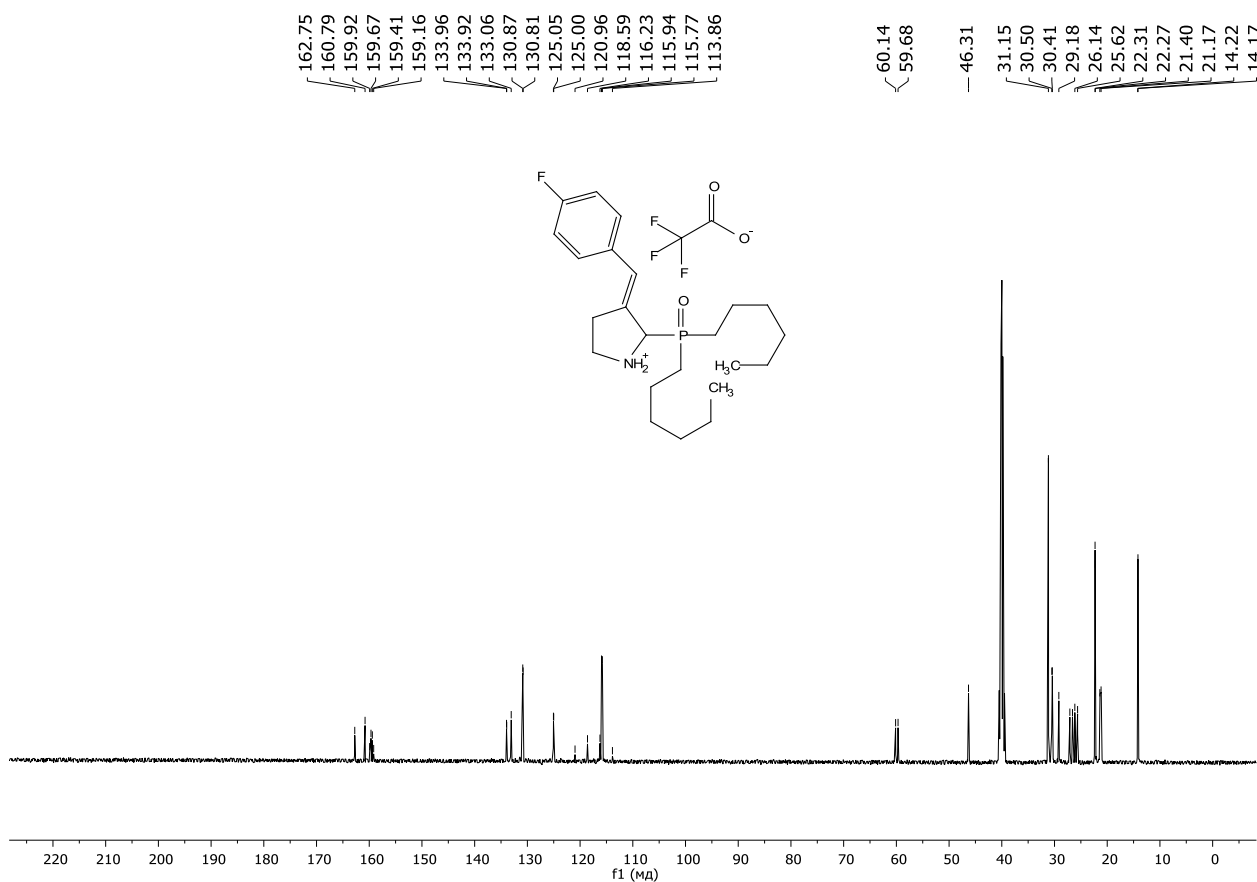


Figure S47. $^{13}\text{C}\{^1\text{H}\}$ NMR (DMSO- d_6 , 150 MHz) spectrum of the compound 3ao

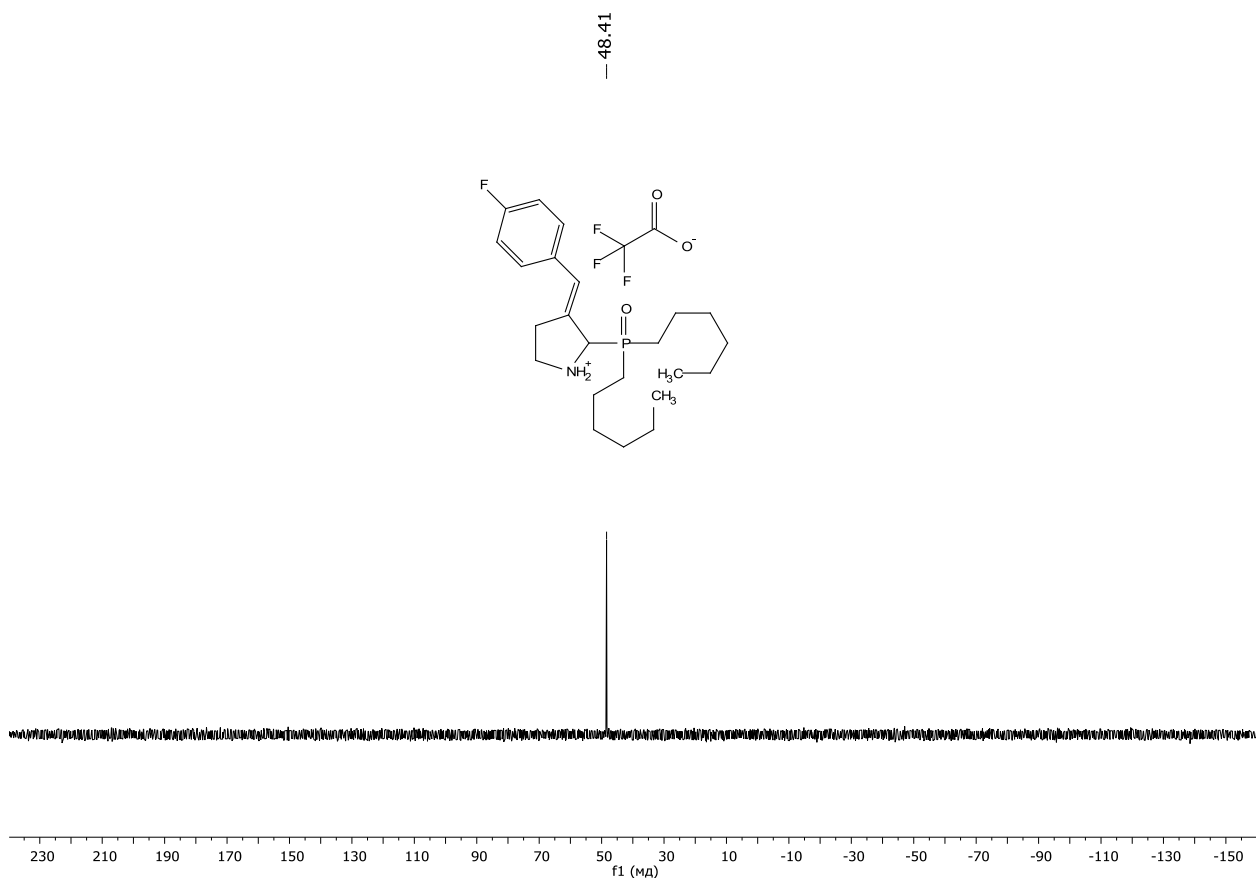


Figure S48. $^{31}\text{P}\{^1\text{H}\}$ NMR ($\text{DMSO-}d_6$, 161 MHz) spectrum of the compound **3ao**

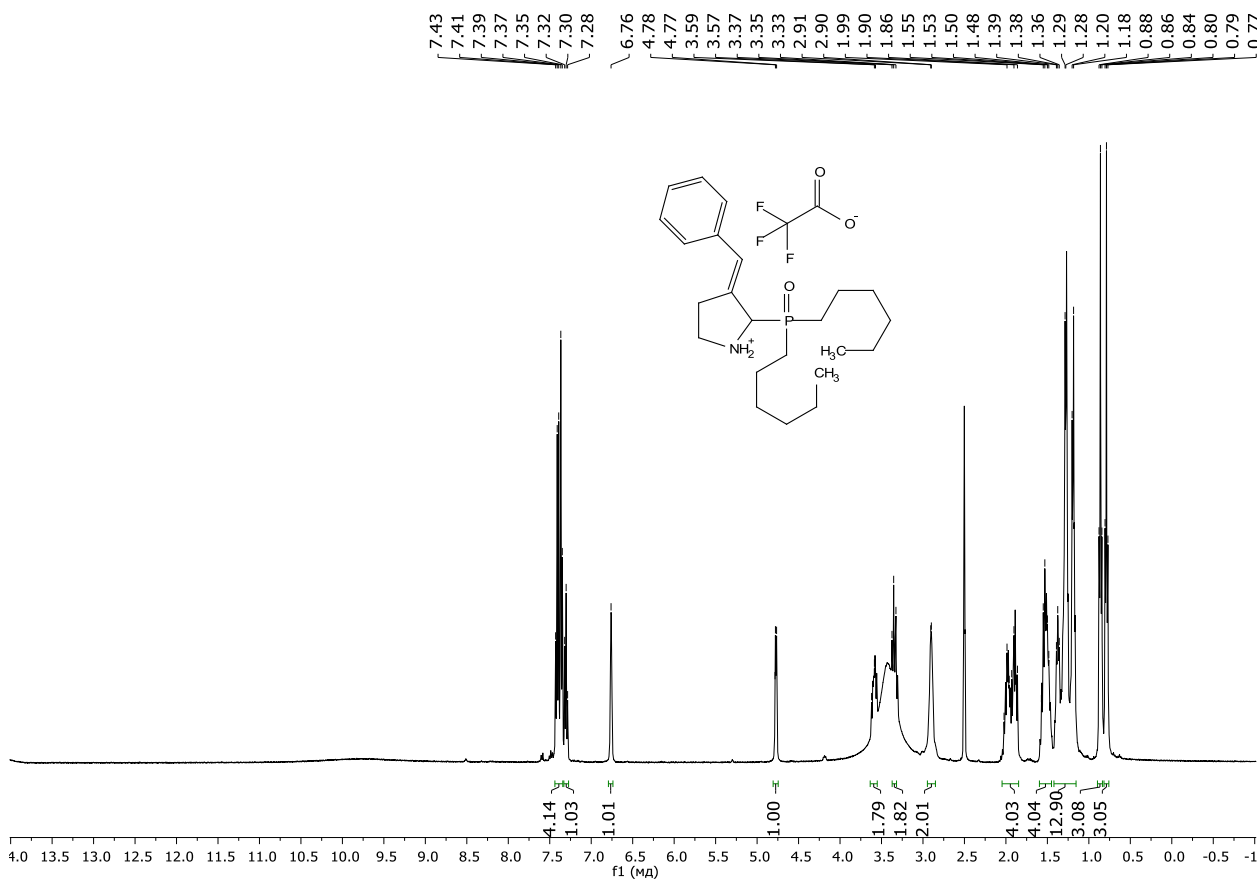


Figure S49. ^1H NMR ($\text{DMSO-}d_6$, 600 MHz) spectrum of the compound **3ap**

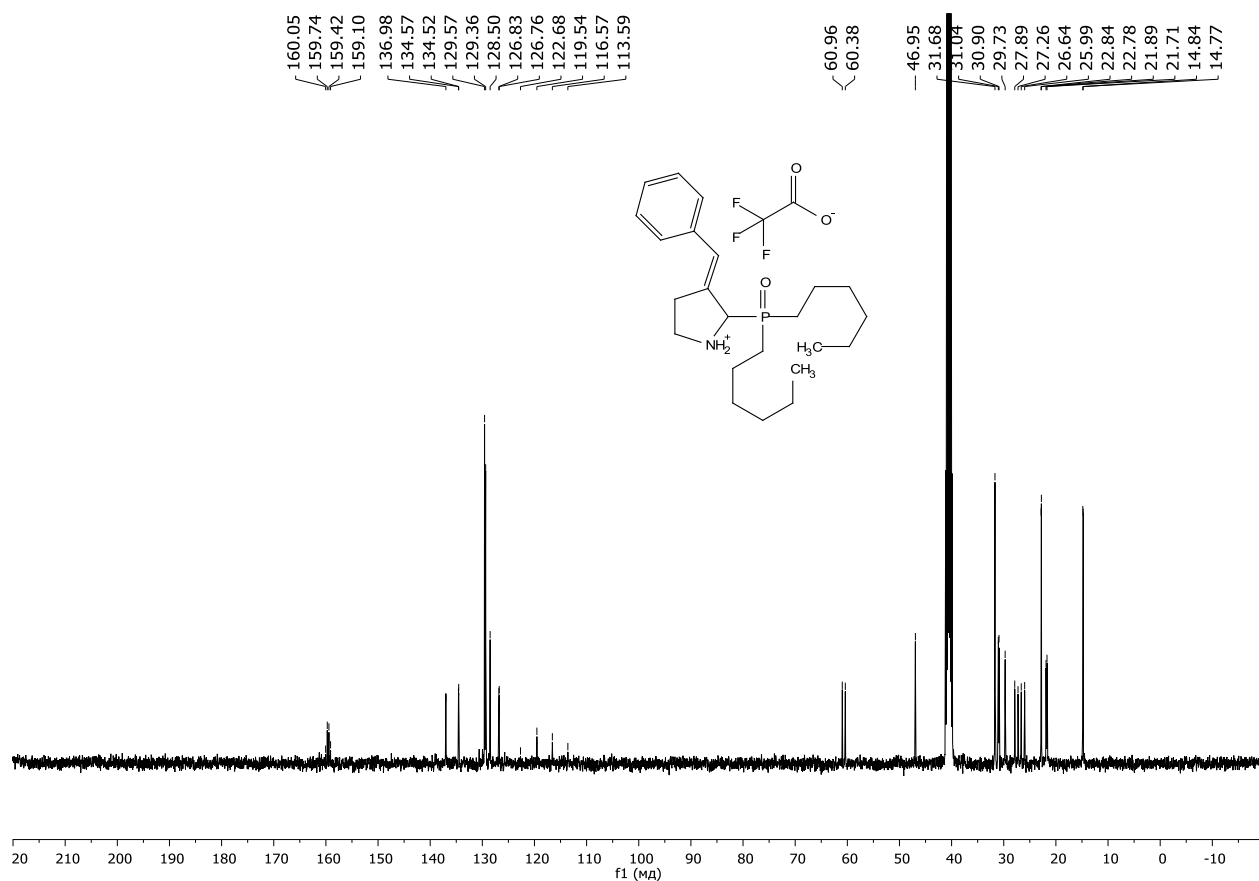


Figure S50. $^{13}\text{C}\{^1\text{H}\}$ NMR (DMSO- d_6 , 150 MHz) spectrum of the compound **3ap**

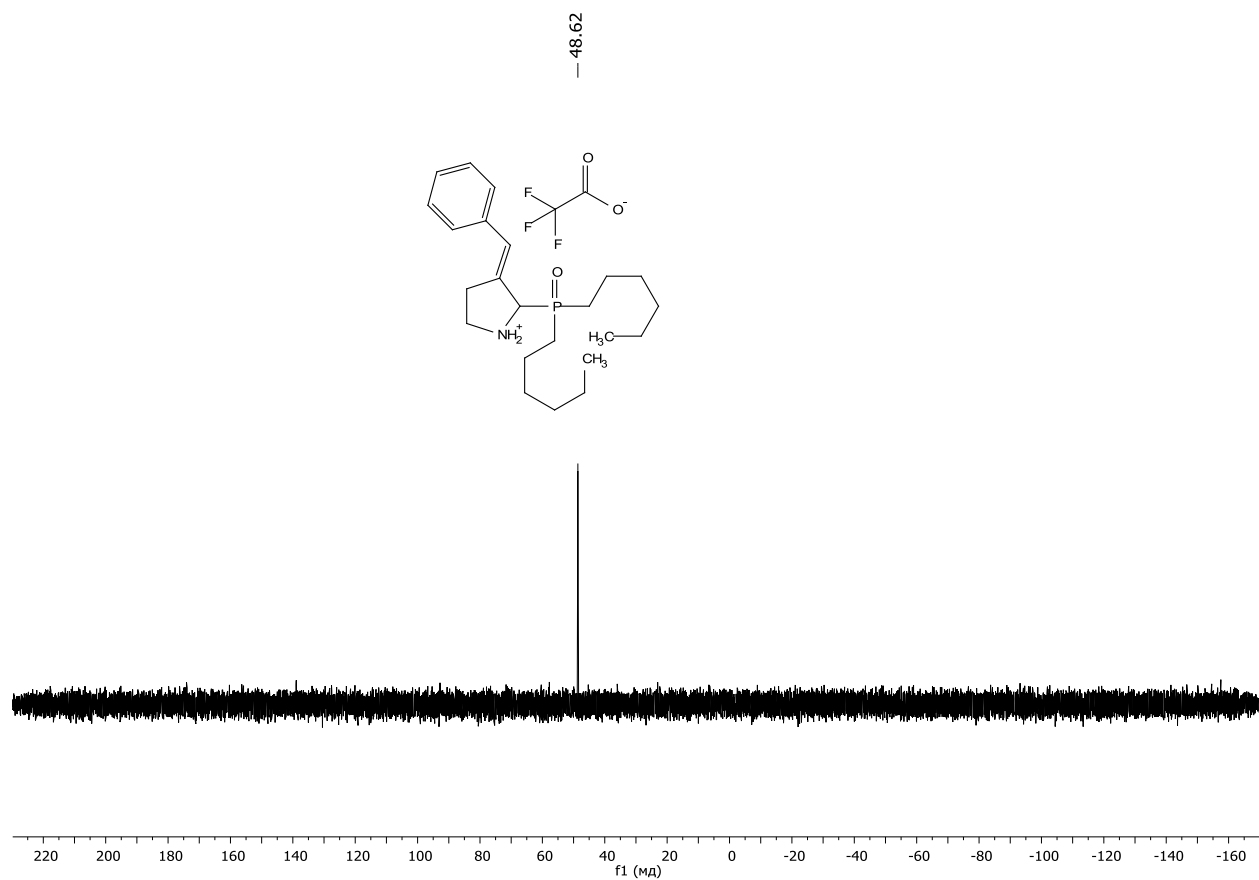


Figure S51. $^{31}\text{P}\{^1\text{H}\}$ NMR (DMSO- d_6 , 161 MHz) spectrum of the compound **3ap**

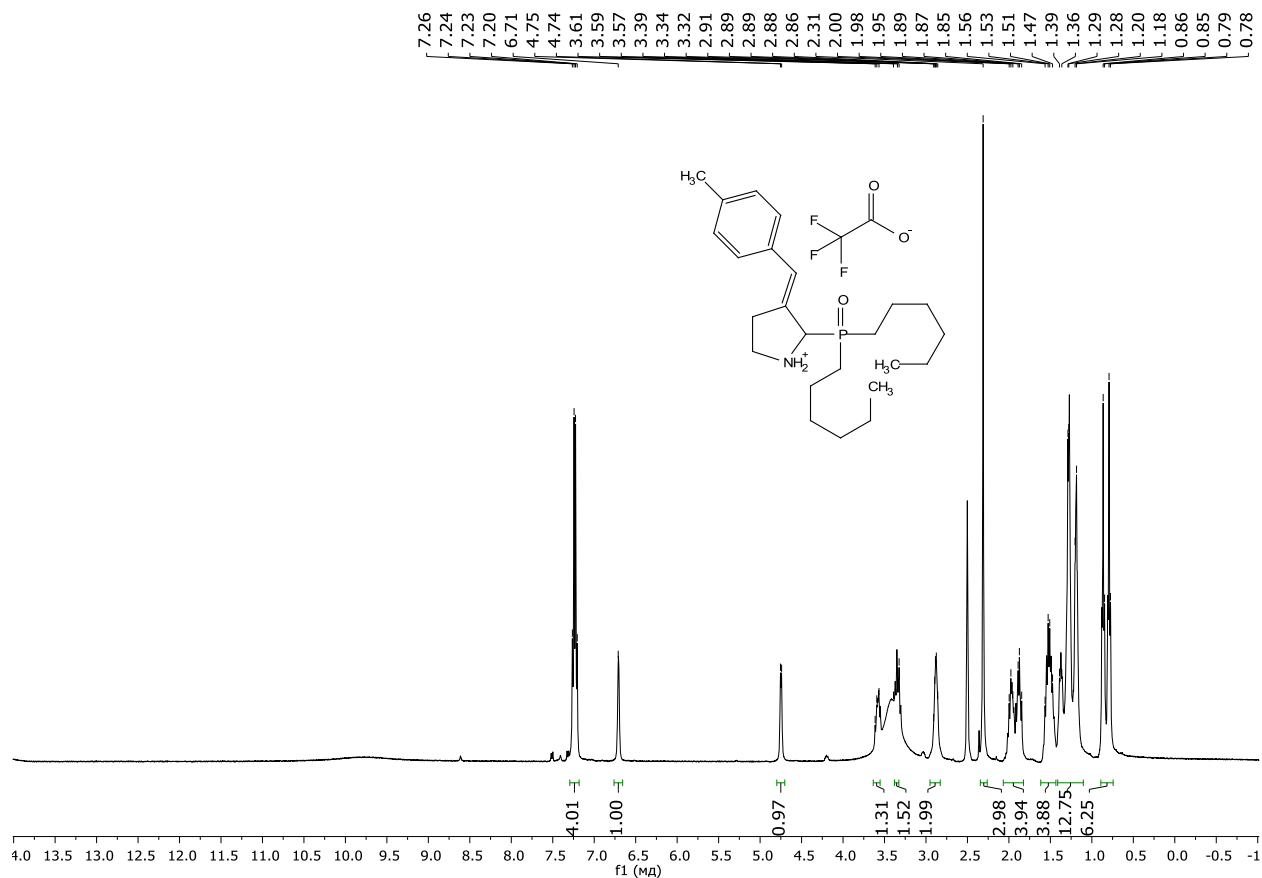


Figure S52. ¹H NMR (DMSO-*d*₆, 600 MHz) spectrum of the compound 3aq

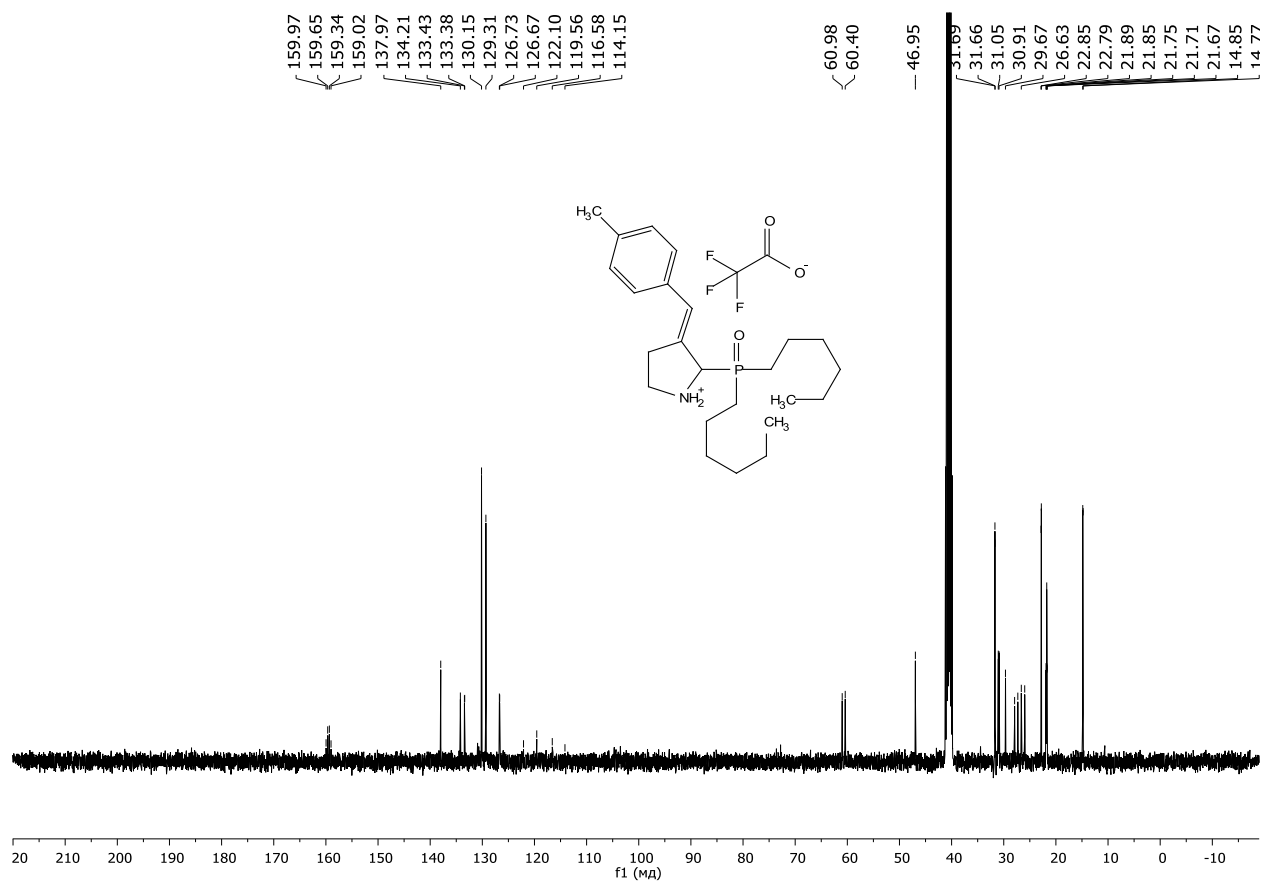


Figure S53. ¹³C{¹H} NMR (DMSO-*d*₆, 150 MHz) spectrum of the compound 3aq

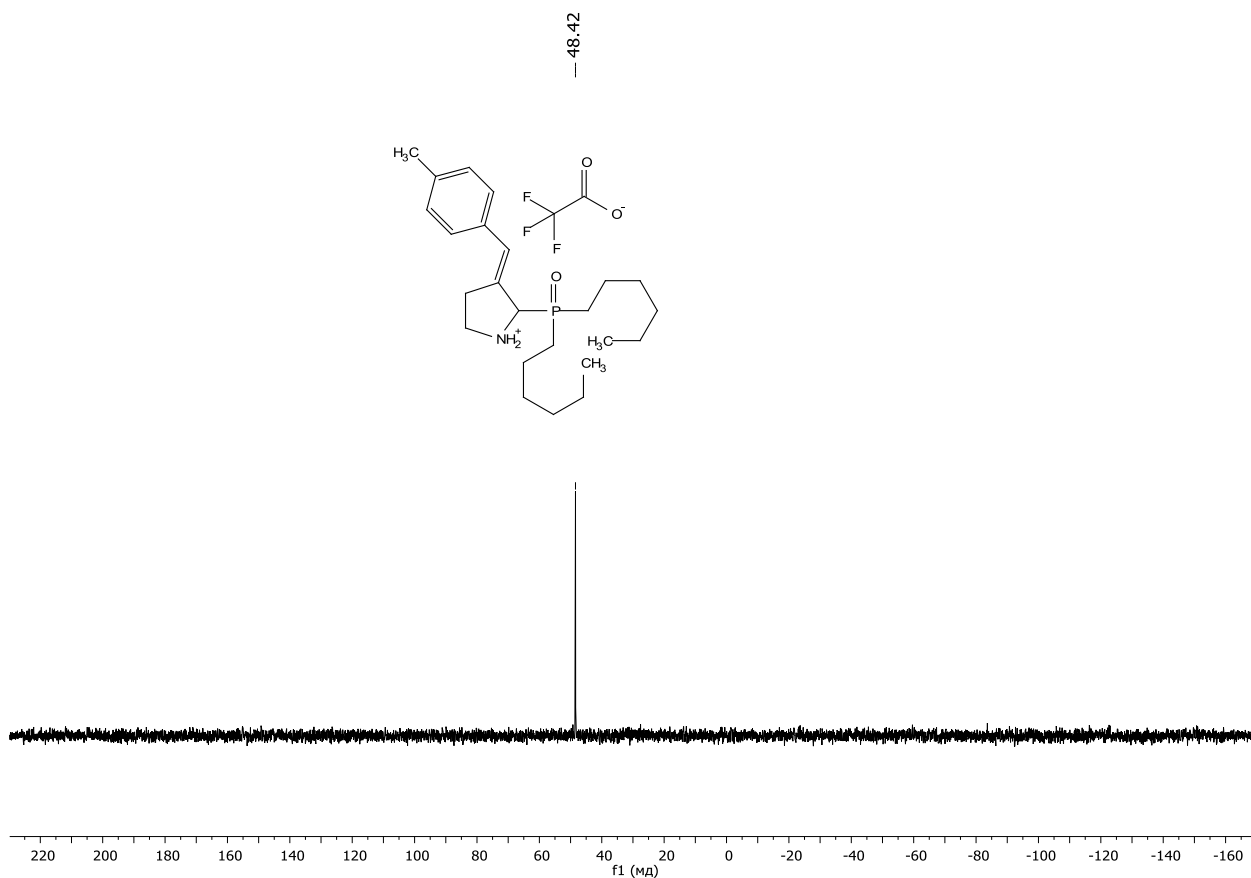


Figure S54. $^{31}\text{P}\{^1\text{H}\}$ NMR (DMSO- d_6 , 161 MHz) spectrum of the compound **3aq**

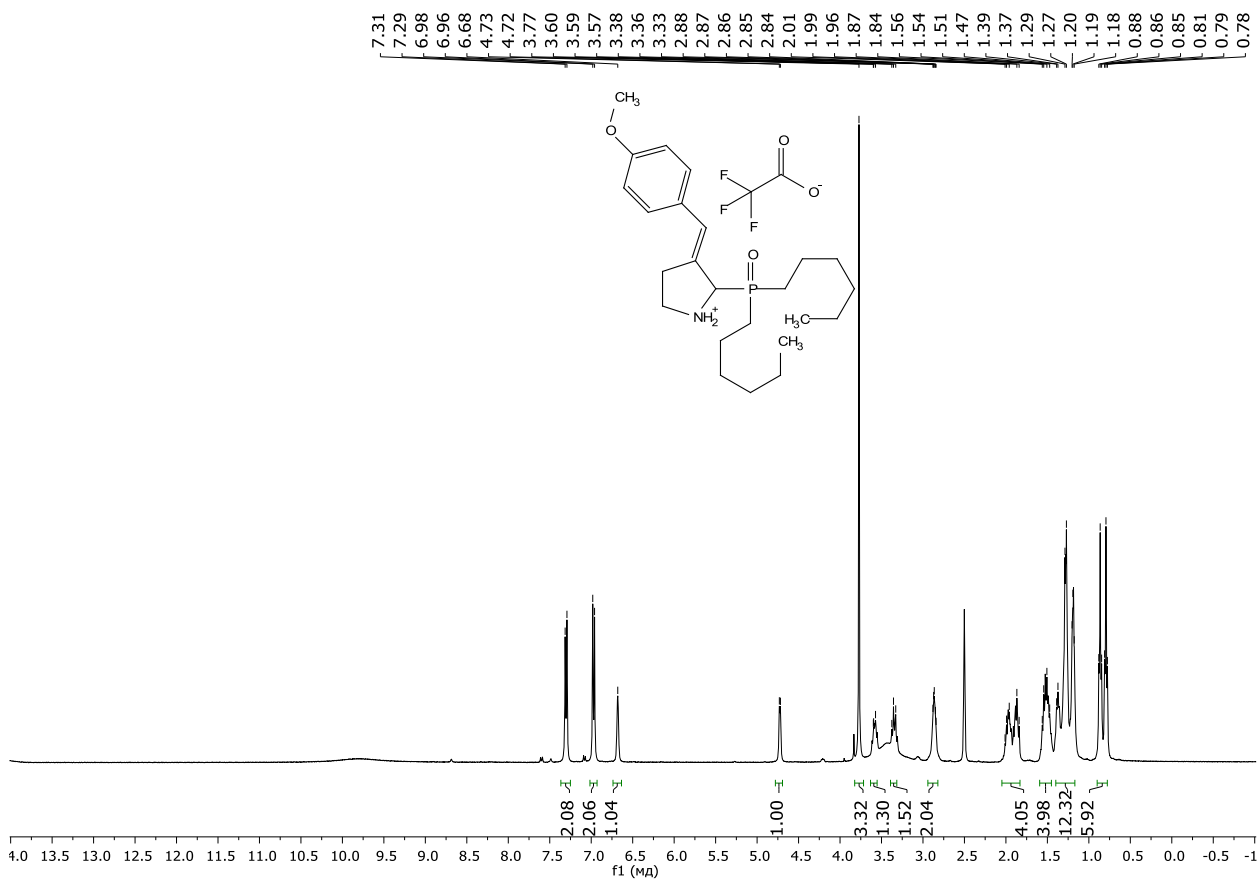


Figure S55. ^1H NMR (DMSO- d_6 , 600 MHz) spectrum of the compound **3ar**

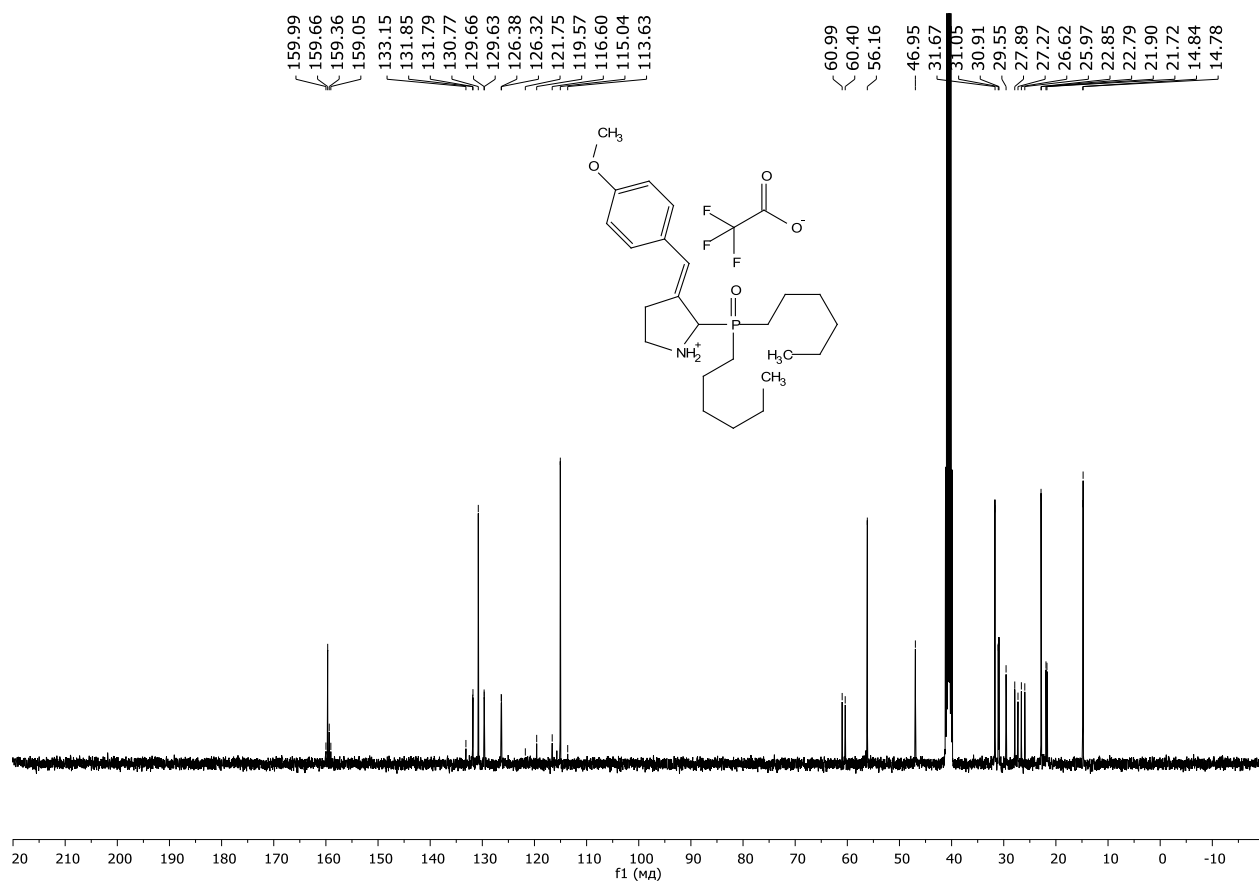


Figure S56. ¹³C{¹H} NMR (DMSO-*d*₆, 150 MHz) spectrum of the compound **3ar**

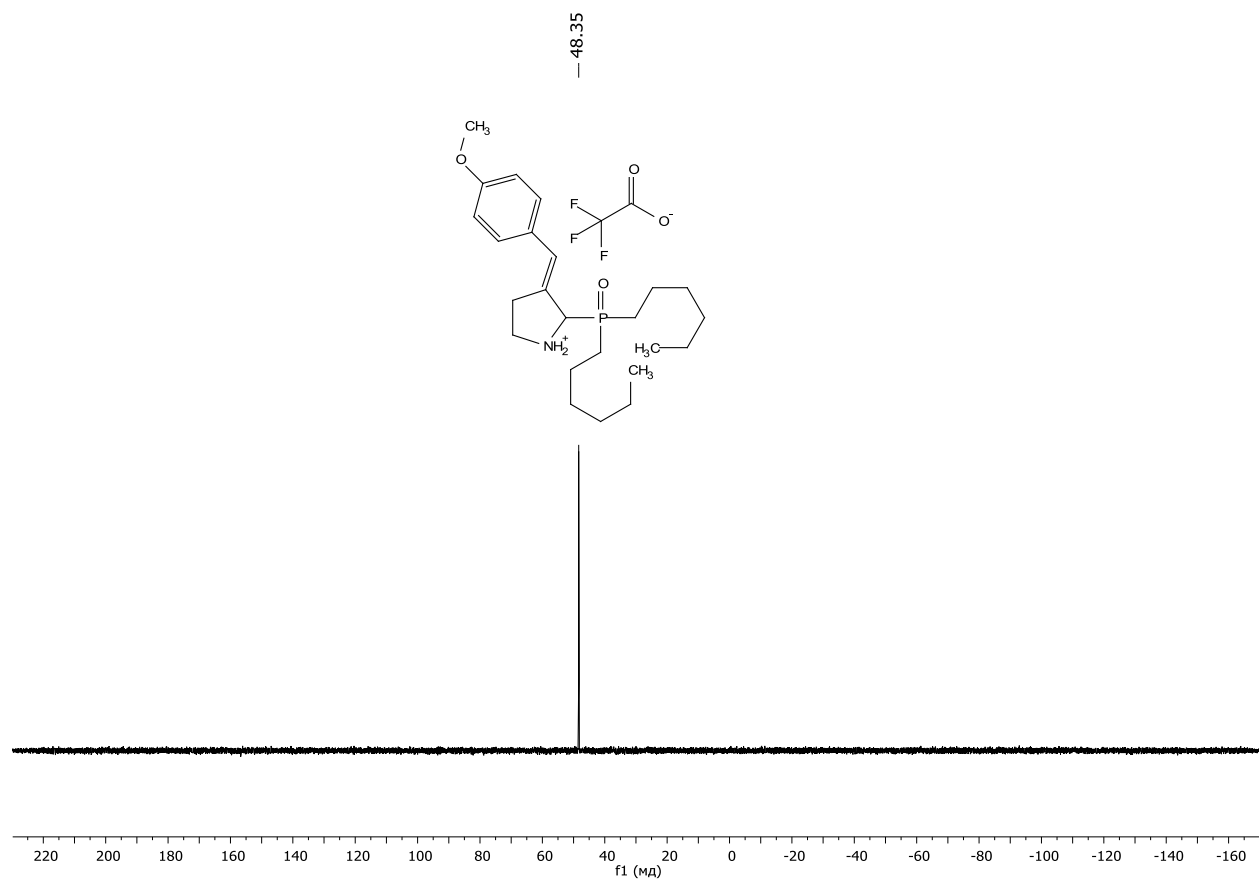


Figure S57. ³¹P{¹H} NMR (DMSO-*d*₆, 161 MHz) spectrum of the compound **3ar**

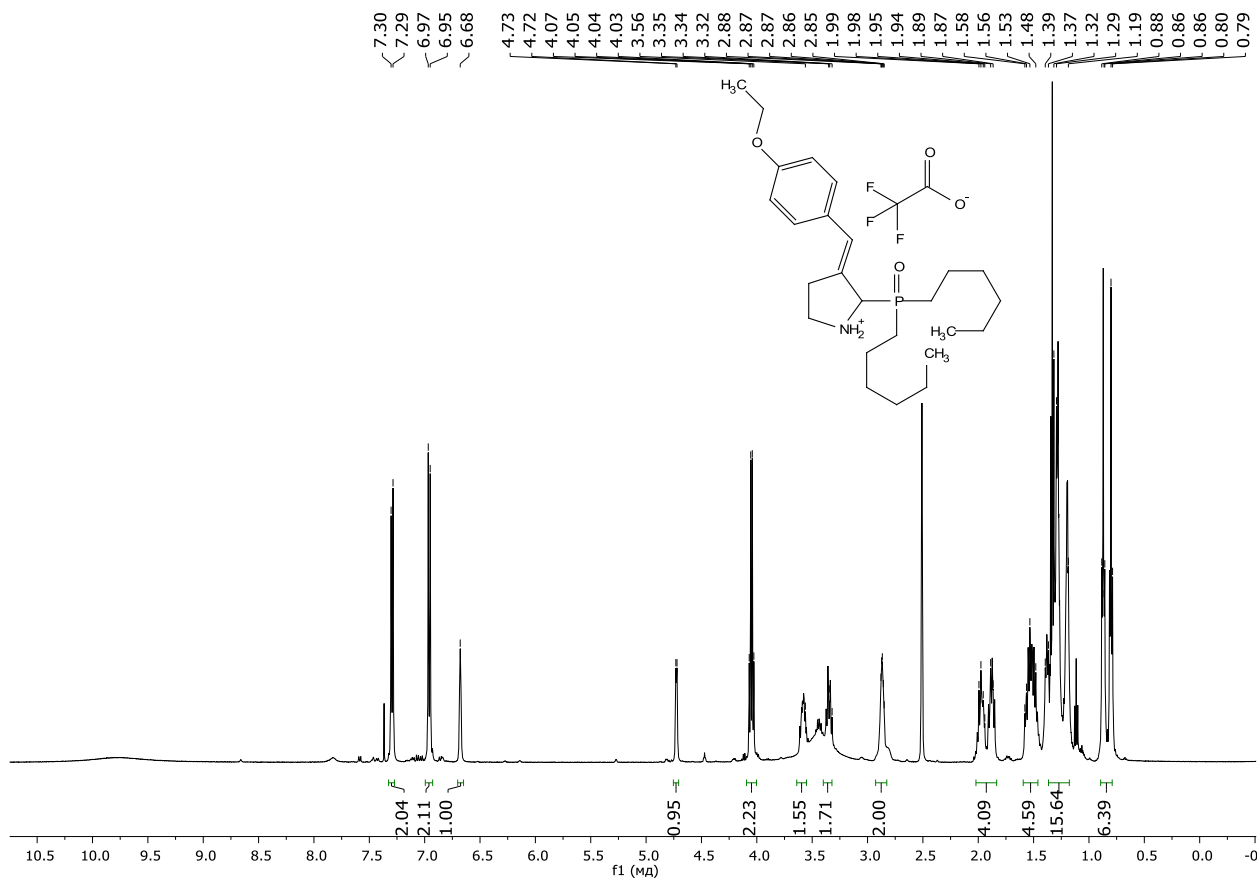


Figure S58. $^1\text{H NMR}$ (DMSO- d_6 , 600 MHz) spectrum of the compound 3as

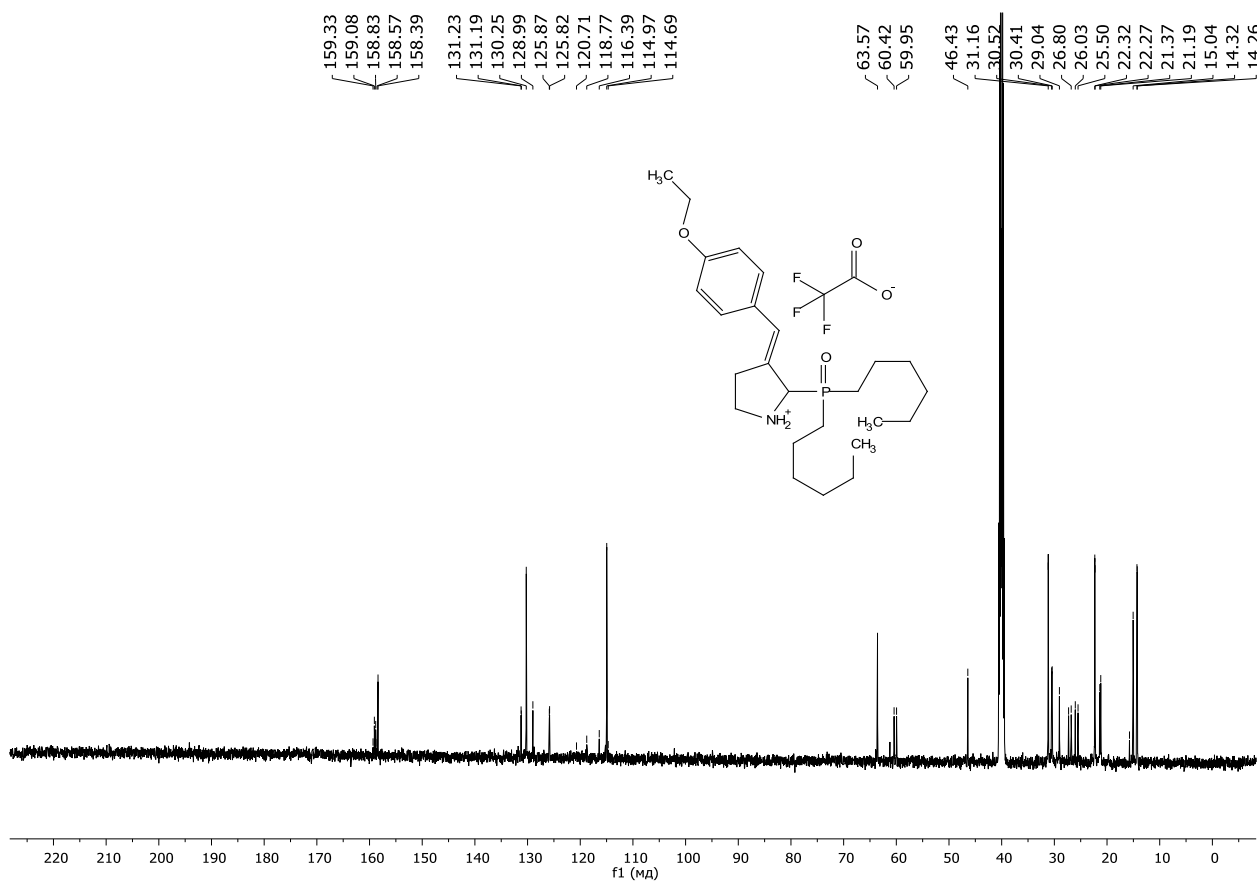


Figure S59. $^{13}\text{C}\{^1\text{H}\}$ NMR (DMSO- d_6 , 150 MHz) spectrum of the compound 3as

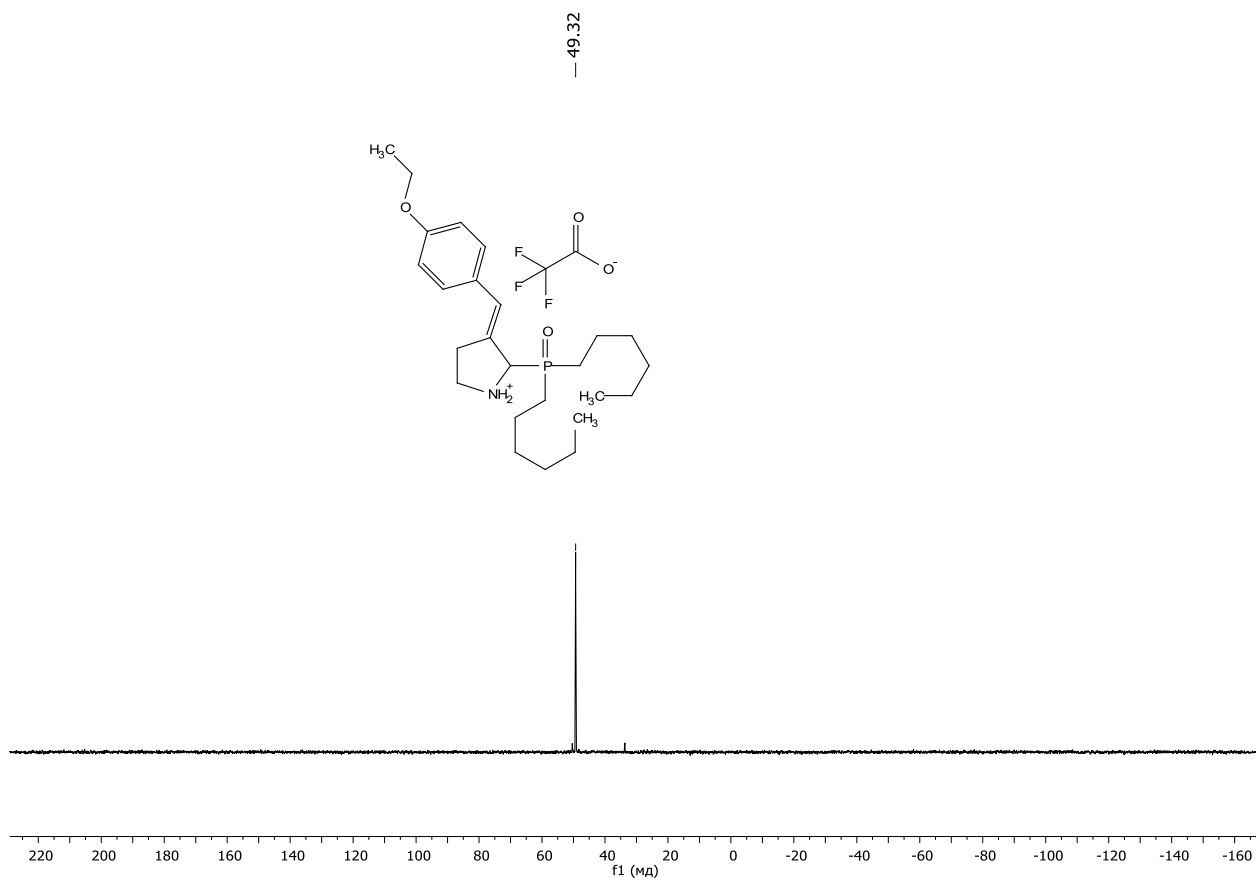


Figure S60. $^{31}\text{P}\{^1\text{H}\}$ NMR ($\text{DMSO-}d_6$, 161 MHz) spectrum of the compound **3as**

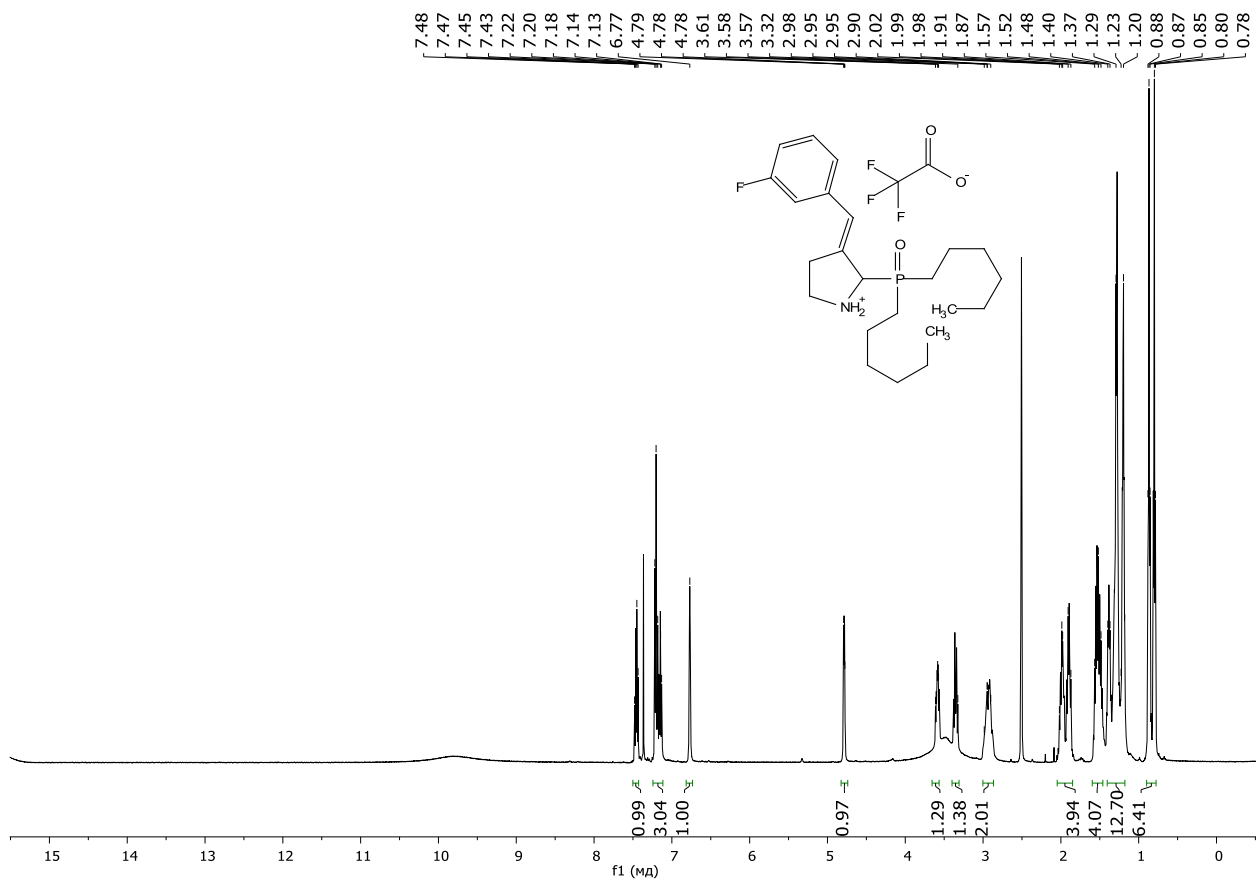


Figure S61. ^1H NMR ($\text{DMSO-}d_6$, 600 MHz) spectrum of the compound **3at**

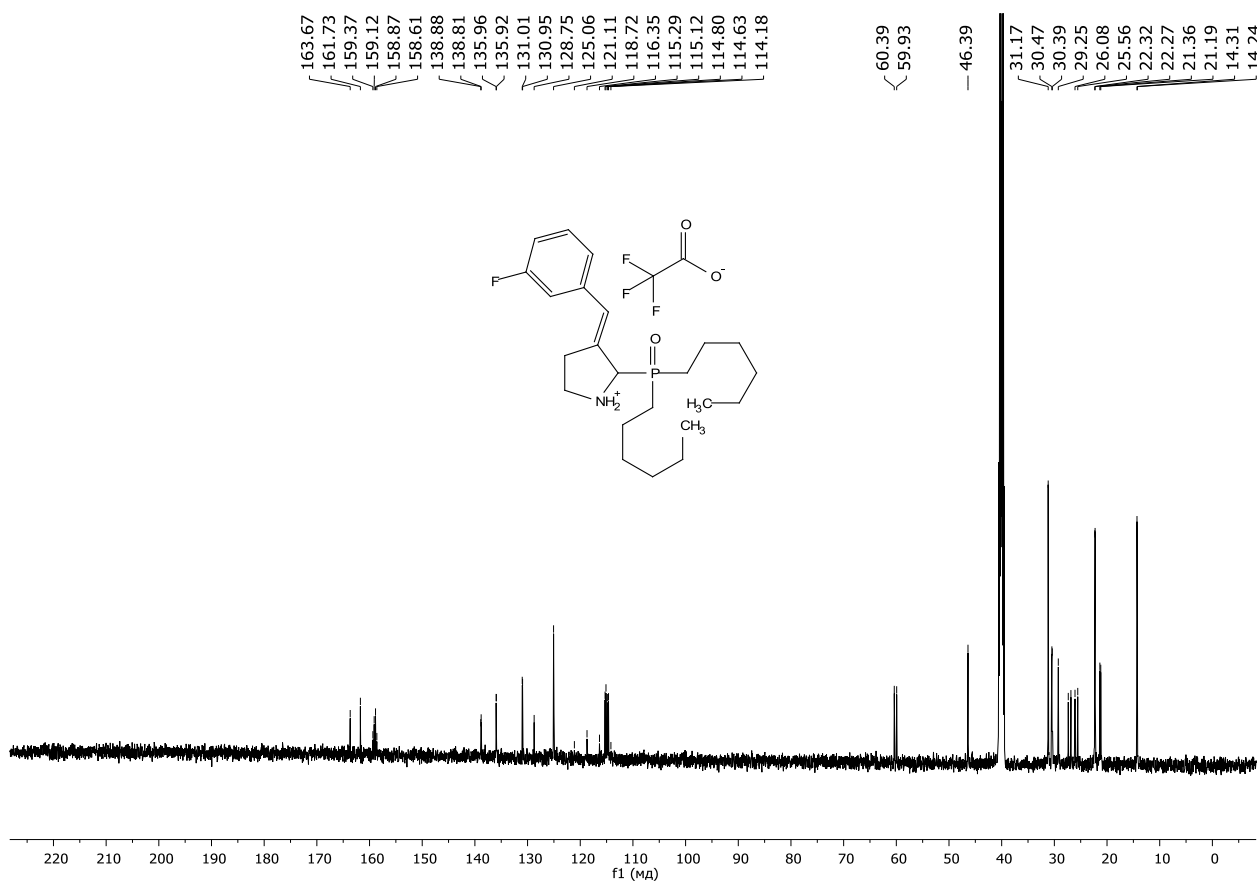


Figure S62. $^{13}\text{C}\{^1\text{H}\}$ NMR (DMSO- d_6 , 150 MHz) spectrum of the compound 3at

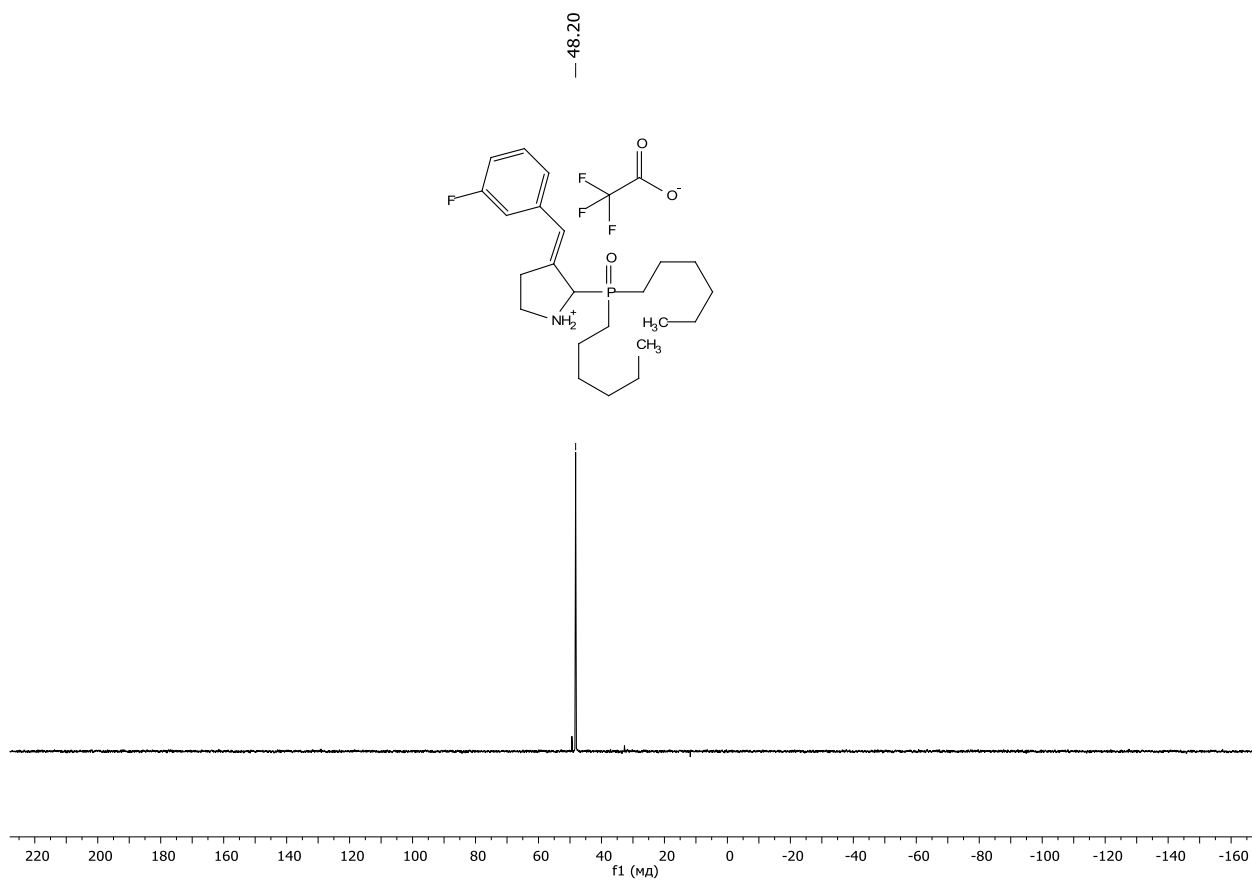


Figure S63. $^{31}\text{P}\{^1\text{H}\}$ NMR (DMSO- d_6 , 161 MHz) spectrum of the compound 3at

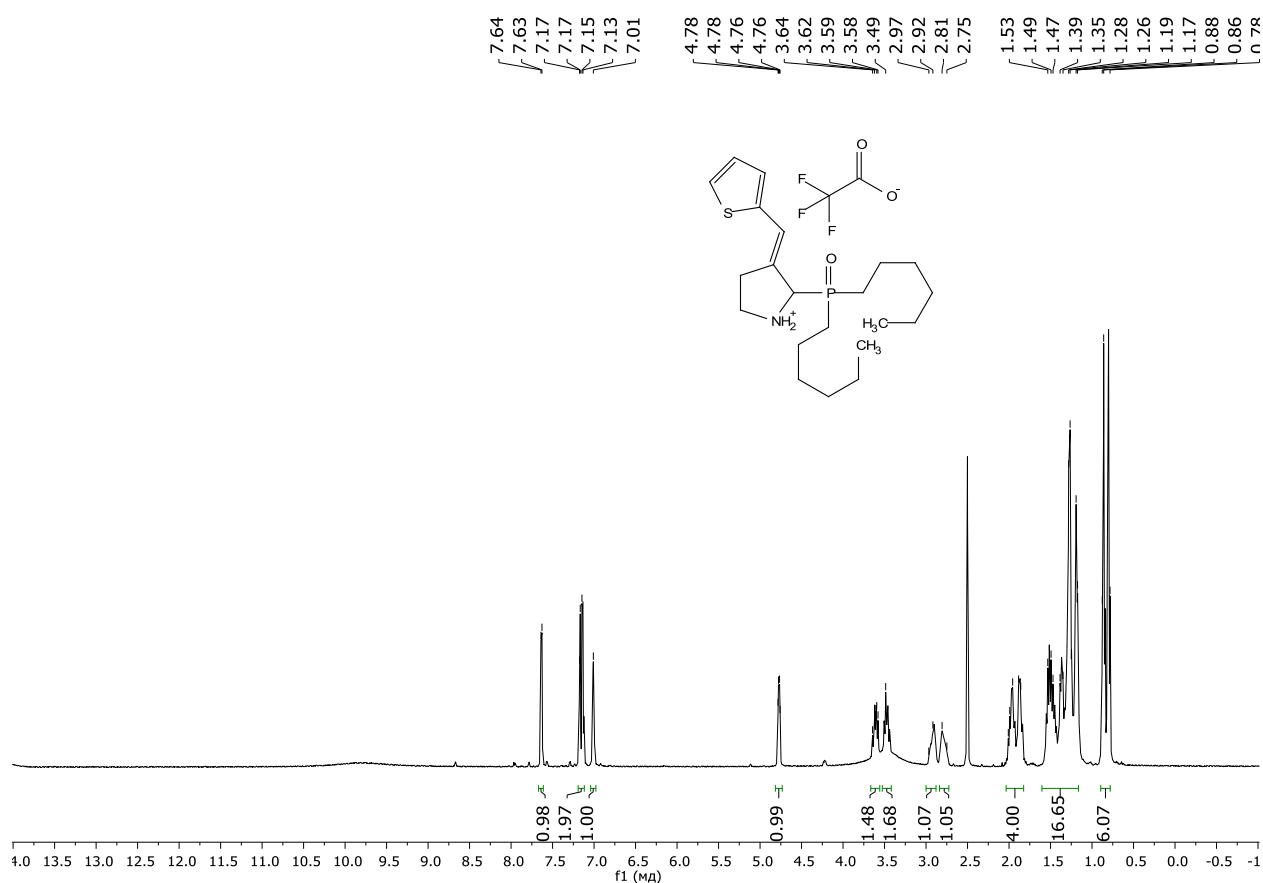


Figure S64. ^1H NMR (DMSO- d_6 , 600 MHz) spectrum of the compound 3au

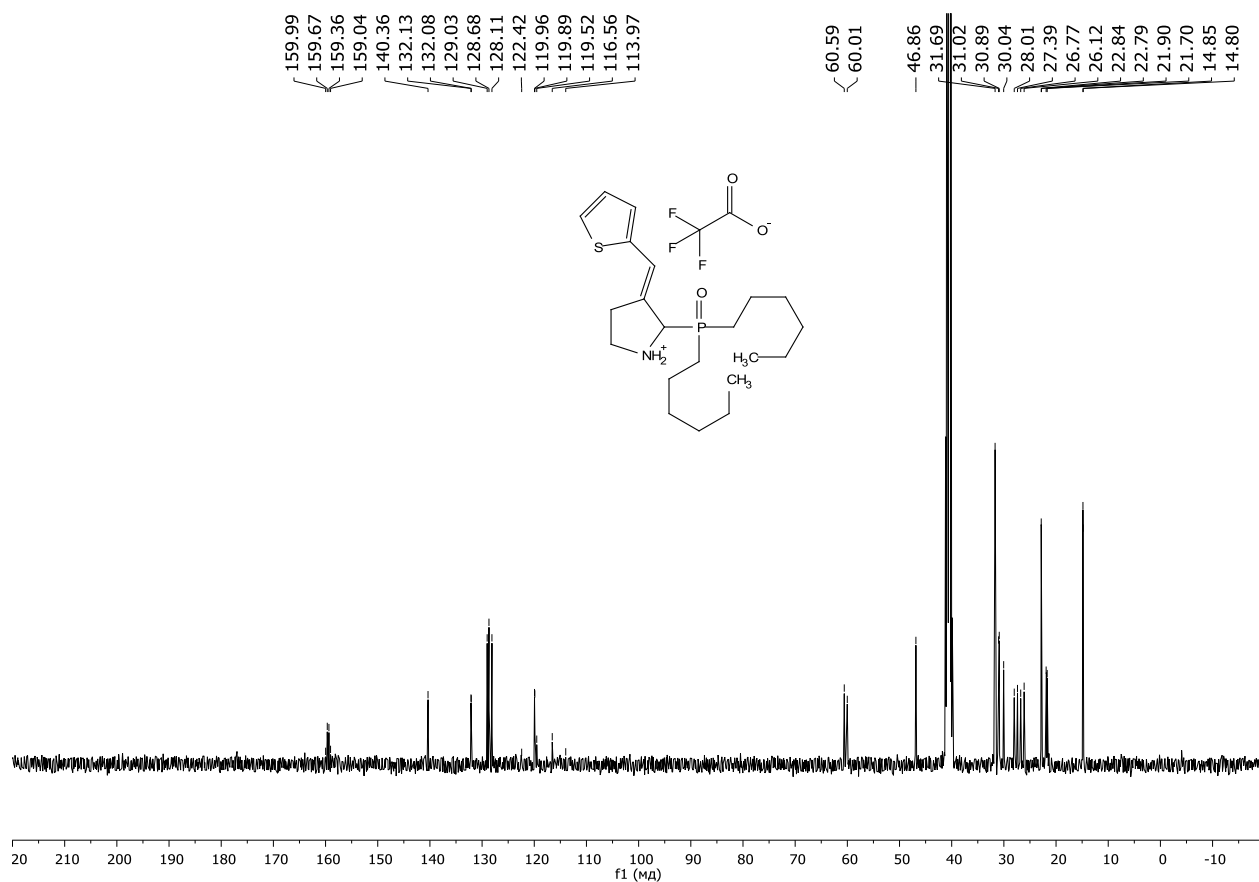


Figure S65. $^{13}\text{C}\{^1\text{H}\}$ NMR (DMSO- d_6 , 150 MHz) spectrum of the compound 3au

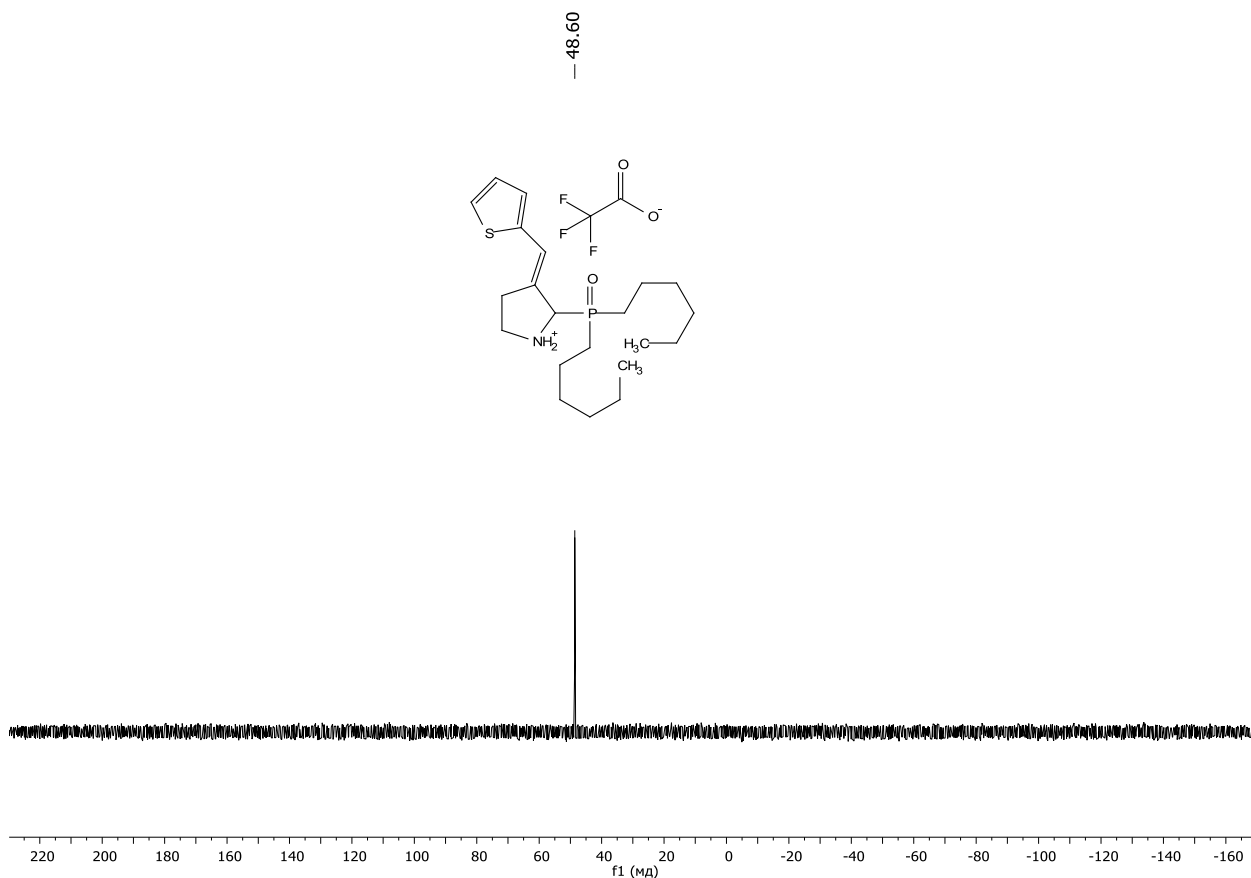


Figure S66. $^{31}\text{P}\{^1\text{H}\}$ NMR (DMSO- d_6 , 161 MHz) spectrum of the compound 3au

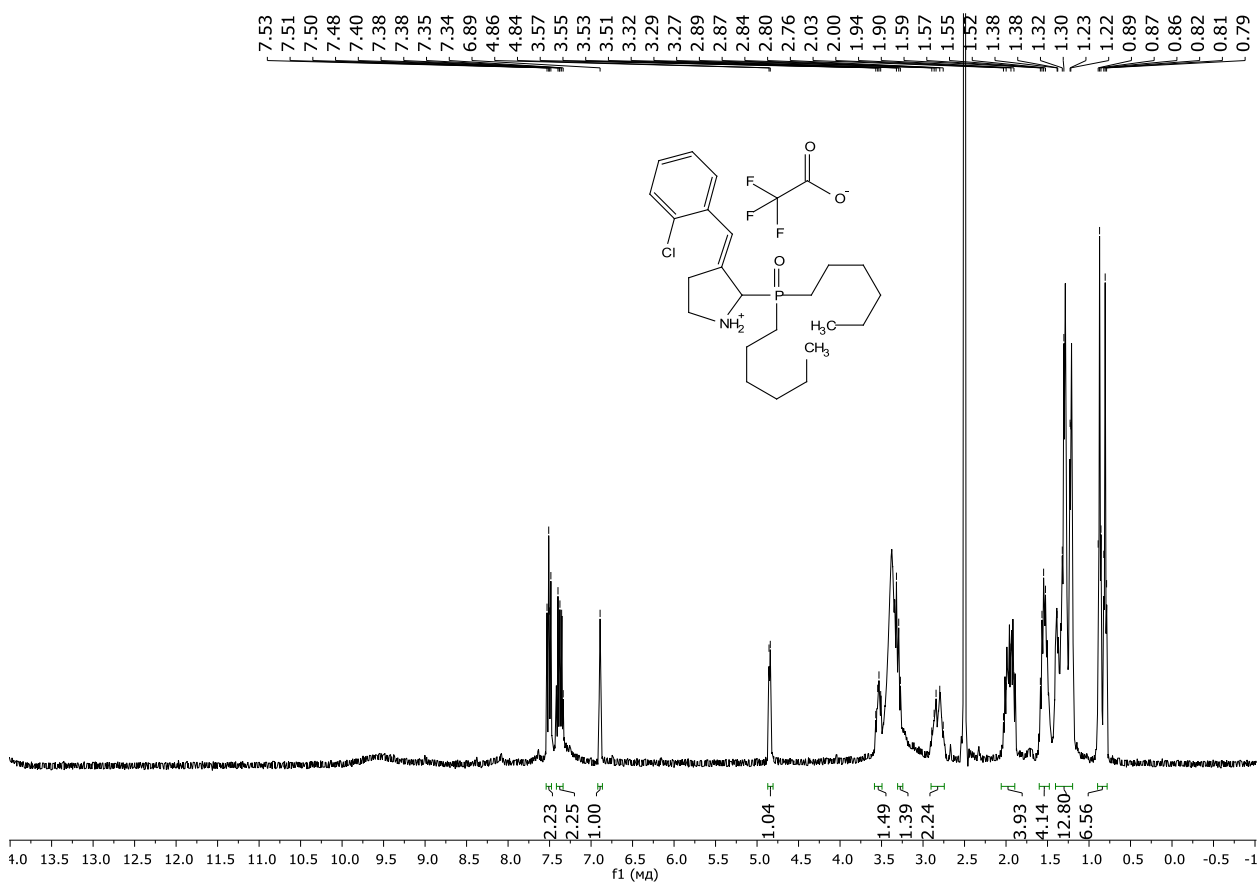


Figure S67. ^1H NMR (DMSO- d_6 , 600 MHz) spectrum of the compound 3av

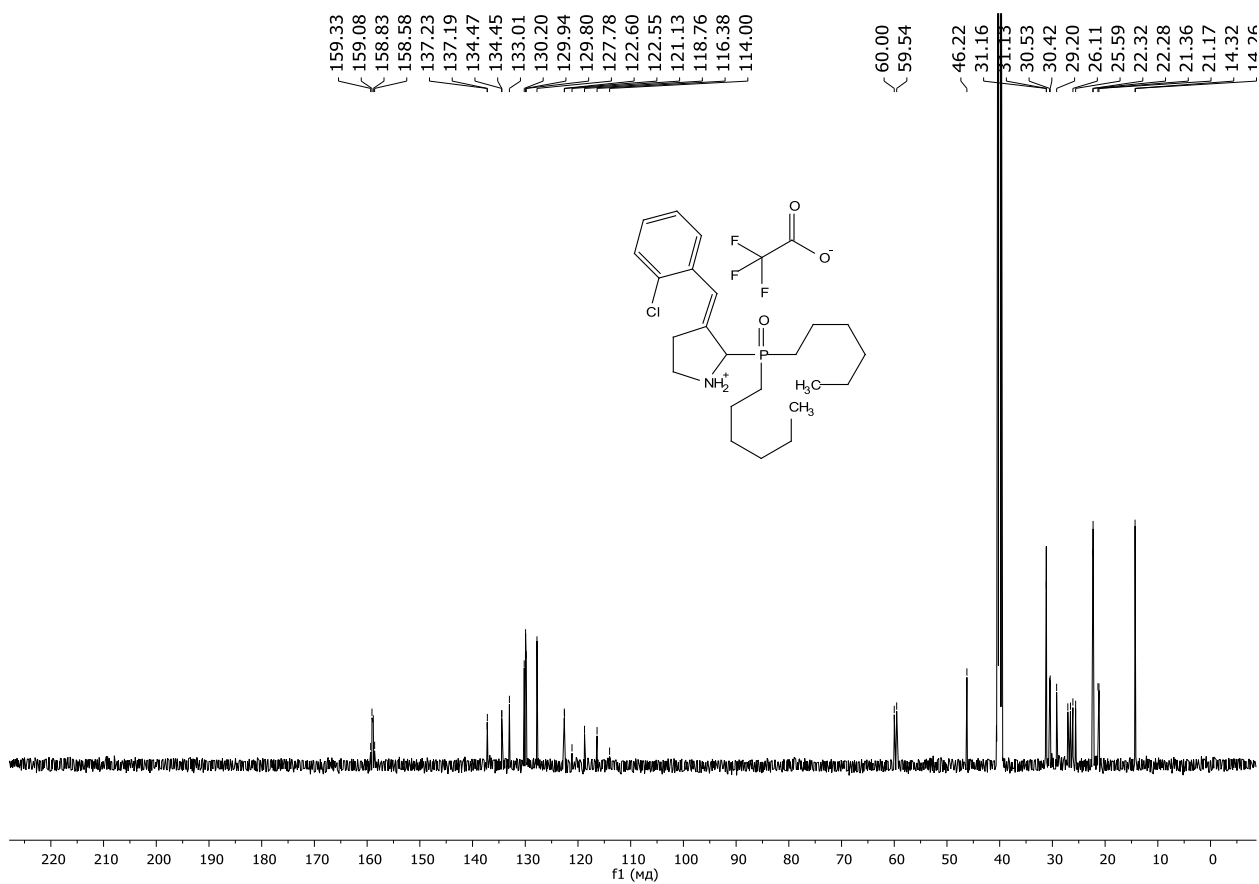


Figure S68. $^{13}\text{C}\{^1\text{H}\}$ NMR (DMSO- d_6 , 150 MHz) spectrum of the compound 3av

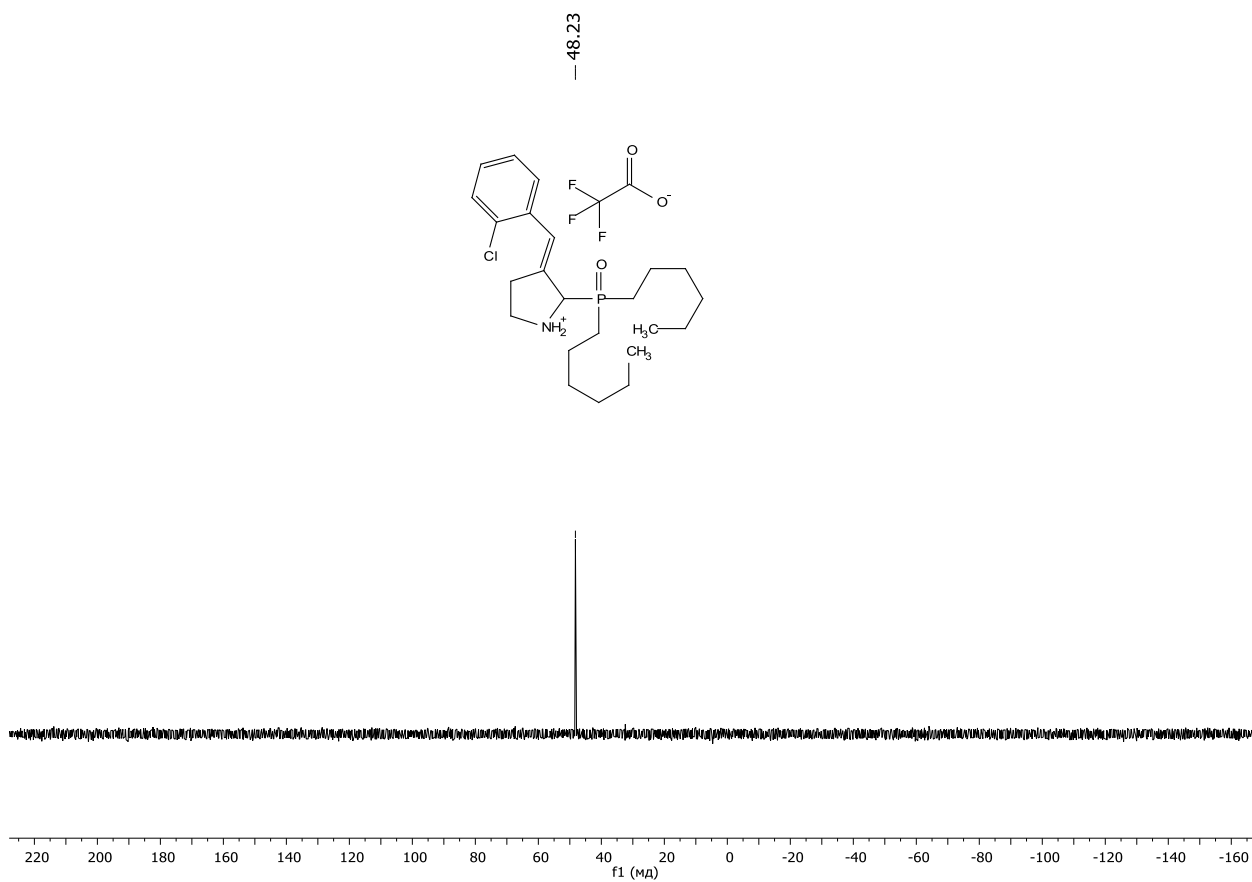


Figure S69. $^{31}\text{P}\{^1\text{H}\}$ NMR (DMSO- d_6 , 161 MHz) spectrum of the compound 3av

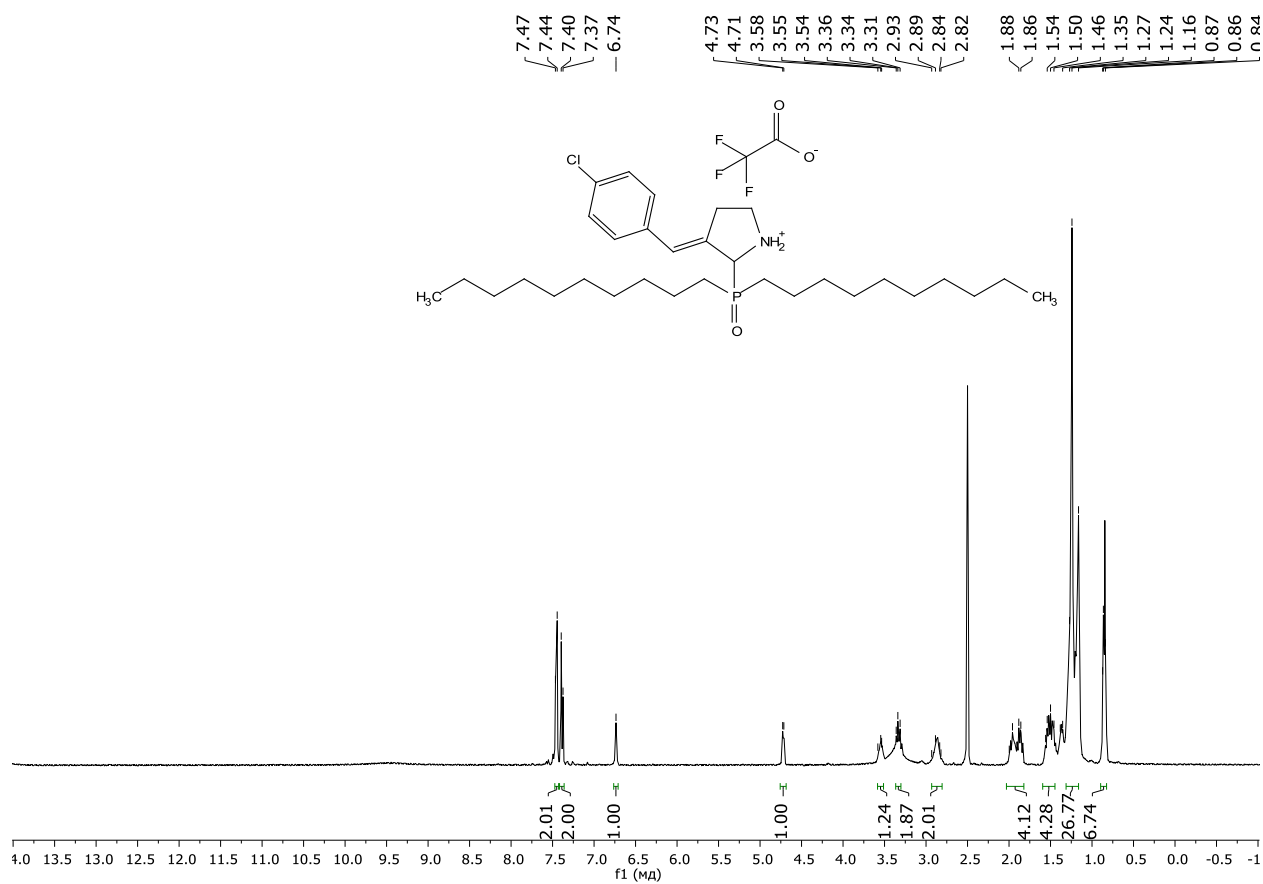


Figure S70. ¹H NMR (DMSO-*d*₆, 600 MHz) spectrum of the compound **3aw**

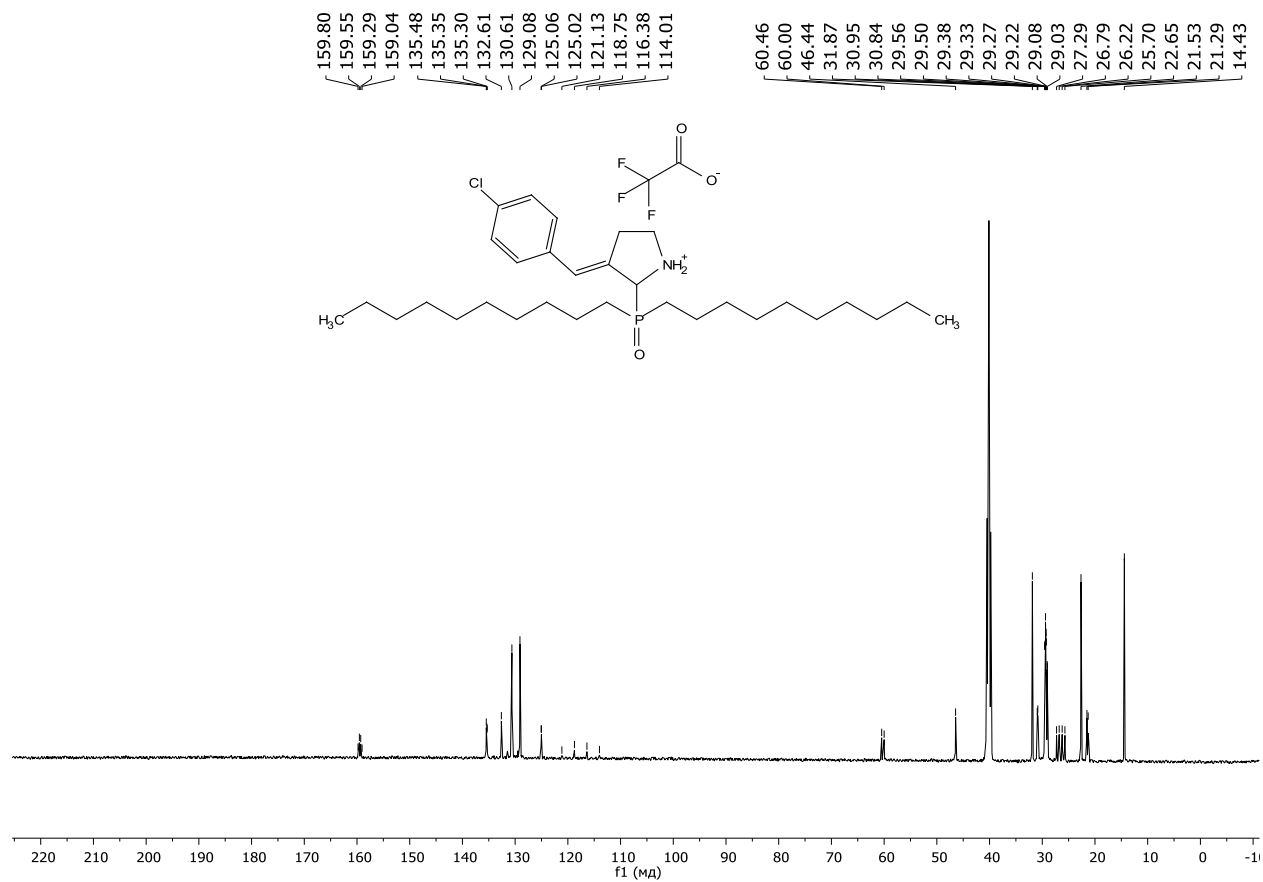


Figure S71. ¹³C{¹H} NMR (DMSO-*d*₆, 150 MHz) spectrum of the compound **3aw**

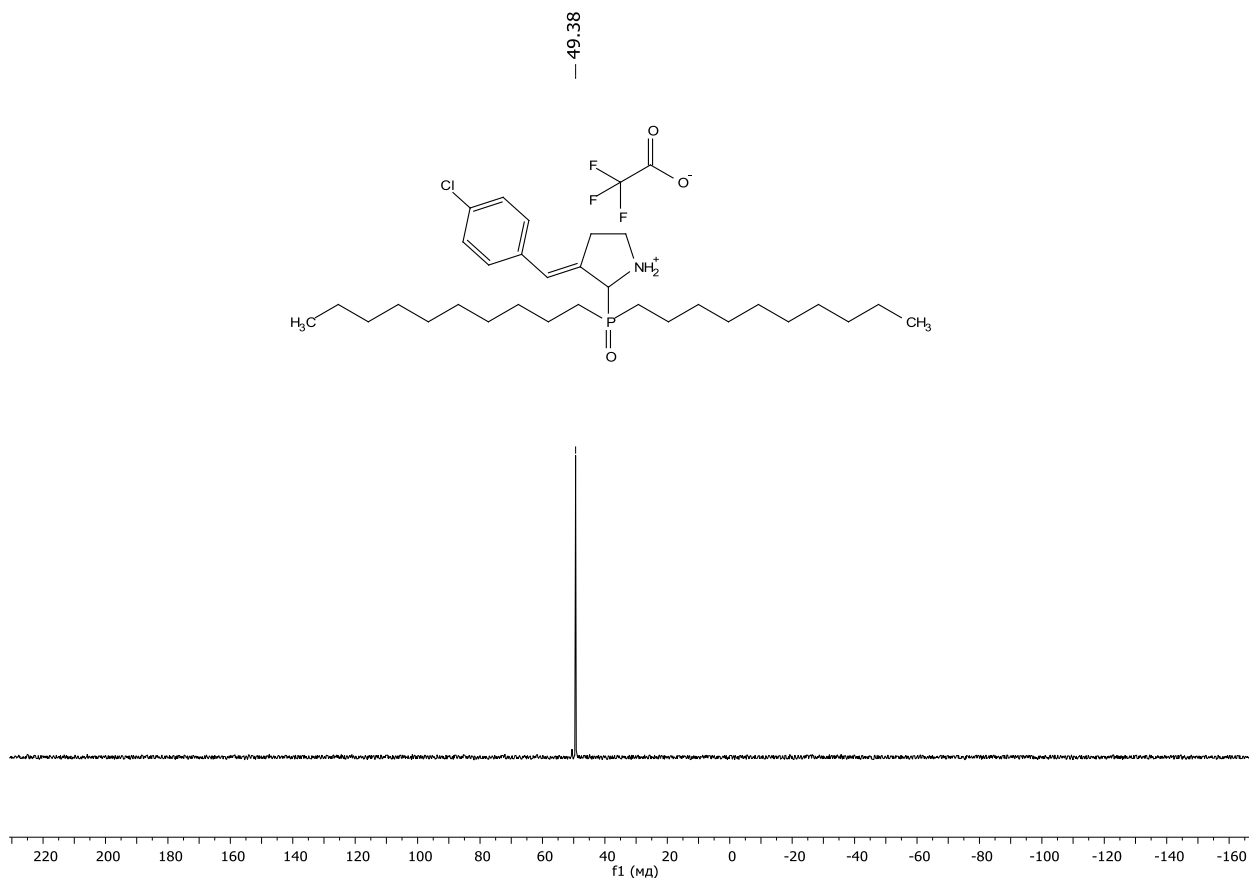


Figure S72. $^{31}\text{P}\{^1\text{H}\}$ NMR ($\text{DMSO-}d_6$, 161 MHz) spectrum of the compound **3aw**

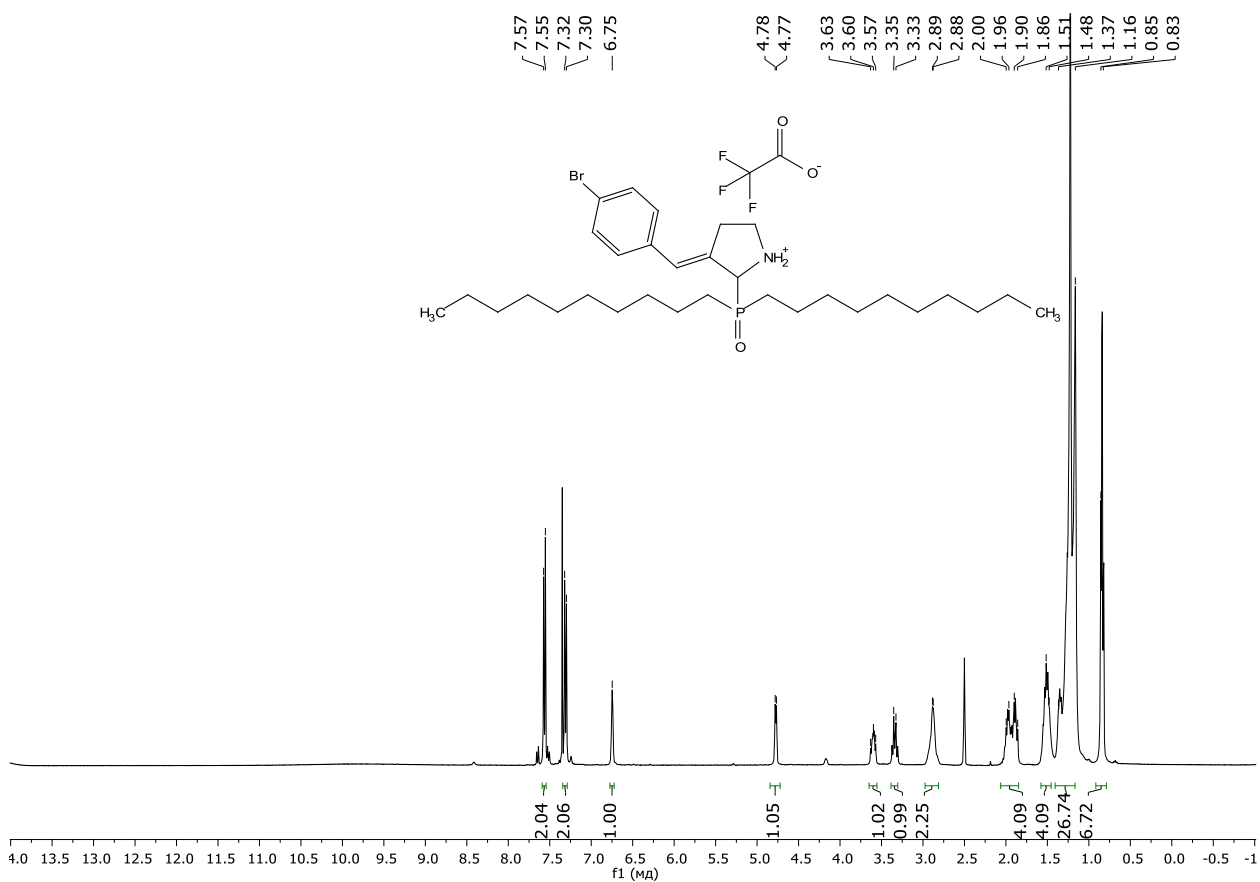


Figure S73. ^1H NMR ($\text{DMSO-}d_6$, 600 MHz) spectrum of the compound **3ax**

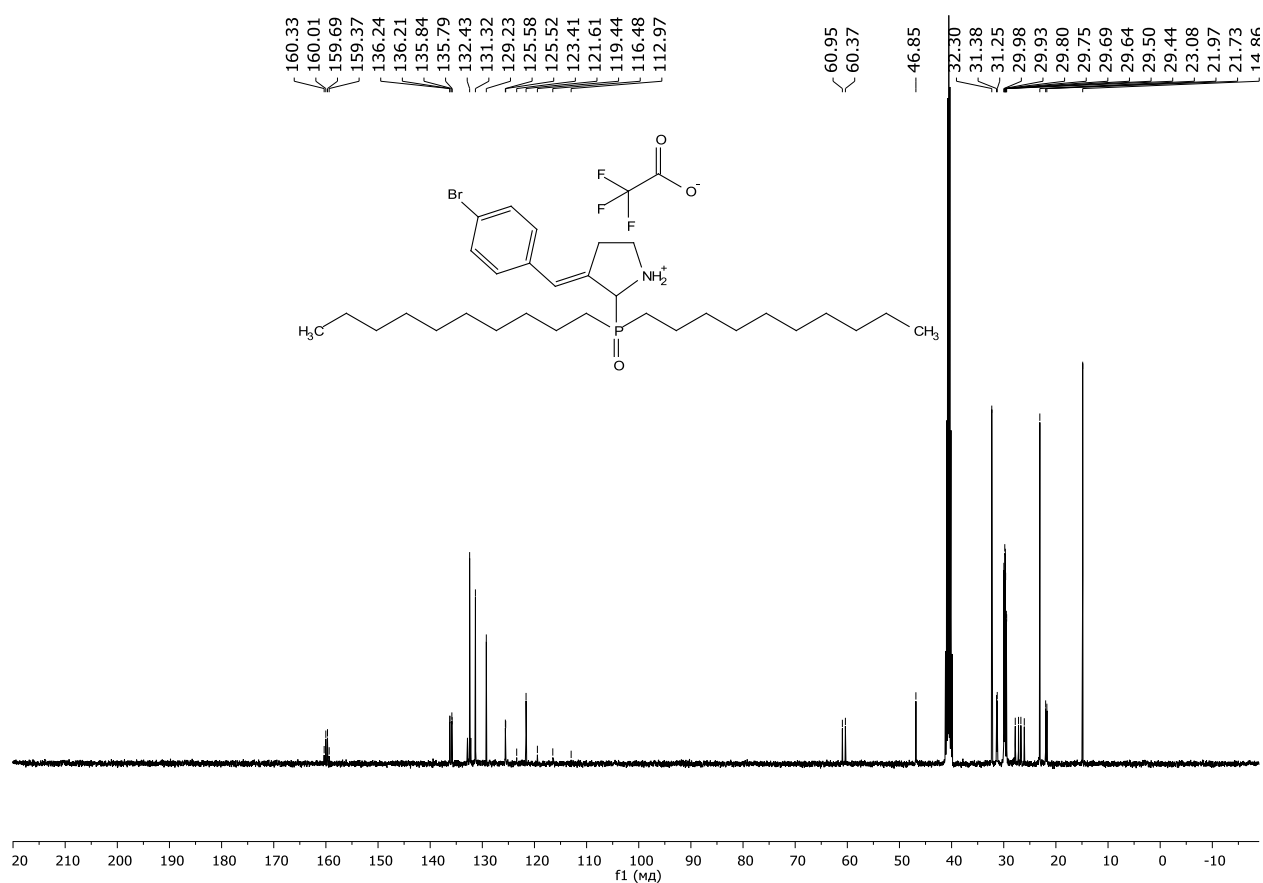


Figure S74. ¹³C{¹H} NMR (DMSO-*d*₆, 150 MHz) spectrum of the compound **3ax**

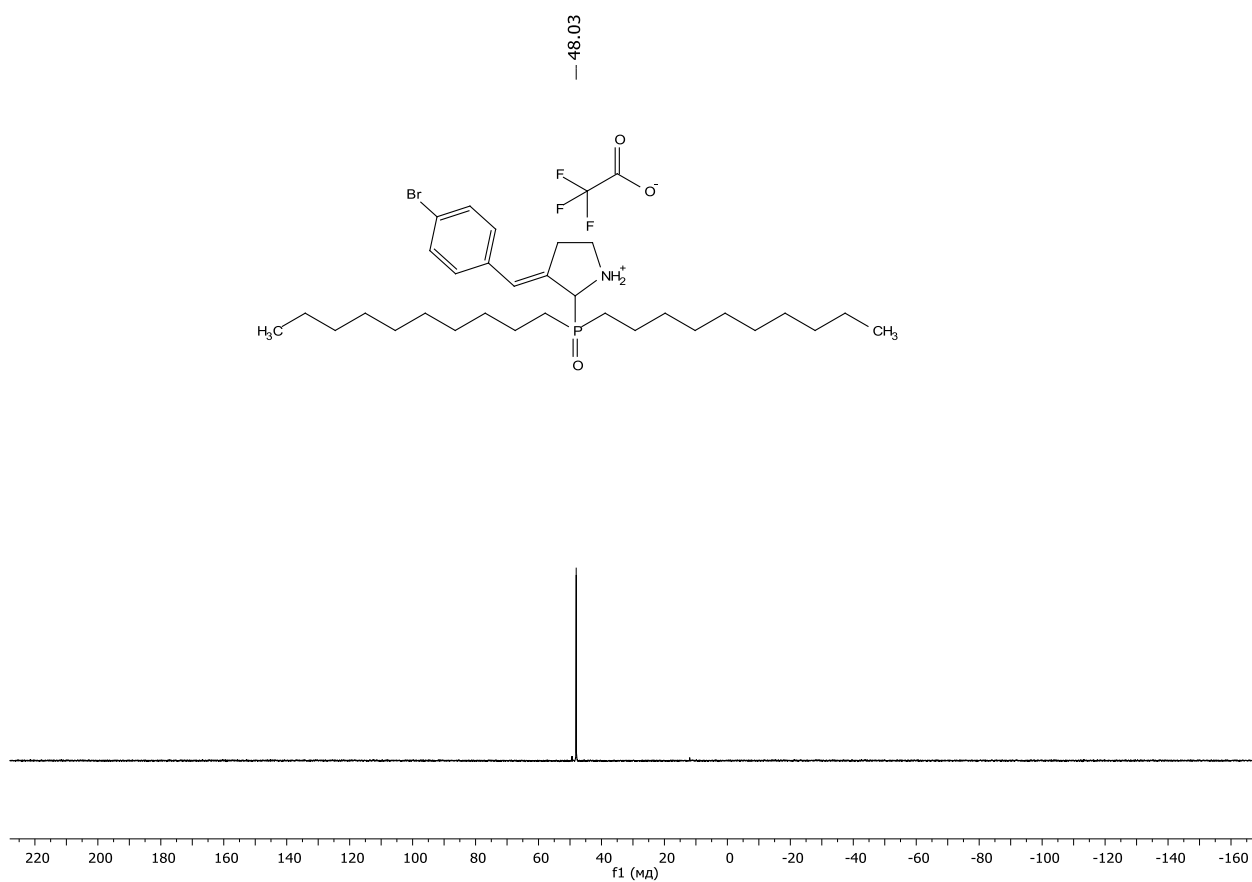


Figure S75. ³¹P{¹H} NMR (DMSO-*d*₆, 161 MHz) spectrum of the compound **3ax**

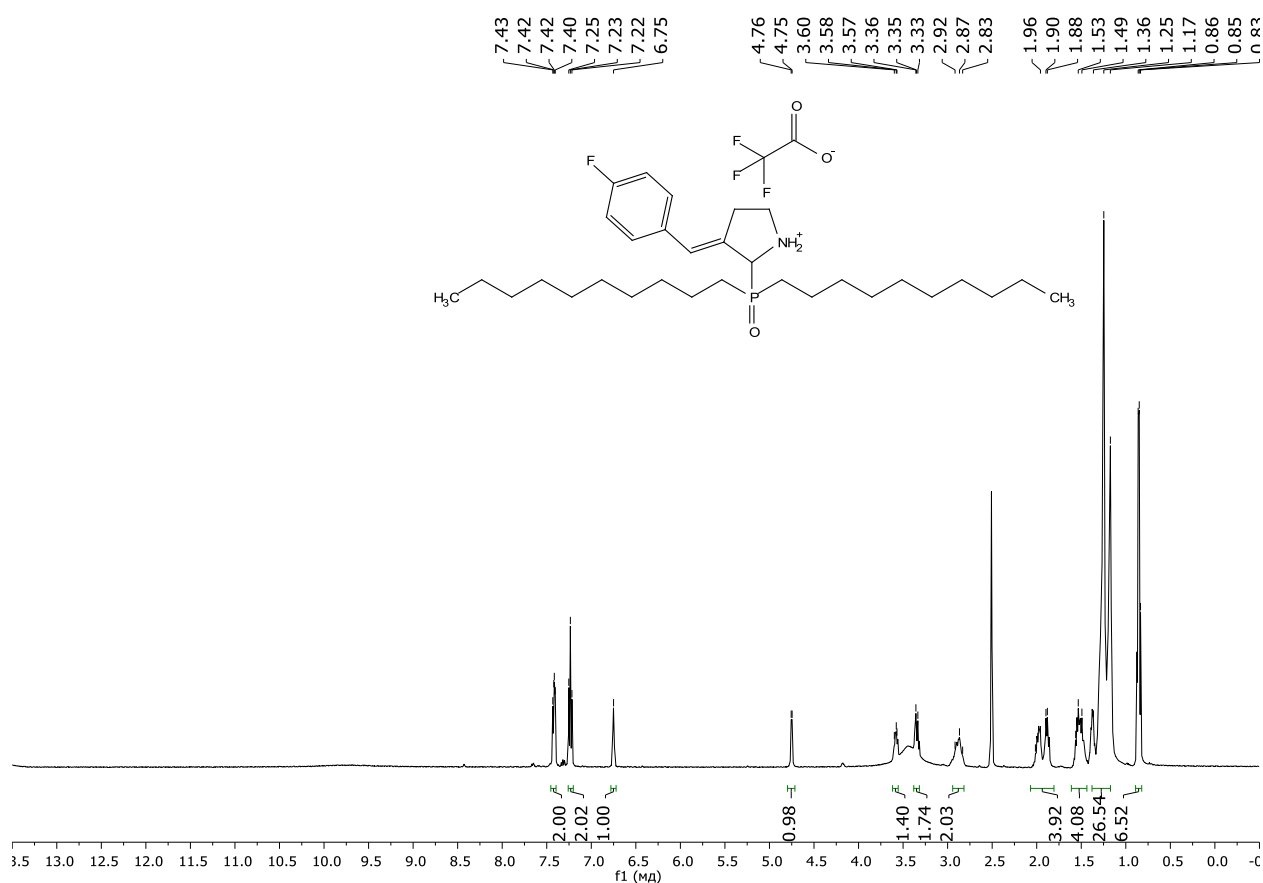


Figure S76. ¹H NMR (DMSO-d₆, 600 MHz) spectrum of the compound 3ay

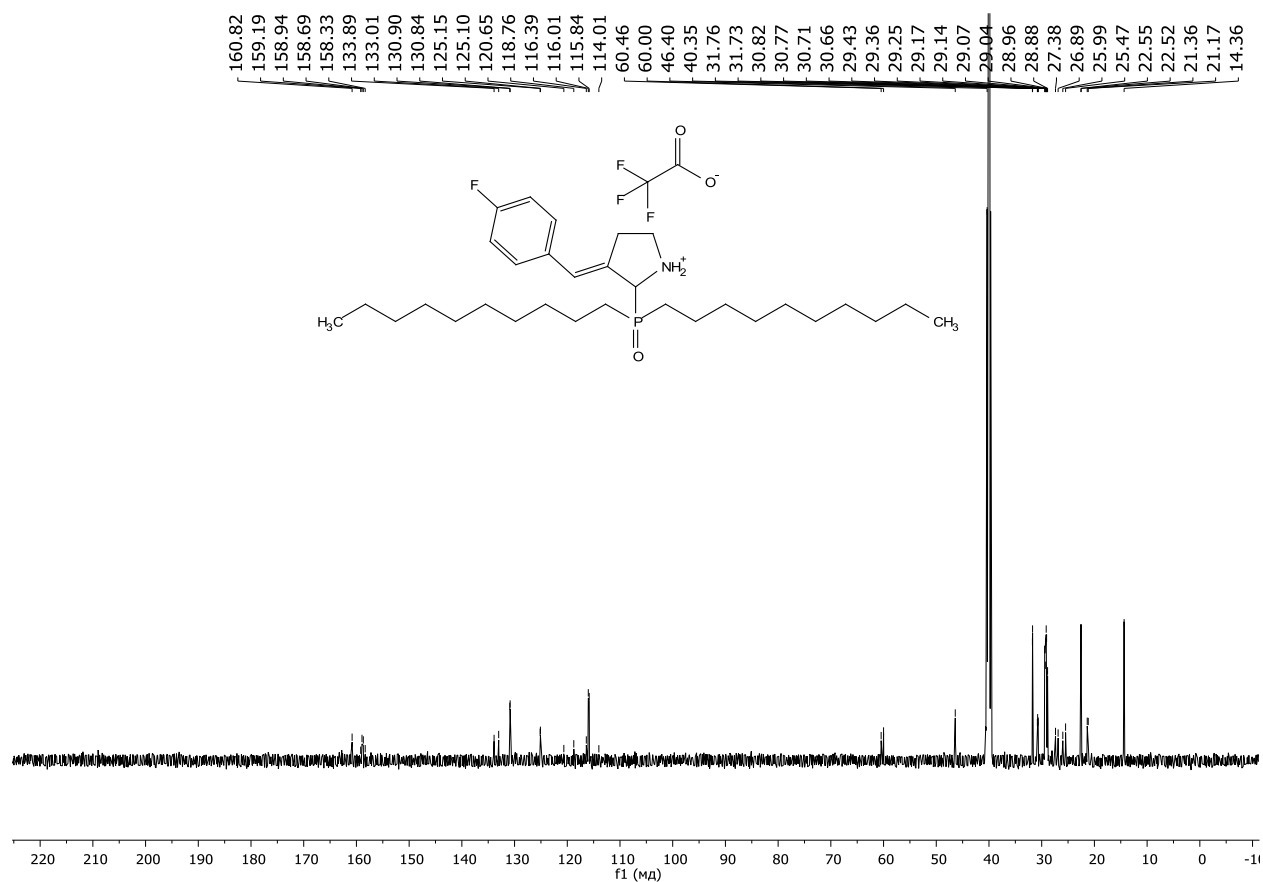


Figure S77. ¹³C{¹H} NMR (DMSO-d₆, 150 MHz) spectrum of the compound 3ay

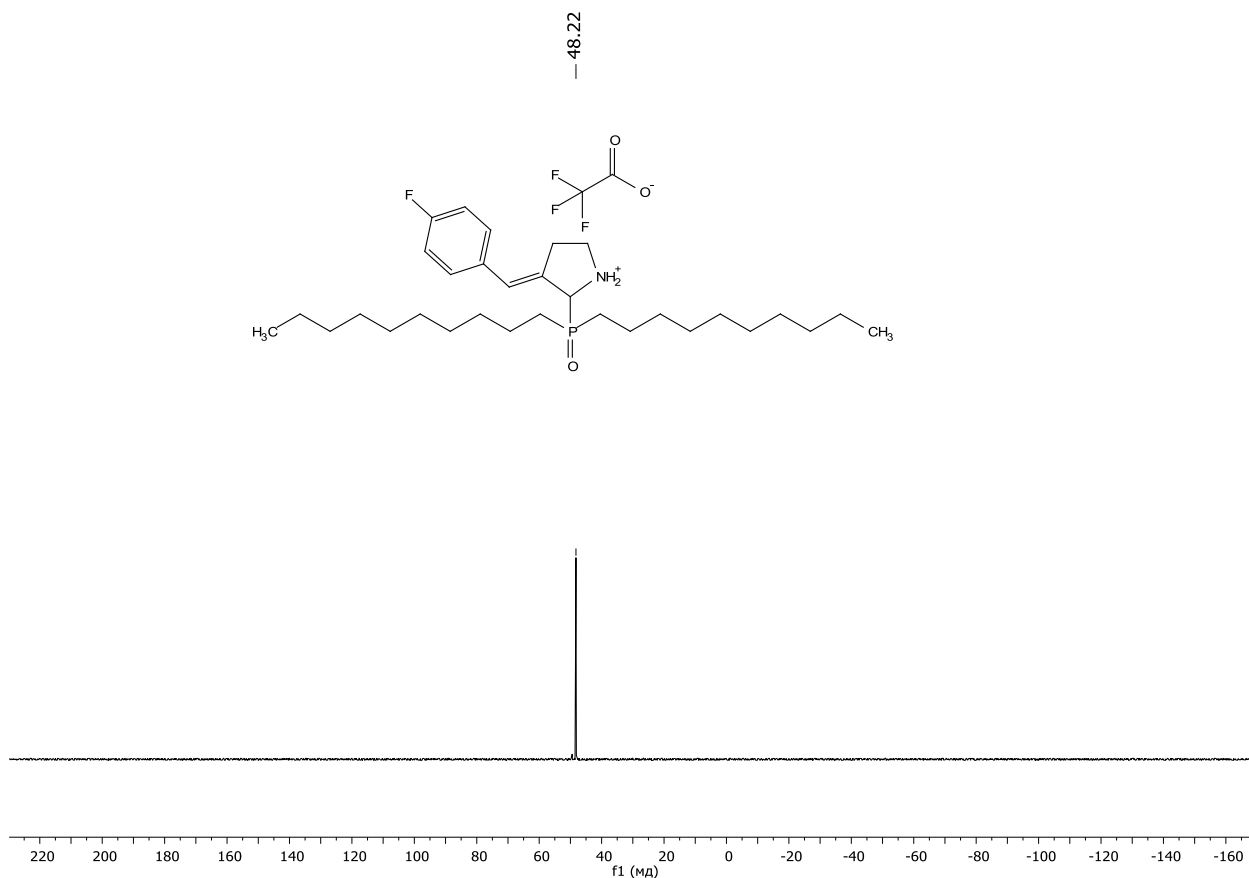


Figure S78. $^{31}\text{P}\{^1\text{H}\}$ NMR (DMSO- d_6 , 161 MHz) spectrum of the compound **3ay**

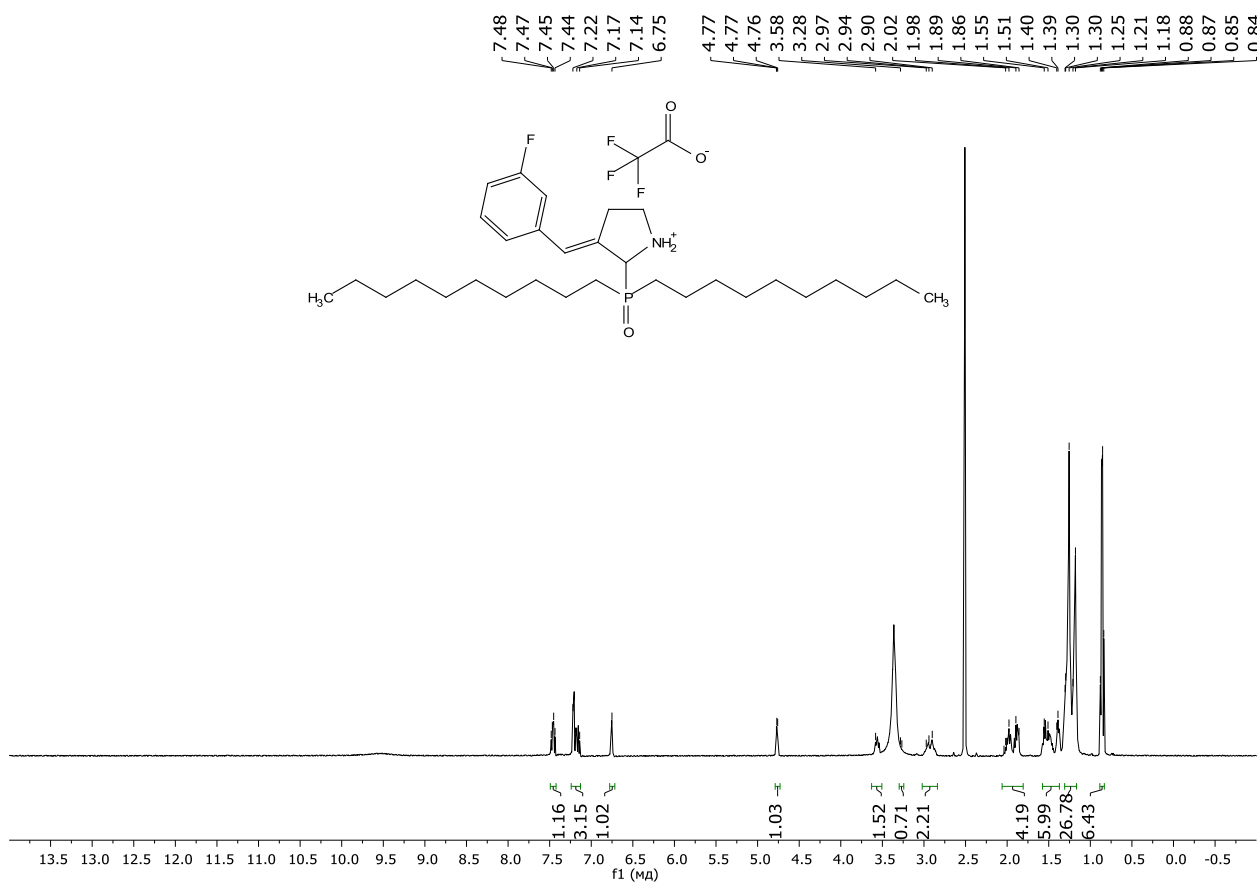


Figure S79. ^1H NMR (DMSO- d_6 , 600 MHz) spectrum of the compound **3az**

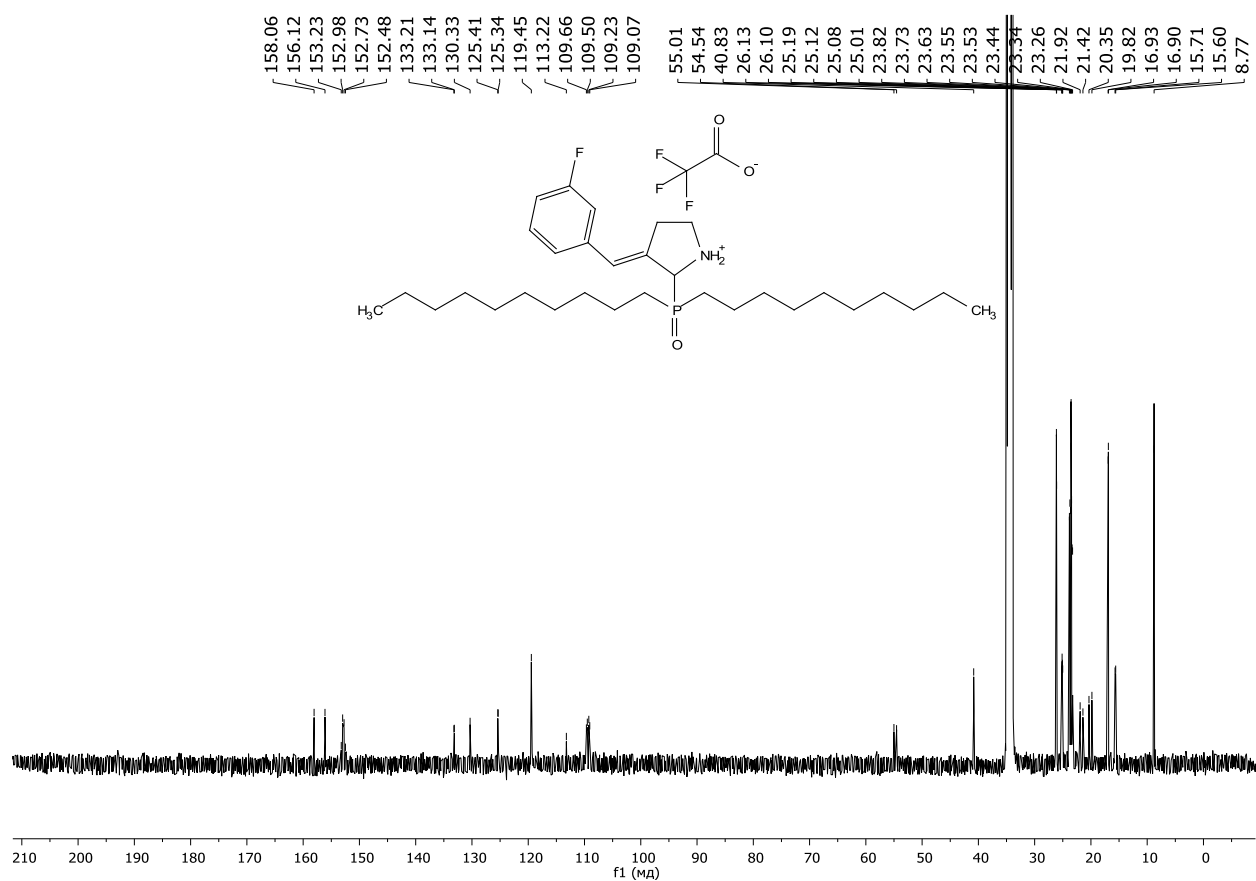


Figure S80. $^{13}\text{C}\{^1\text{H}\}$ NMR ($\text{DMSO-}d_6$, 150 MHz) spectrum of the compound **3az**

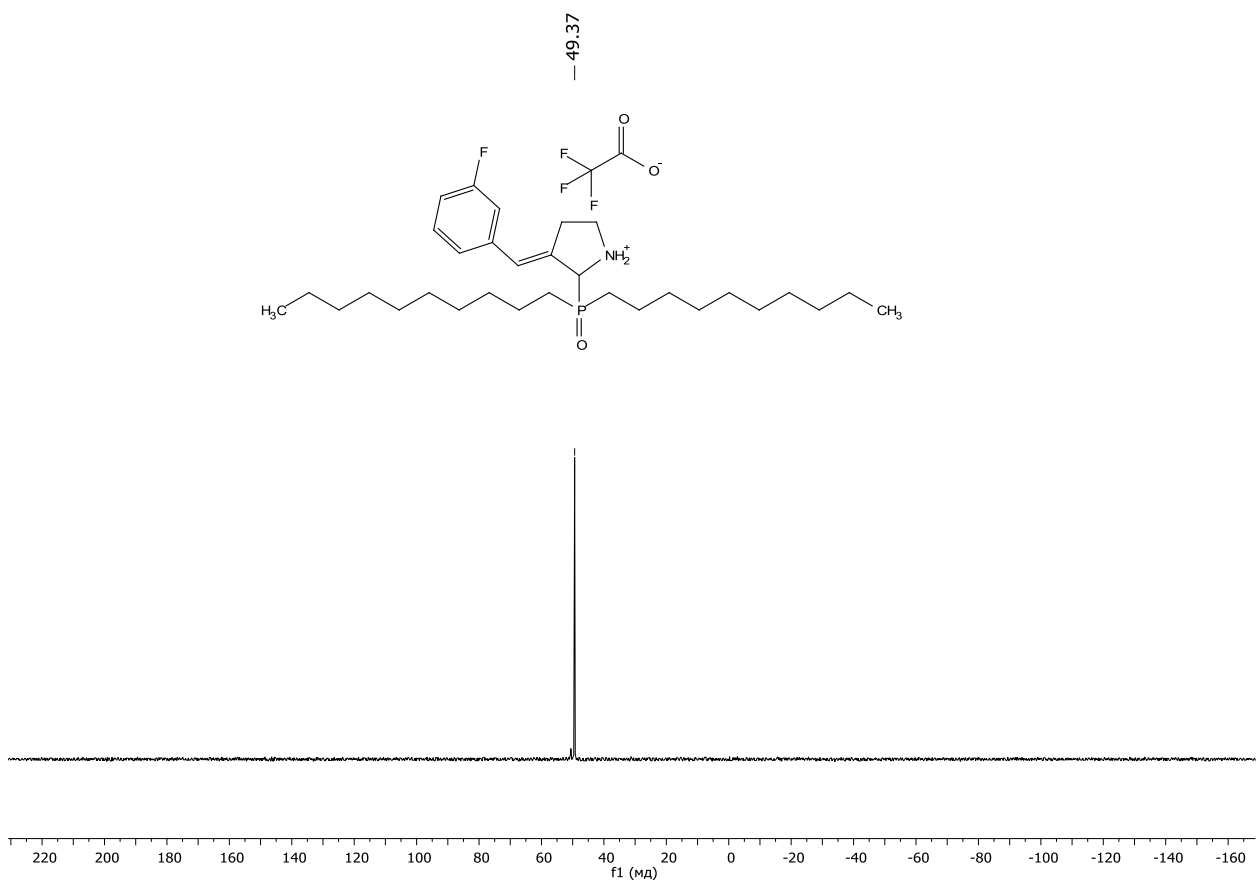


Figure S81. $^{31}\text{P}\{^1\text{H}\}$ NMR ($\text{DMSO-}d_6$, 161 MHz) spectrum of the compound **3az**

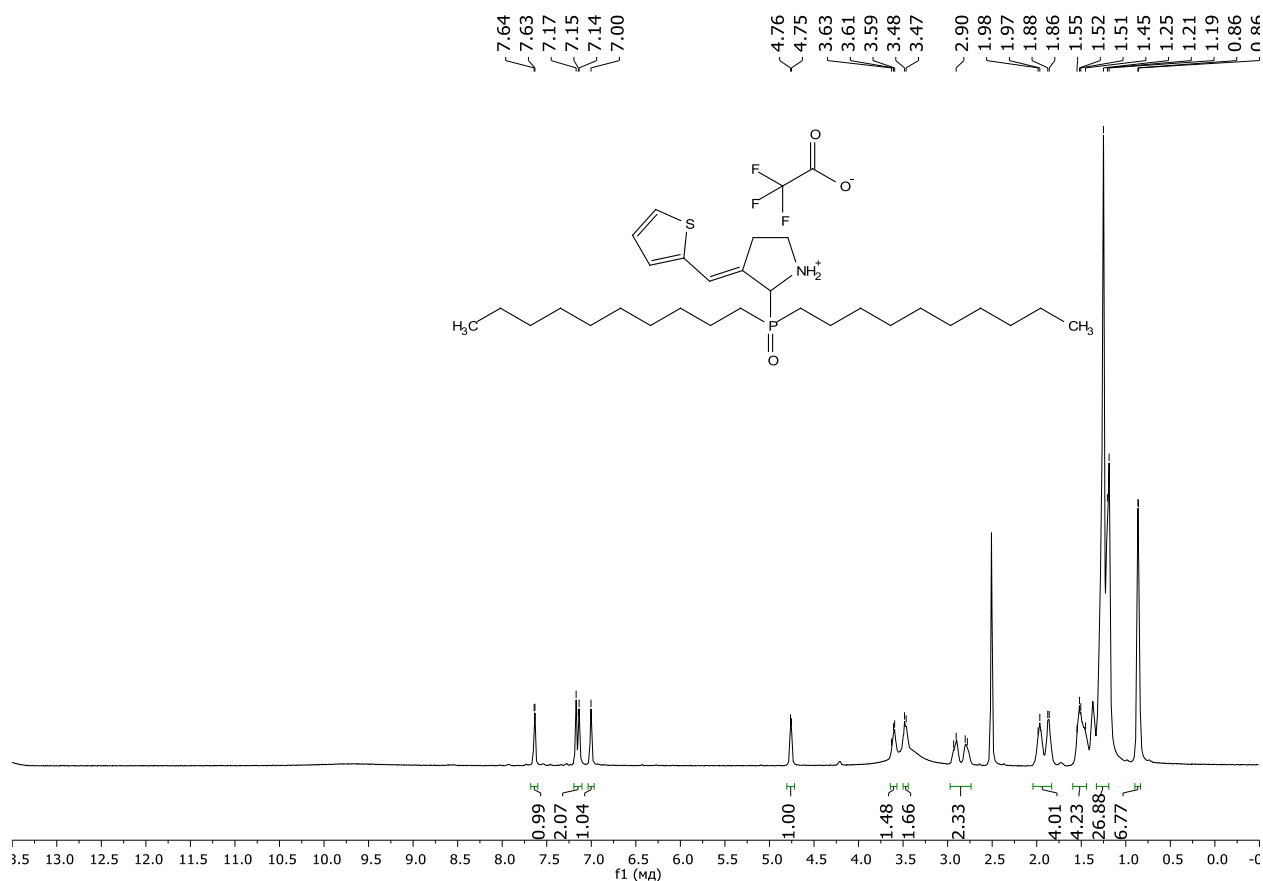


Figure S82. ¹H NMR (DMSO-*d*₆, 600 MHz) spectrum of the compound **3ba**

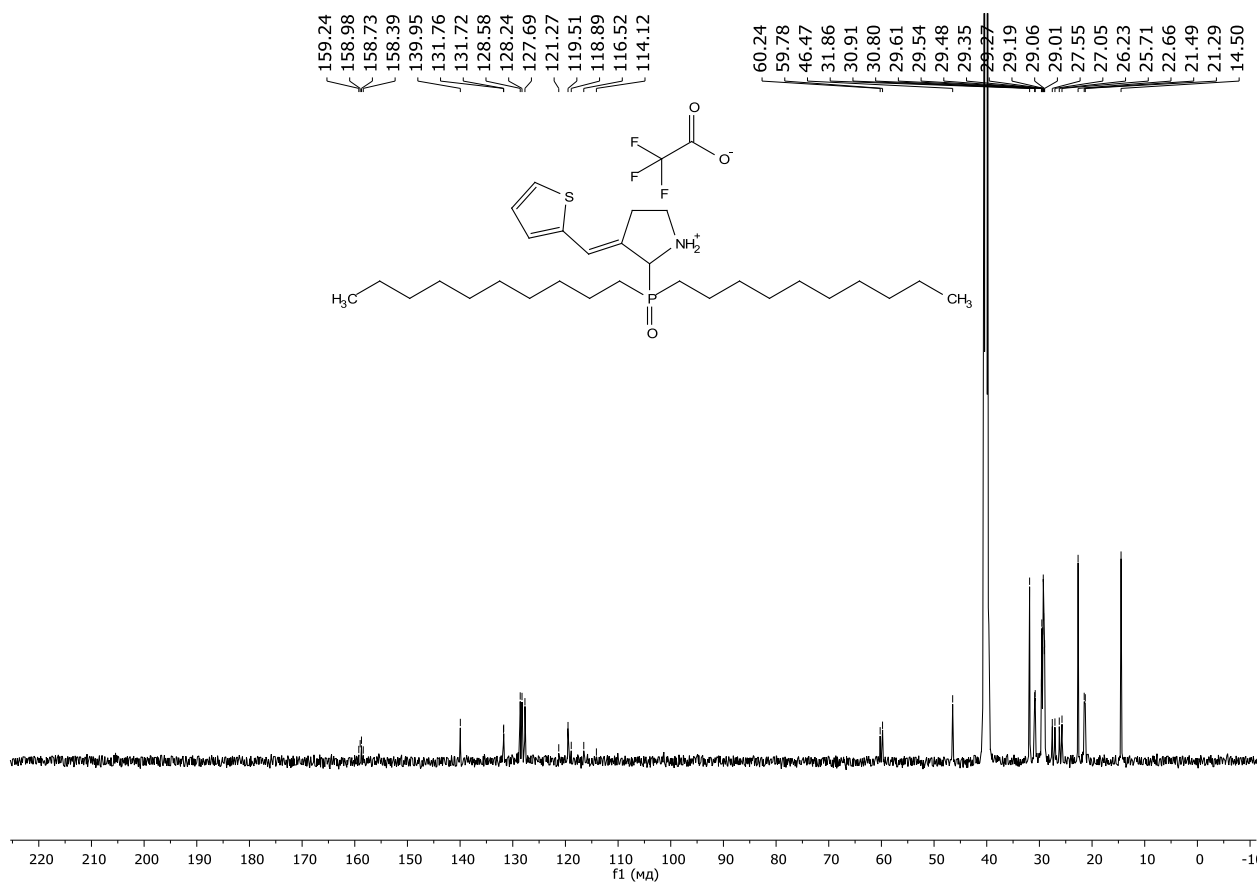


Figure S83. ¹³C{¹H} NMR (DMSO-*d*₆, 150 MHz) spectrum of the compound **3ba**

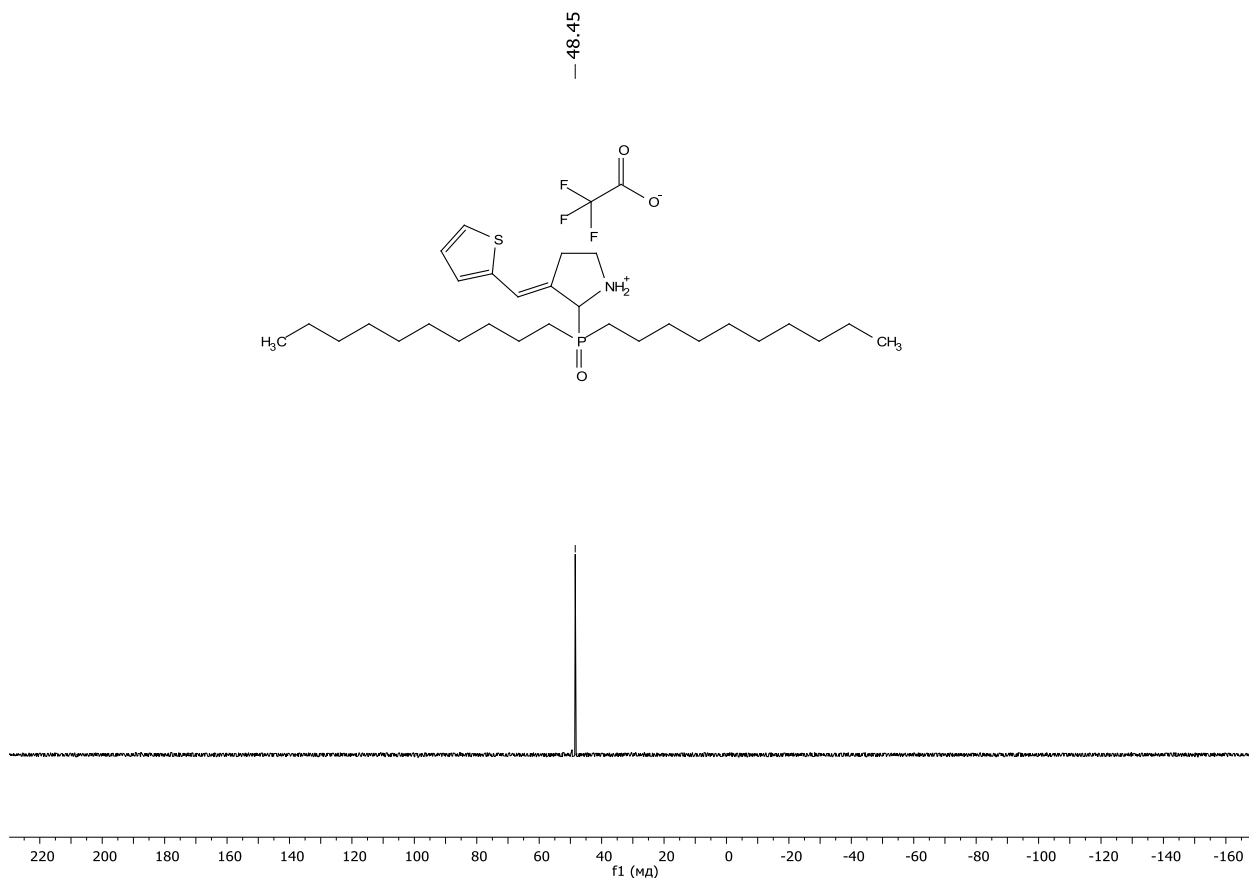


Figure S84. $^{31}\text{P}\{^1\text{H}\}$ NMR (DMSO- d_6 , 161 MHz) spectrum of the compound **3ba**

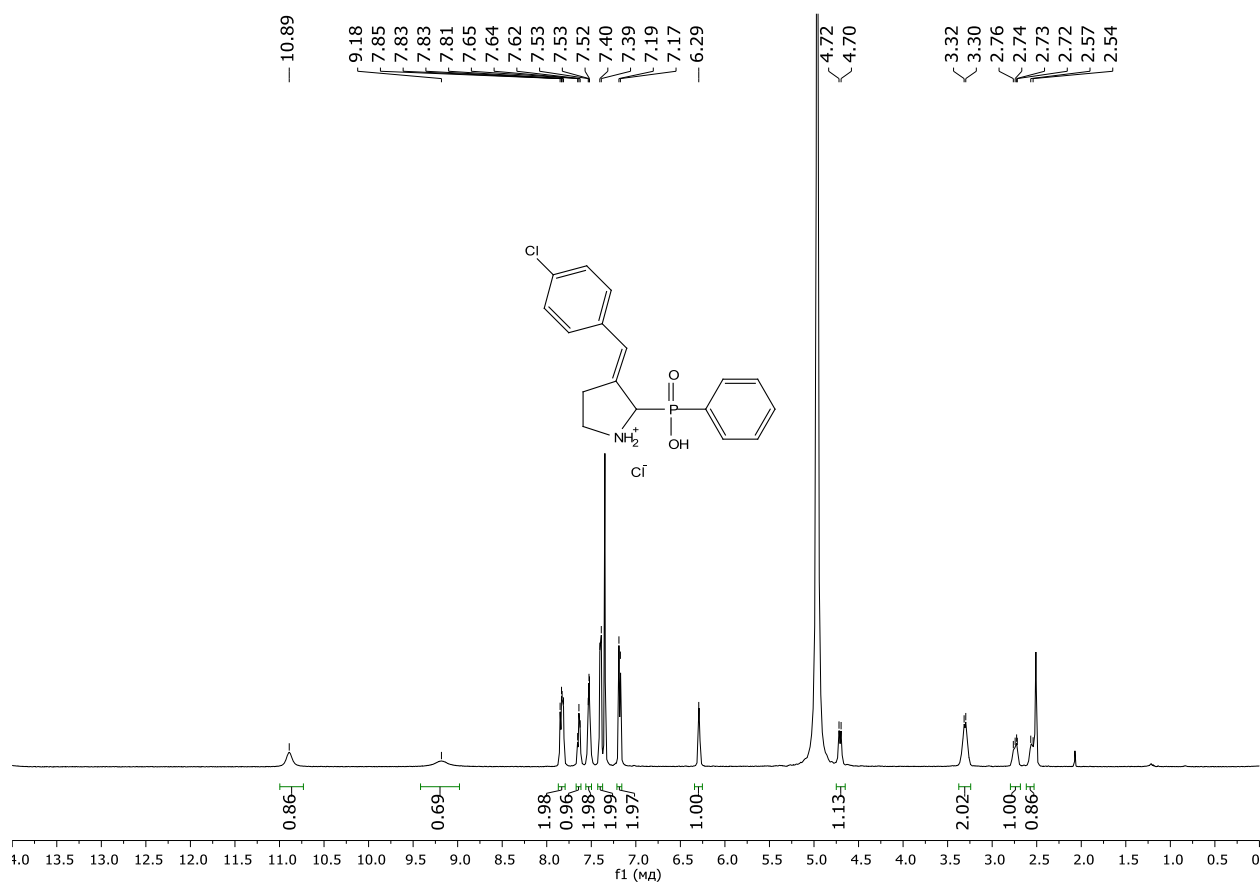


Figure S85. ^1H NMR (DMSO- d_6 , 600 MHz) spectrum of the compound **3bb**

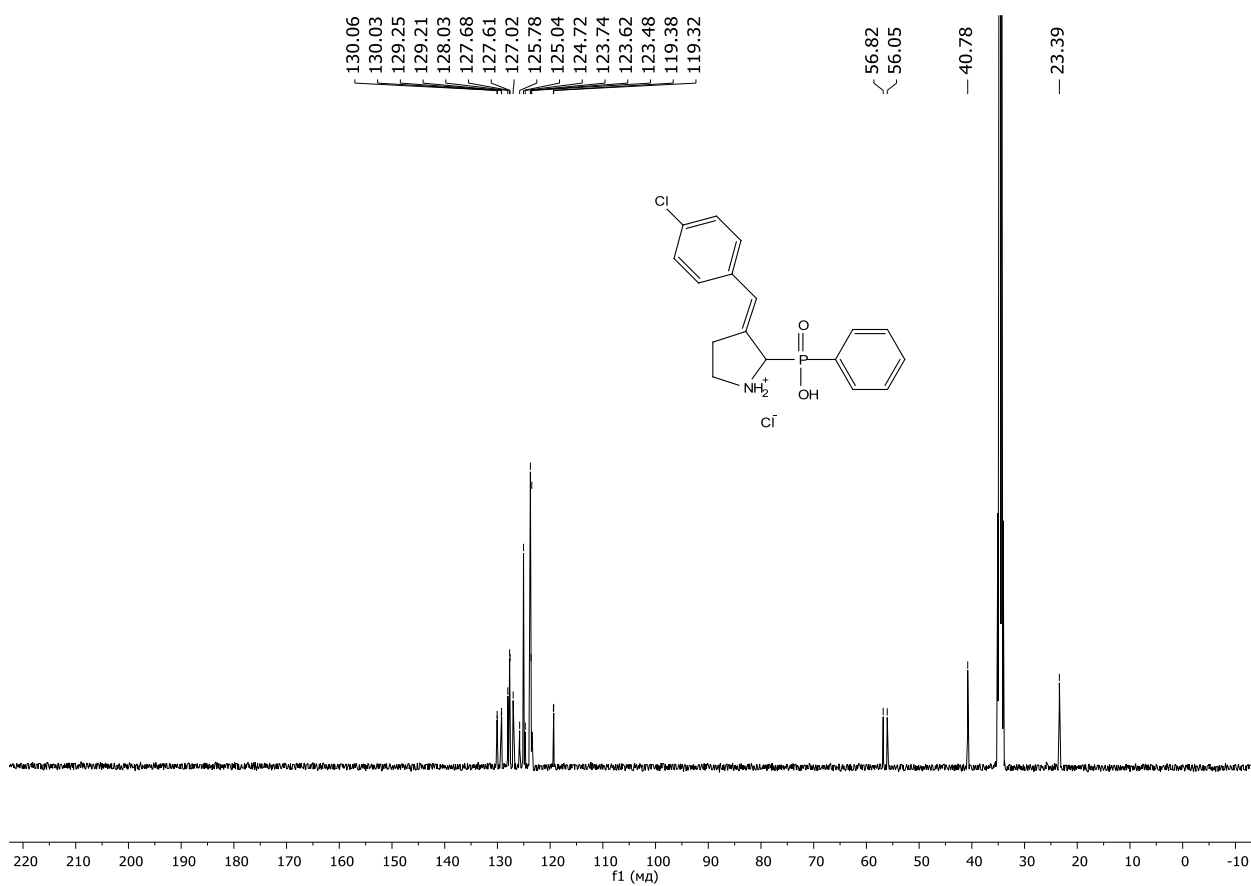


Figure S86. $^{13}\text{C}\{^1\text{H}\}$ NMR (DMSO- d_6 , 150 MHz) spectrum of the compound **3bb**

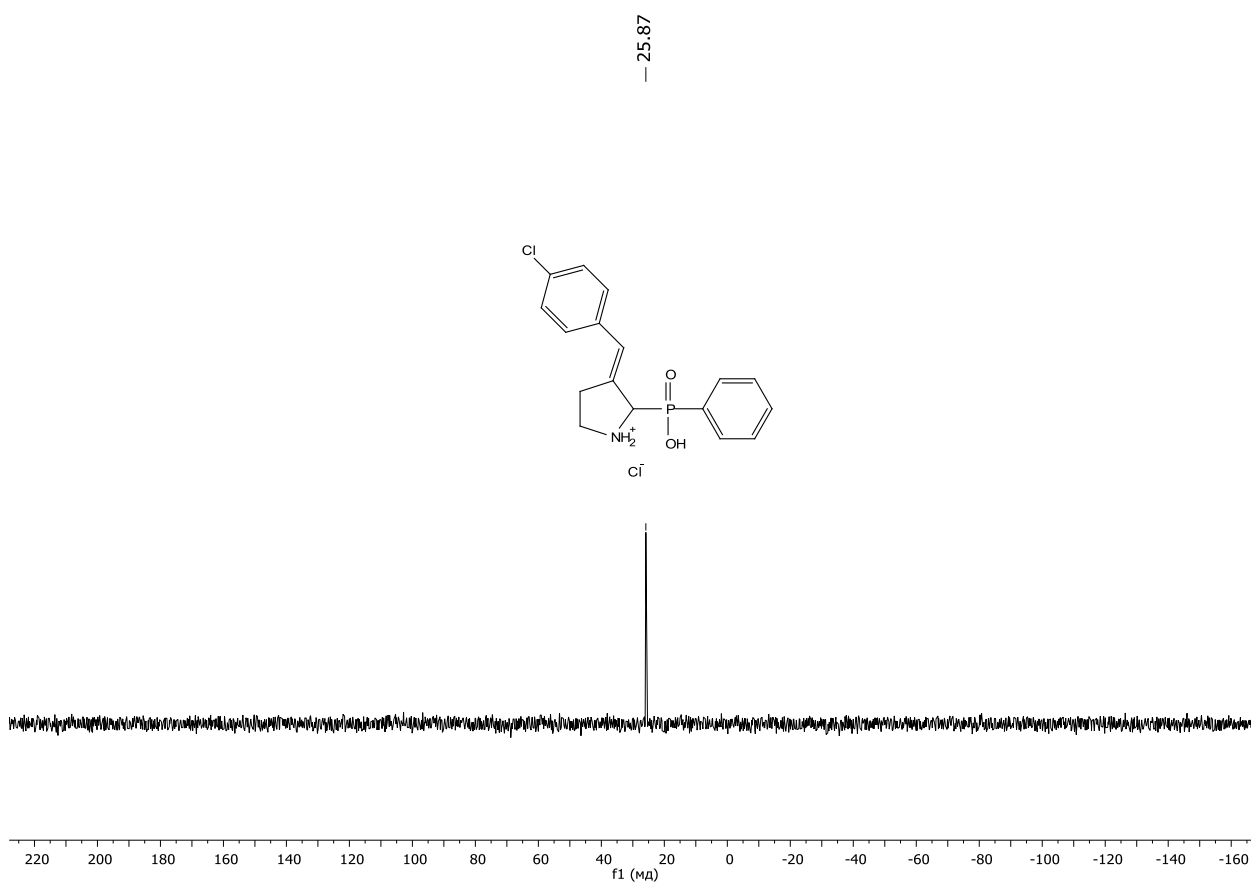
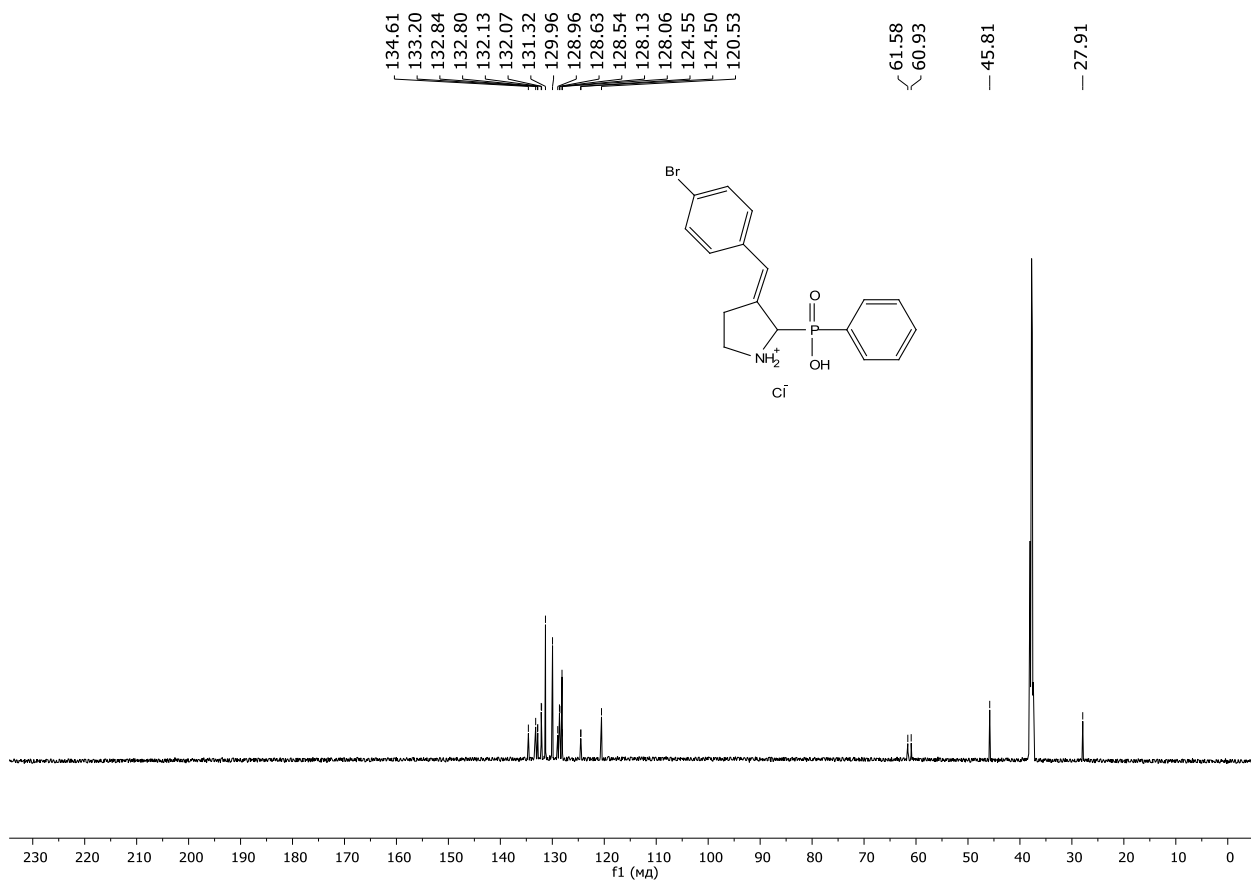
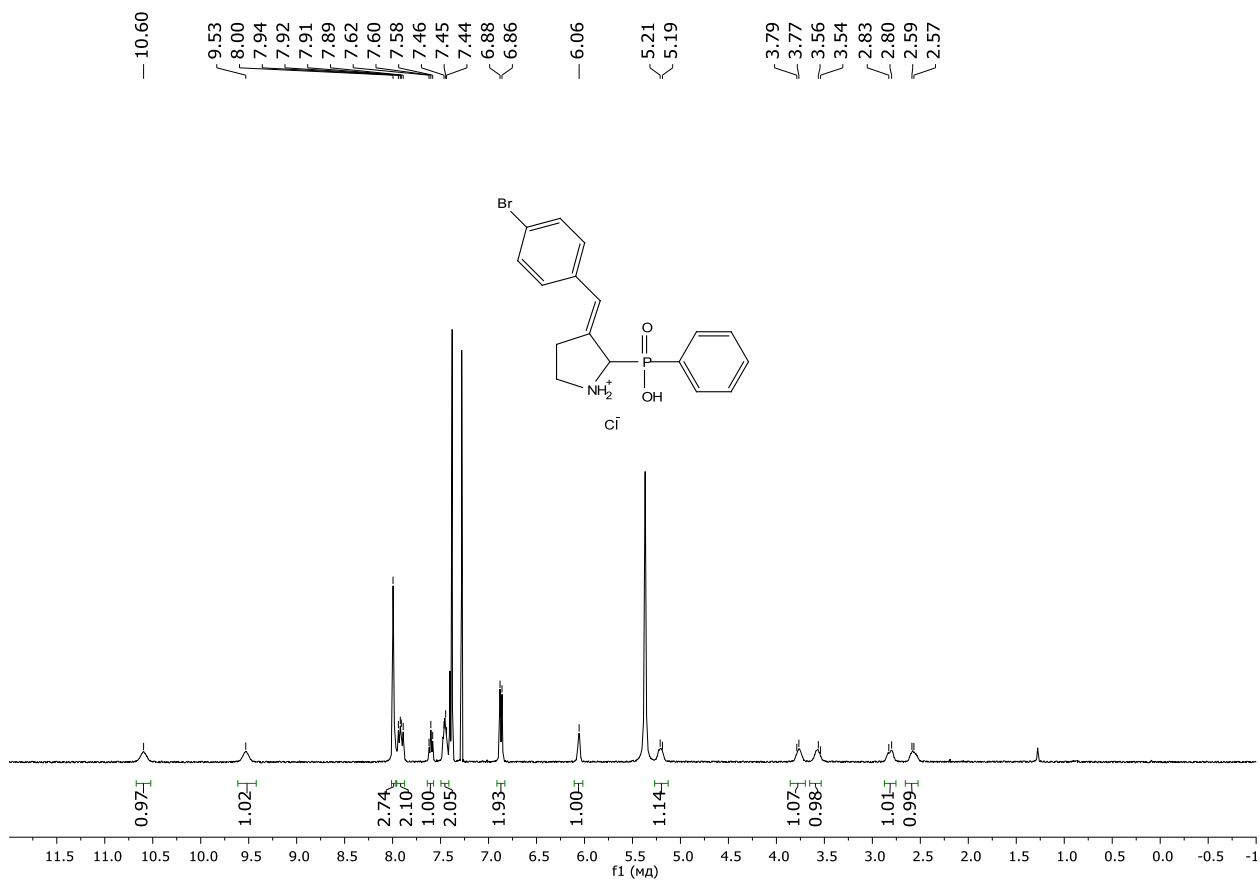


Figure S87. $^{31}\text{P}\{^1\text{H}\}$ NMR (DMSO- d_6 , 161 MHz) spectrum of the compound **3bb**



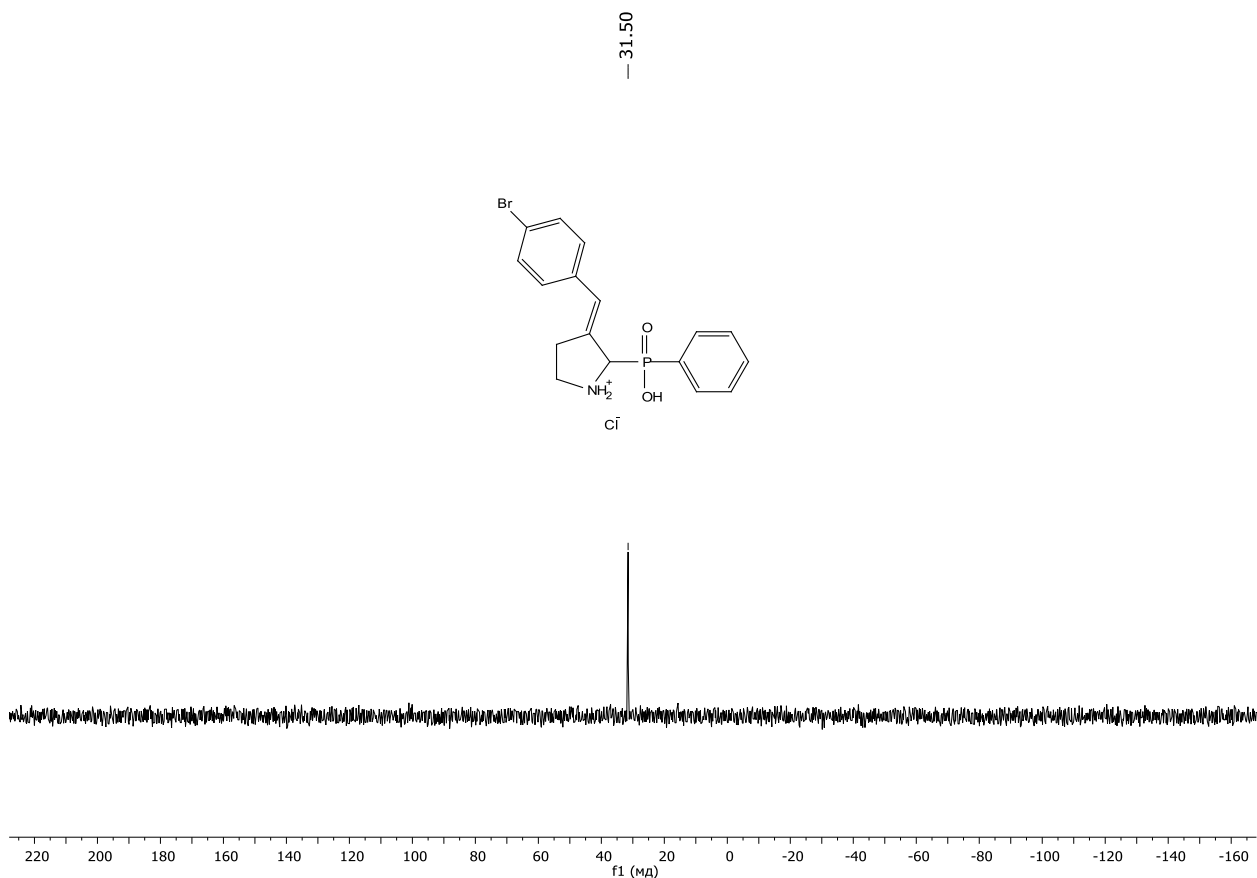


Figure S90. $^{31}\text{P}\{^1\text{H}\}$ NMR ($\text{DMSO-}d_6$, 161 MHz) spectrum of the compound **3bc**

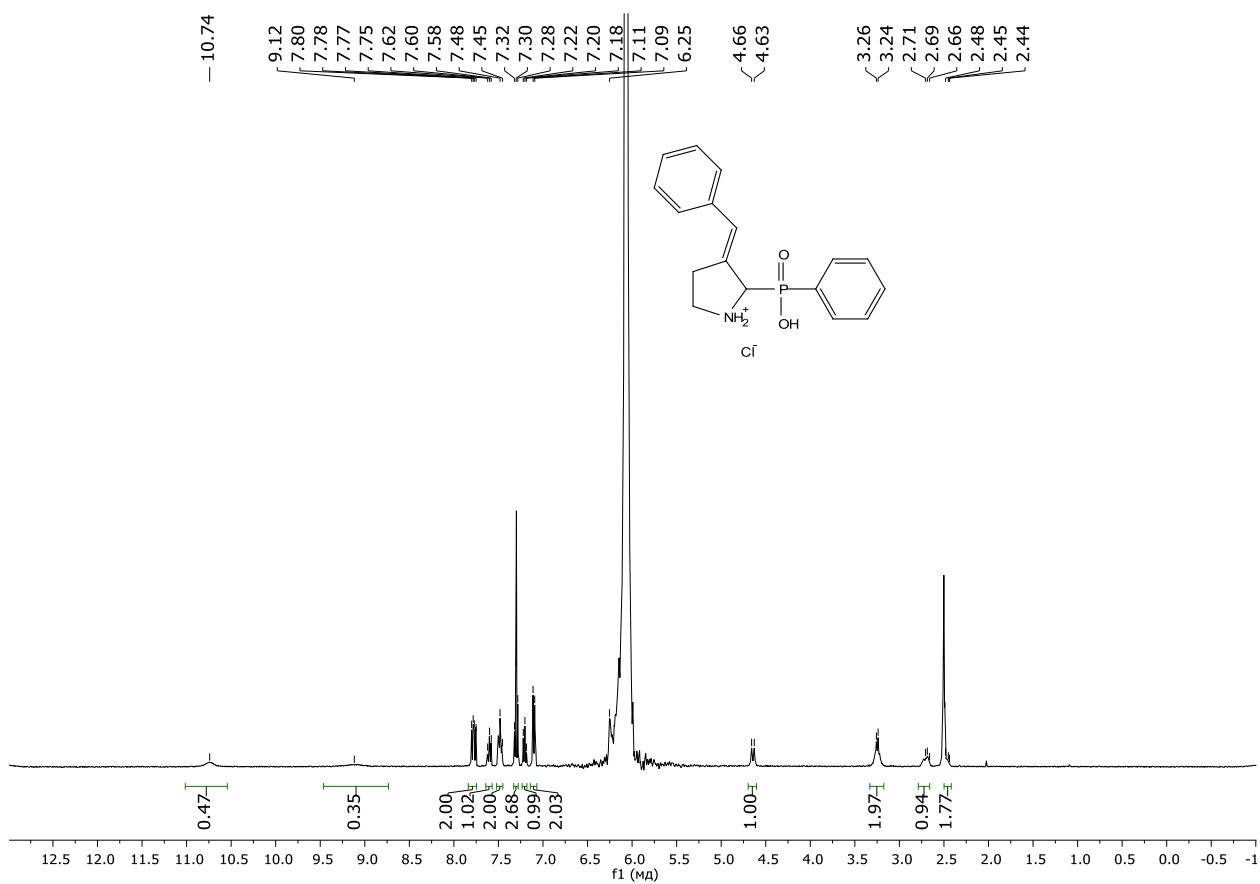


Figure S91. ^1H NMR ($\text{DMSO-}d_6$, 600 MHz) spectrum of the compound **3bd**

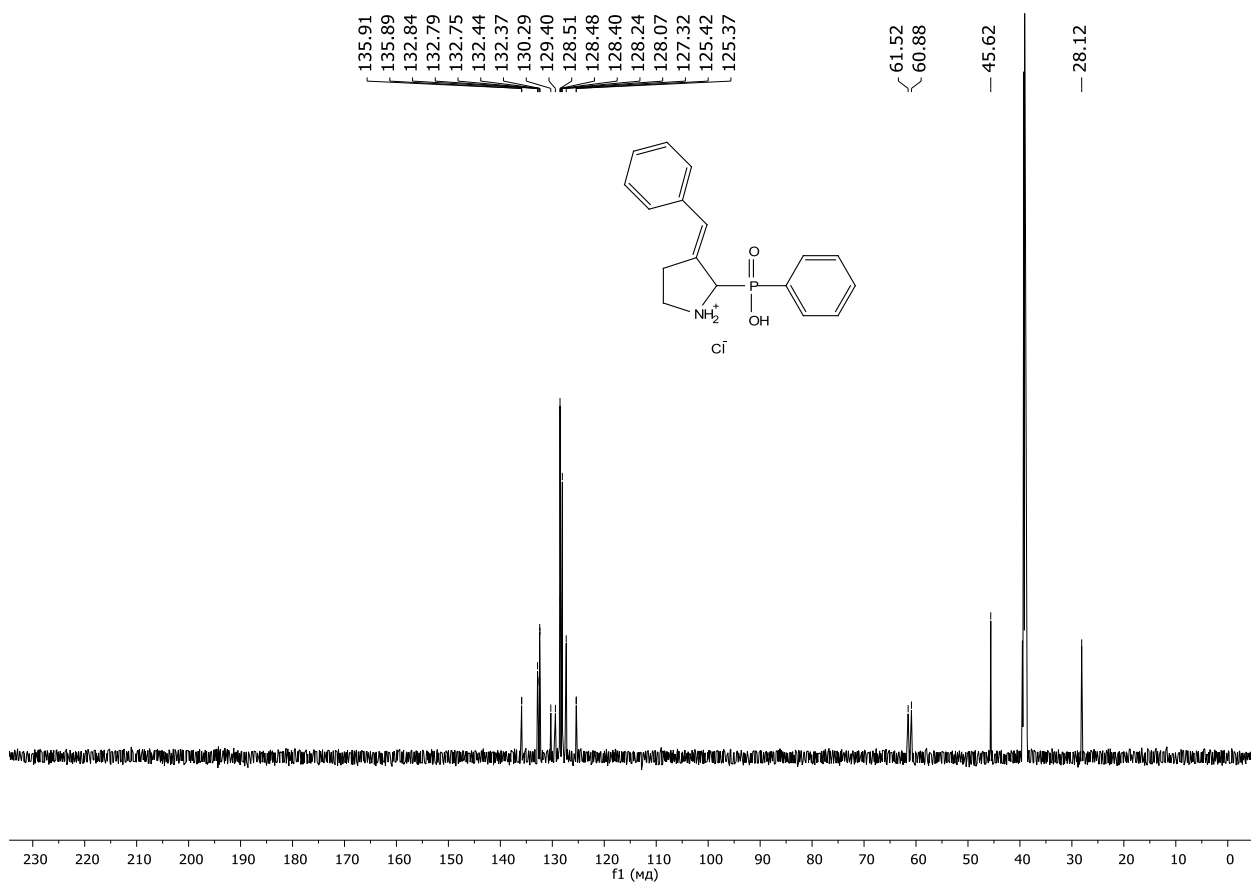


Figure S92. $^{13}\text{C}\{^1\text{H}\}$ NMR (DMSO- d_6 , 150 MHz) spectrum of the compound **3bd**

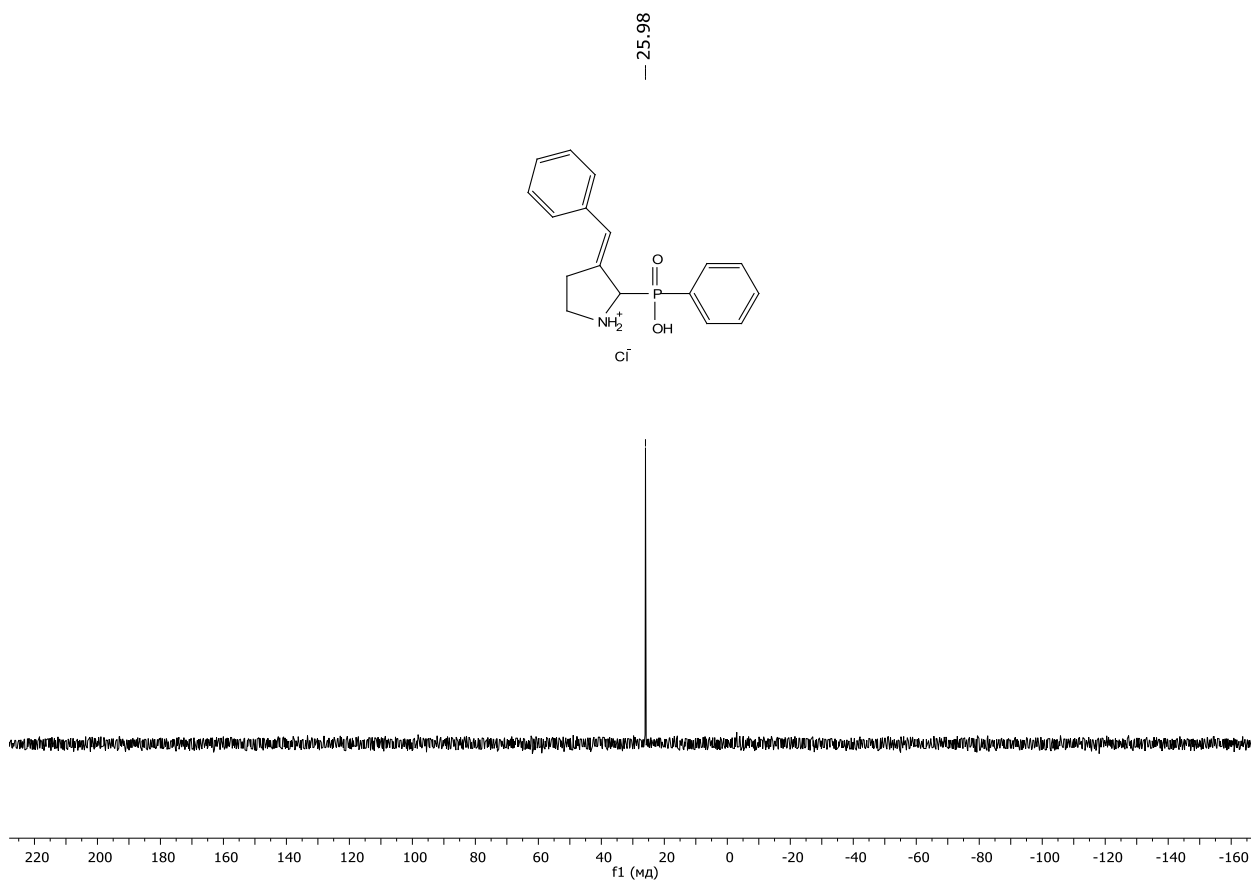


Figure S93. $^{31}\text{P}\{^1\text{H}\}$ NMR (DMSO- d_6 , 161 MHz) spectrum of the compound **3bd**

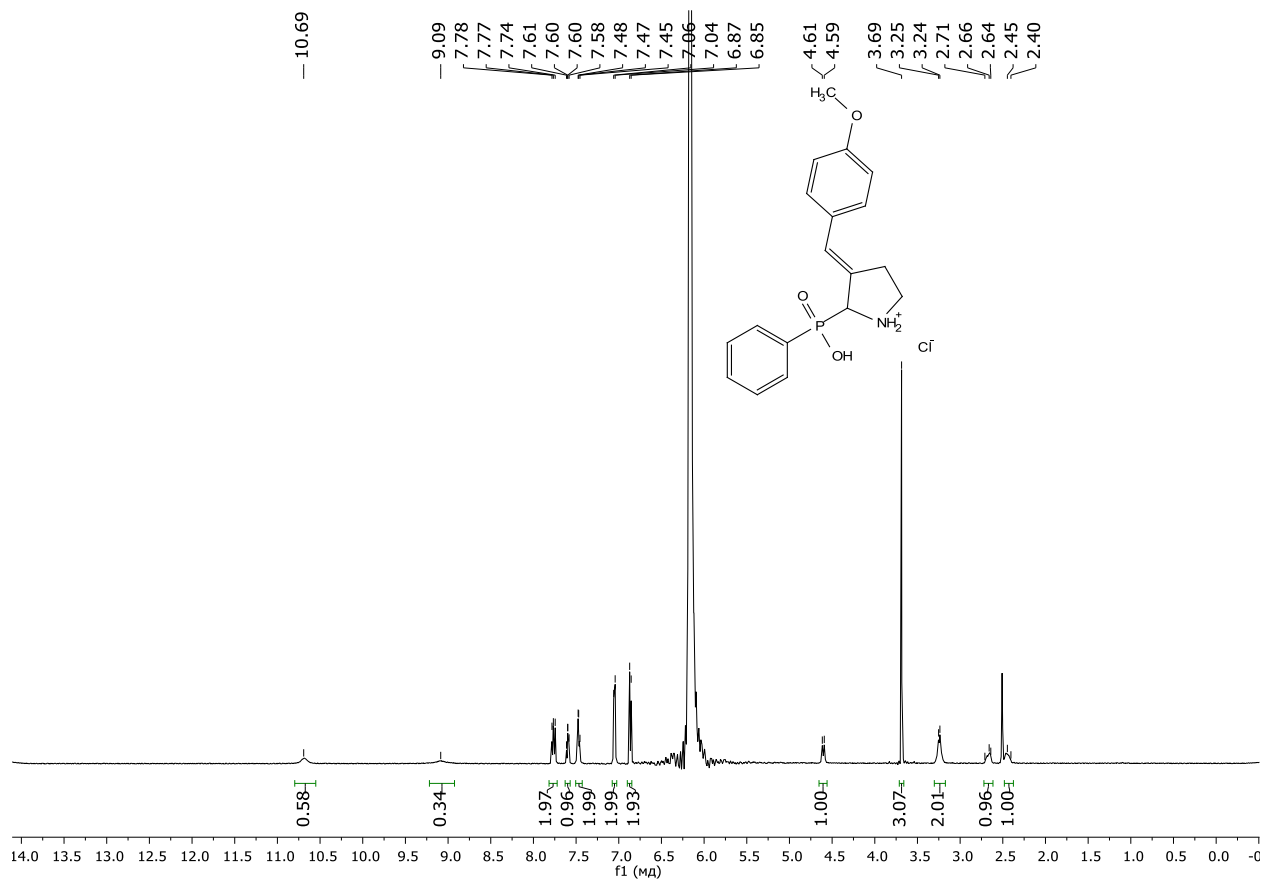


Figure S94. ^1H NMR ($\text{DMSO-}d_6$, 600 MHz) spectrum of the compound **3be**

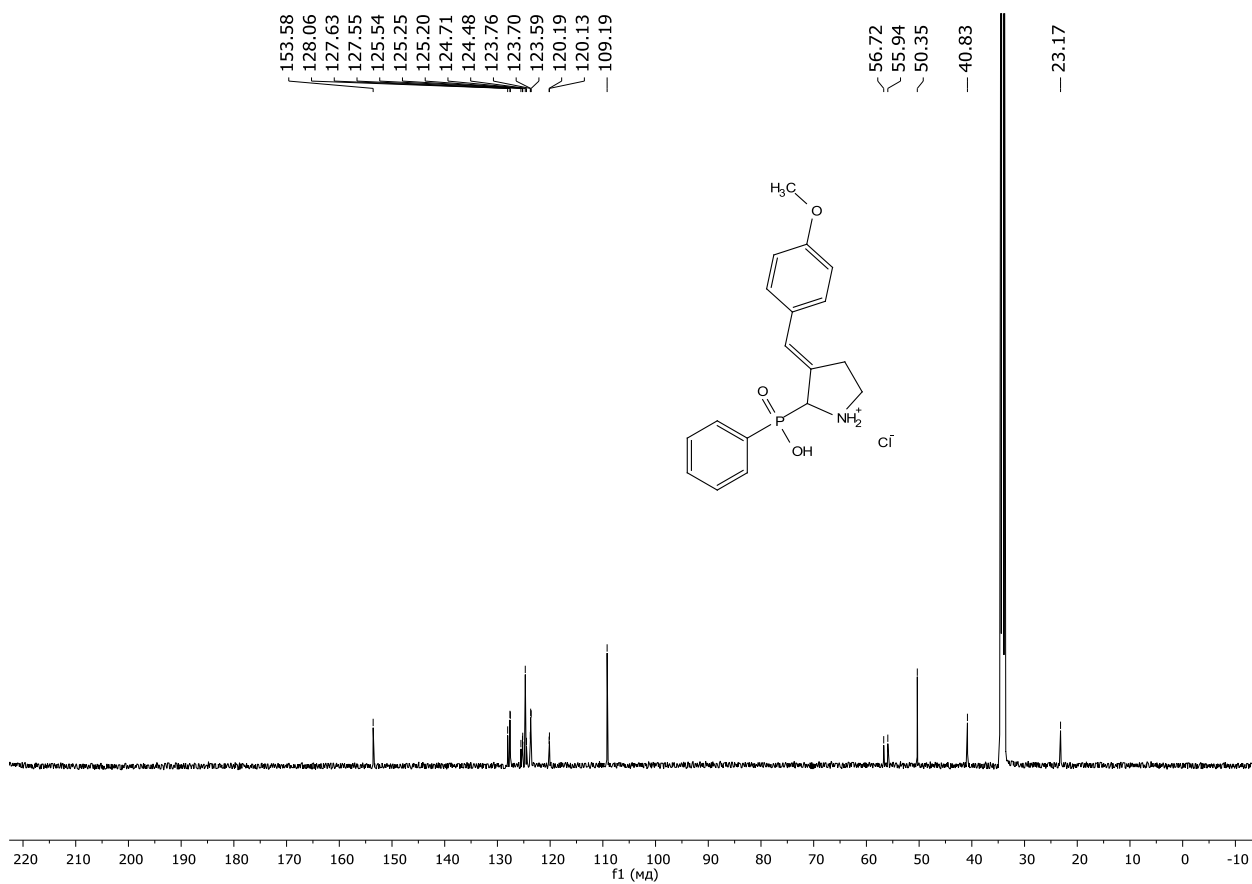


Figure S95. $^{13}\text{C}\{^1\text{H}\}$ NMR ($\text{DMSO-}d_6$, 150 MHz) spectrum of the compound **3be**

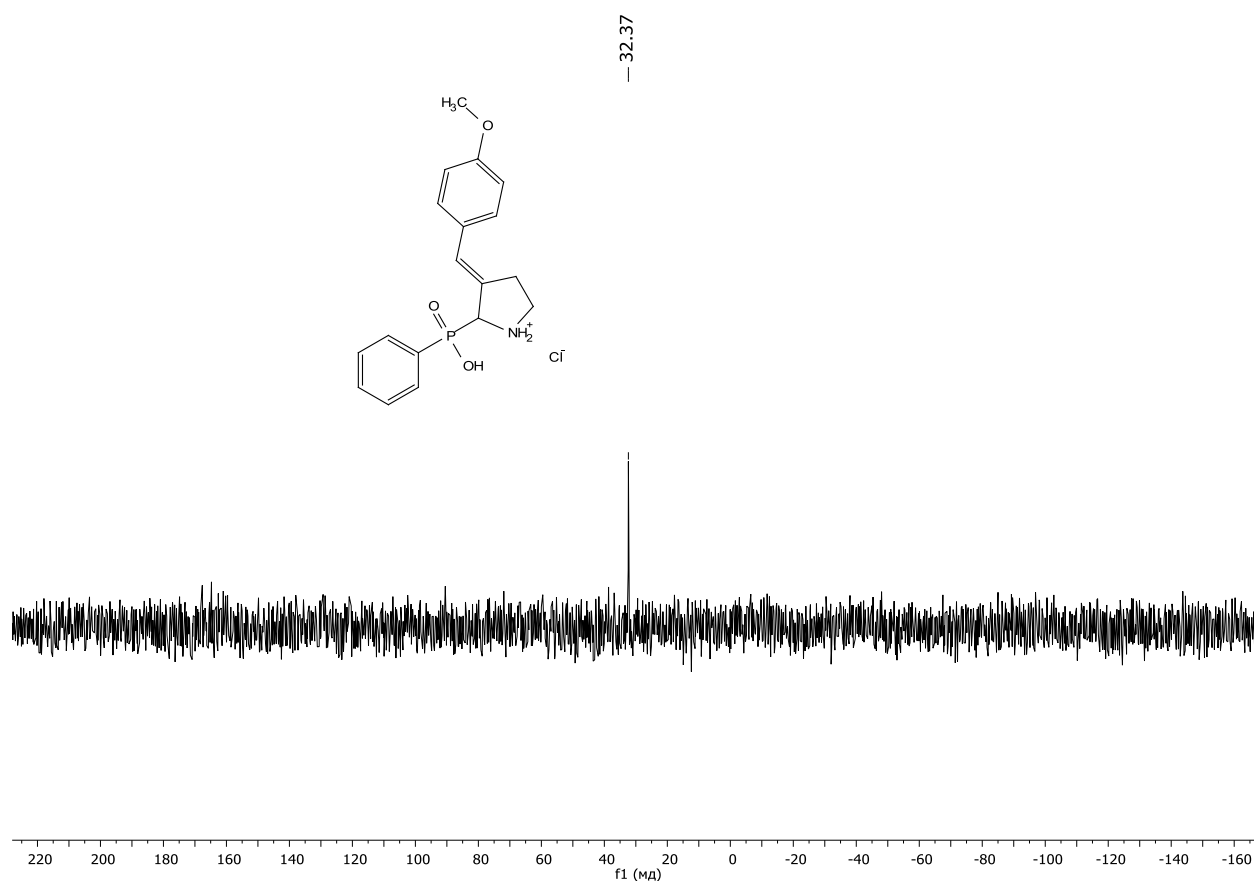


Figure S96. $^{31}\text{P}\{^1\text{H}\}$ NMR ($\text{DMSO-}d_6$, 161 MHz) spectrum of the compound **3be**

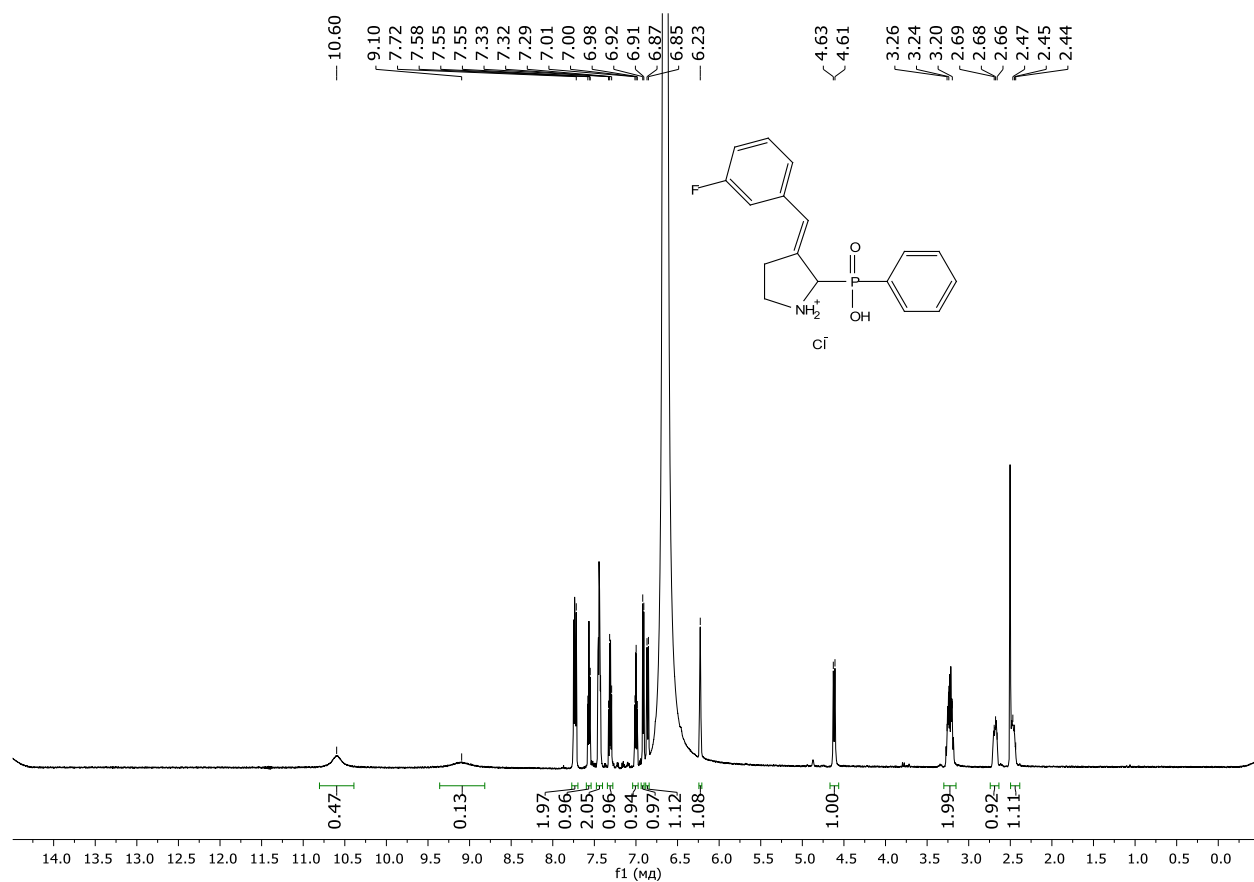


Figure S97. ^1H NMR ($\text{DMSO-}d_6$, 600 MHz) spectrum of the compound **3bf**

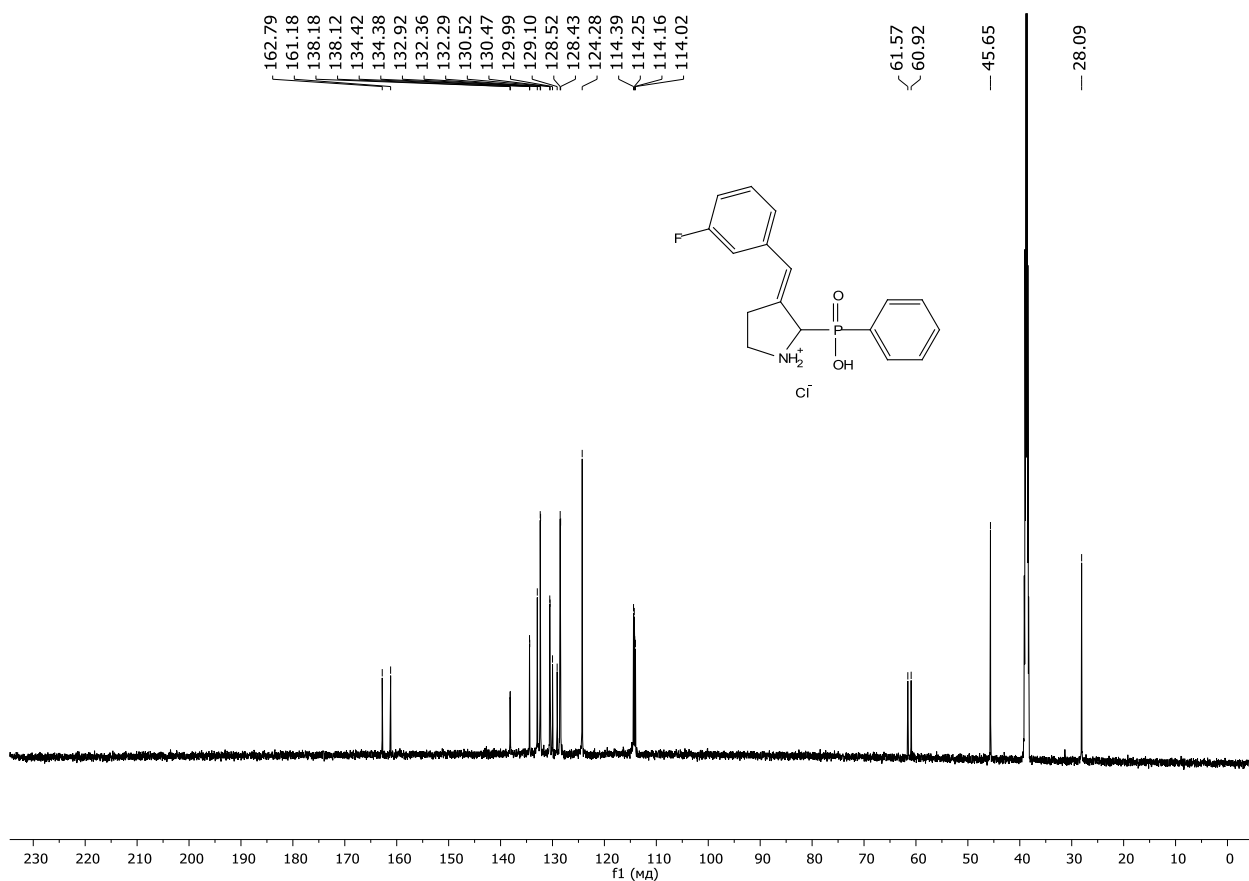


Figure S98. $^{13}\text{C}\{^1\text{H}\}$ NMR (DMSO- d_6 , 150 MHz) spectrum of the compound **3bf**

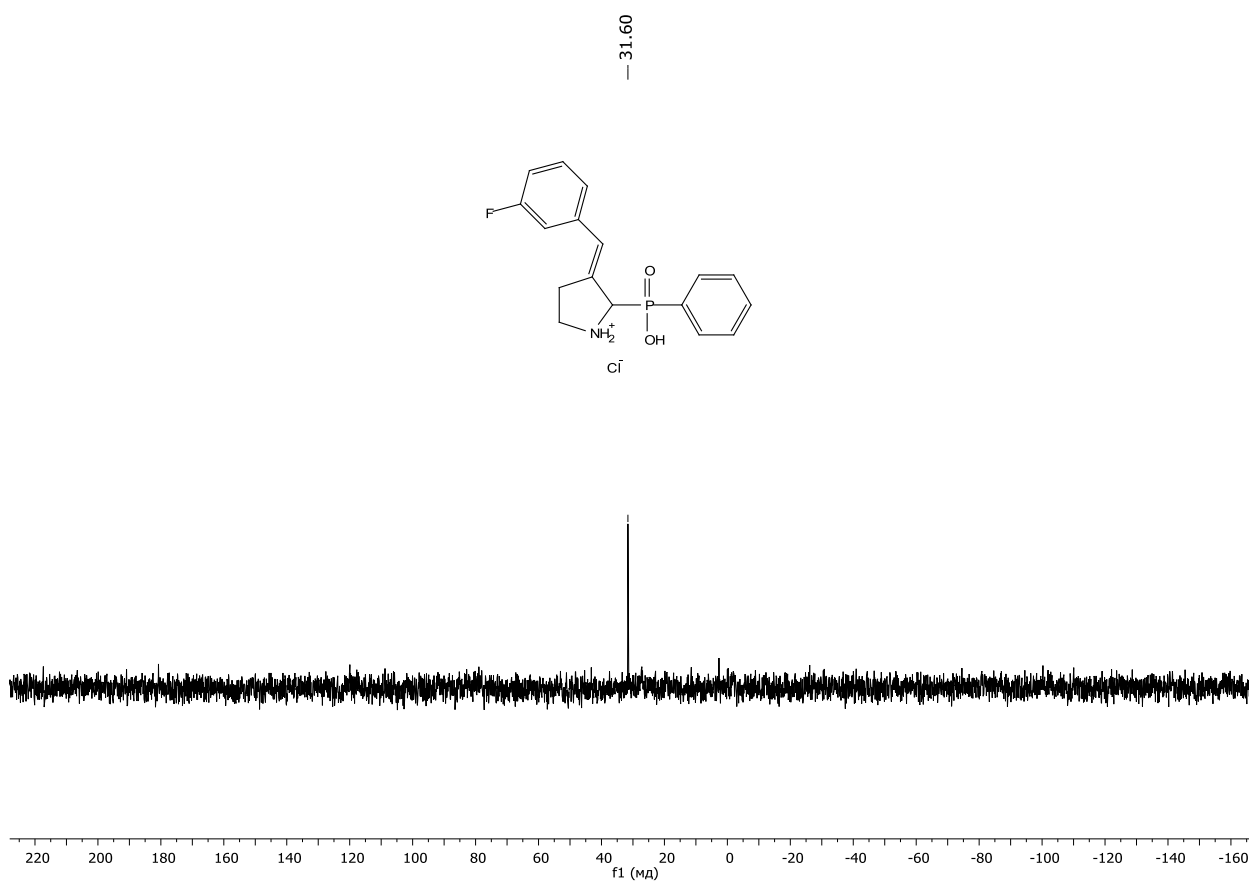


Figure S99. $^{31}\text{P}\{^1\text{H}\}$ NMR (DMSO- d_6 , 161 MHz) spectrum of the compound **3bf**

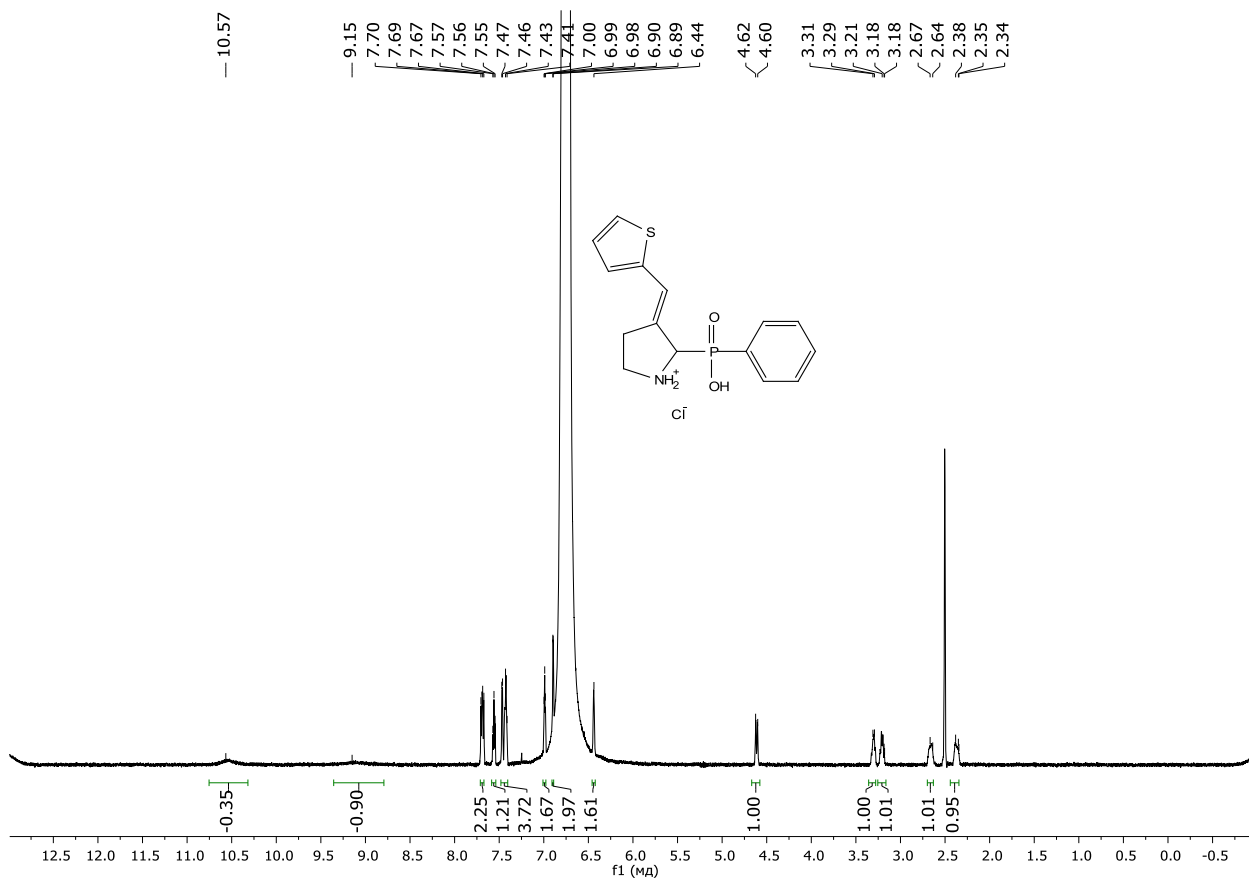


Figure S100. ^1H NMR (DMSO- d_6 , 600 MHz) spectrum of the compound **3bg**

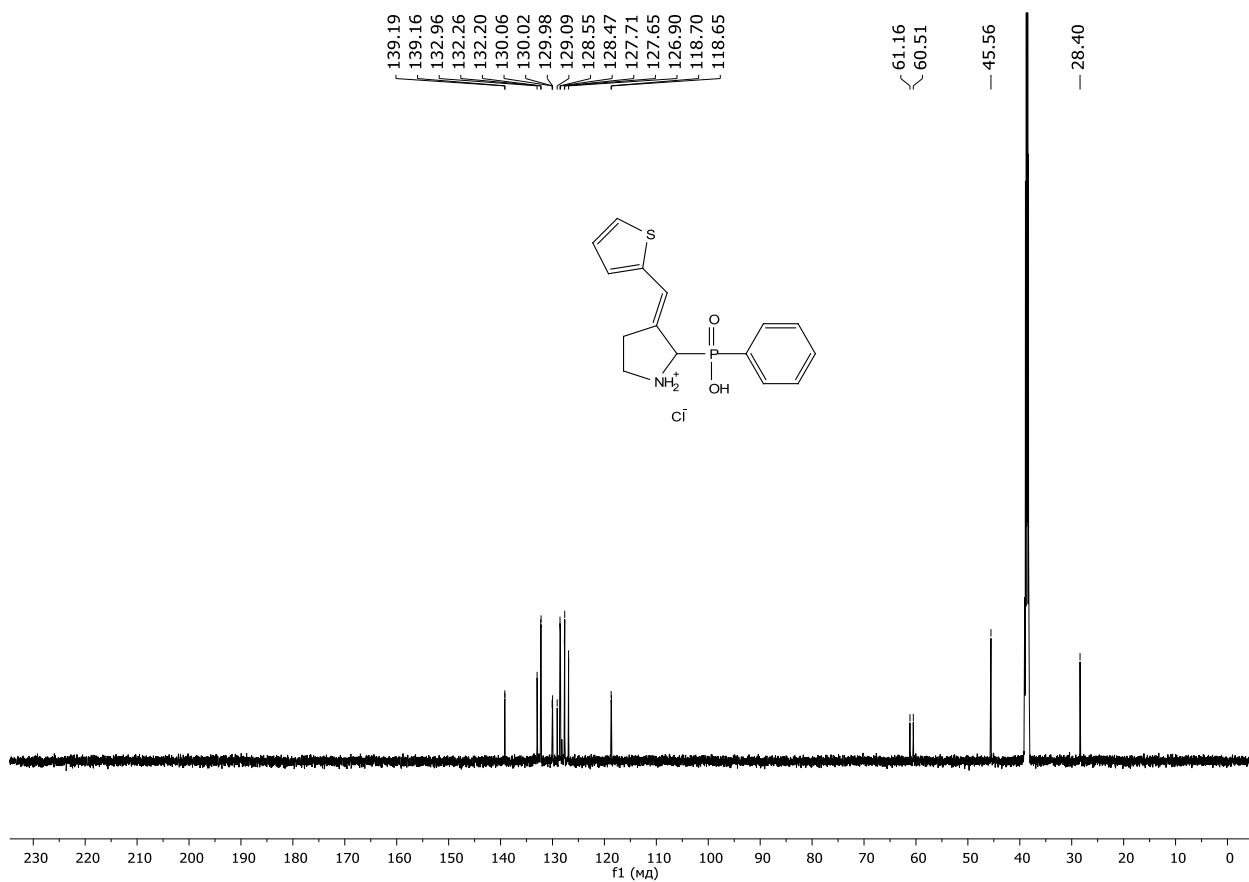


Figure S101. $^{13}\text{C}\{^1\text{H}\}$ NMR (DMSO- d_6 , 150 MHz) spectrum of the compound **3bg**

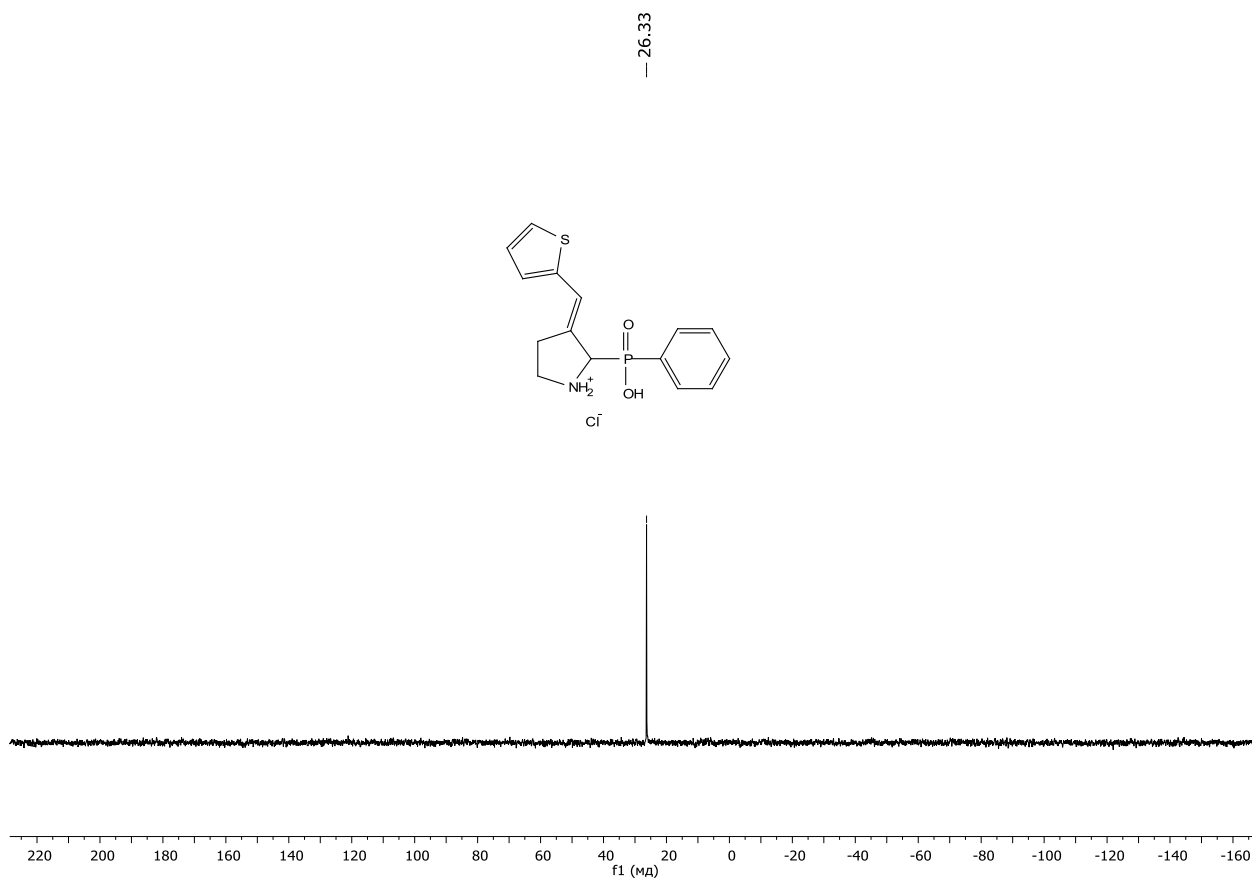


Figure S102. $^{31}\text{P}\{^1\text{H}\}$ NMR (DMSO- d_6 , 161 MHz) spectrum of the compound **3bg**

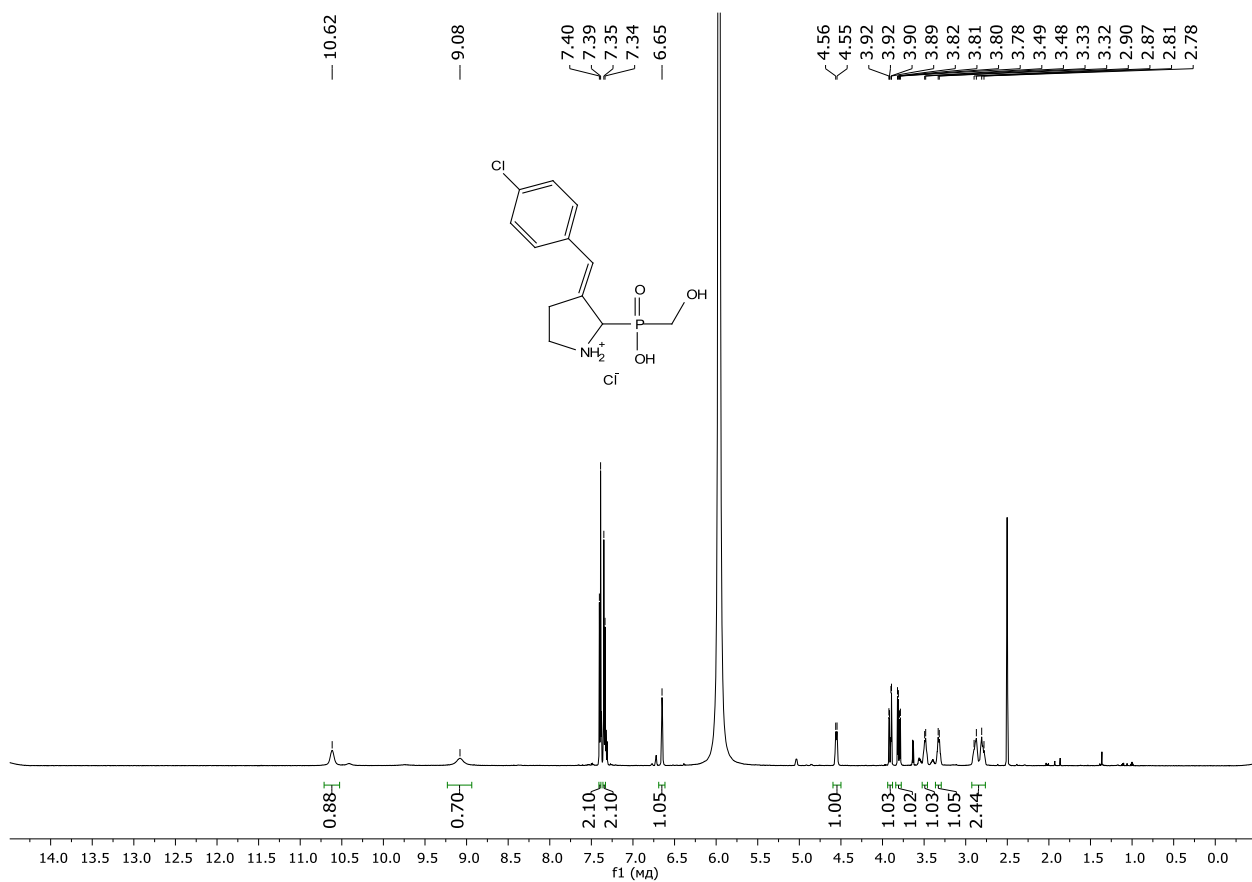


Figure S103. ^1H NMR (DMSO- d_6 , 600 MHz) spectrum of the compound **3bh**

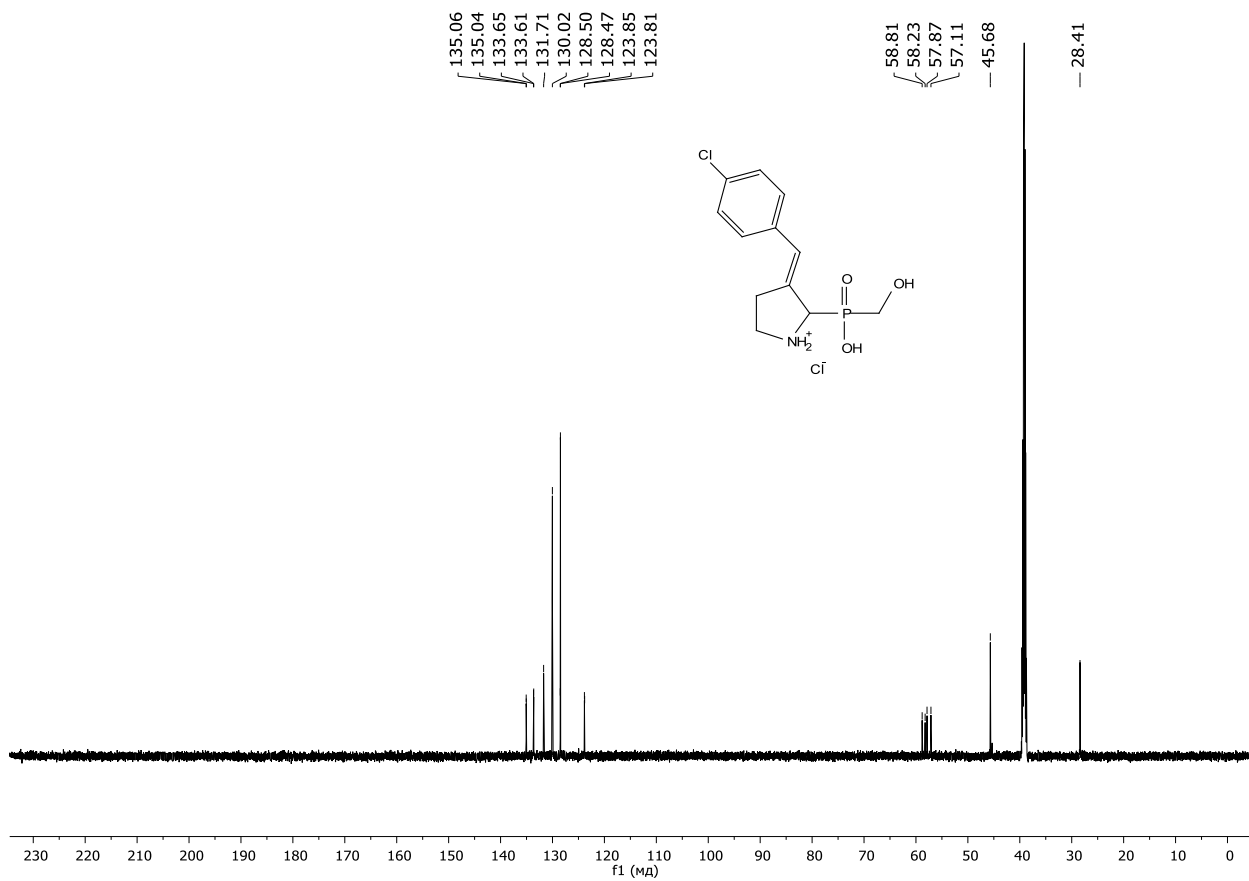


Figure S104. $^{13}\text{C}\{^1\text{H}\}$ NMR (DMSO- d_6 , 150 MHz) spectrum of the compound **3bh**

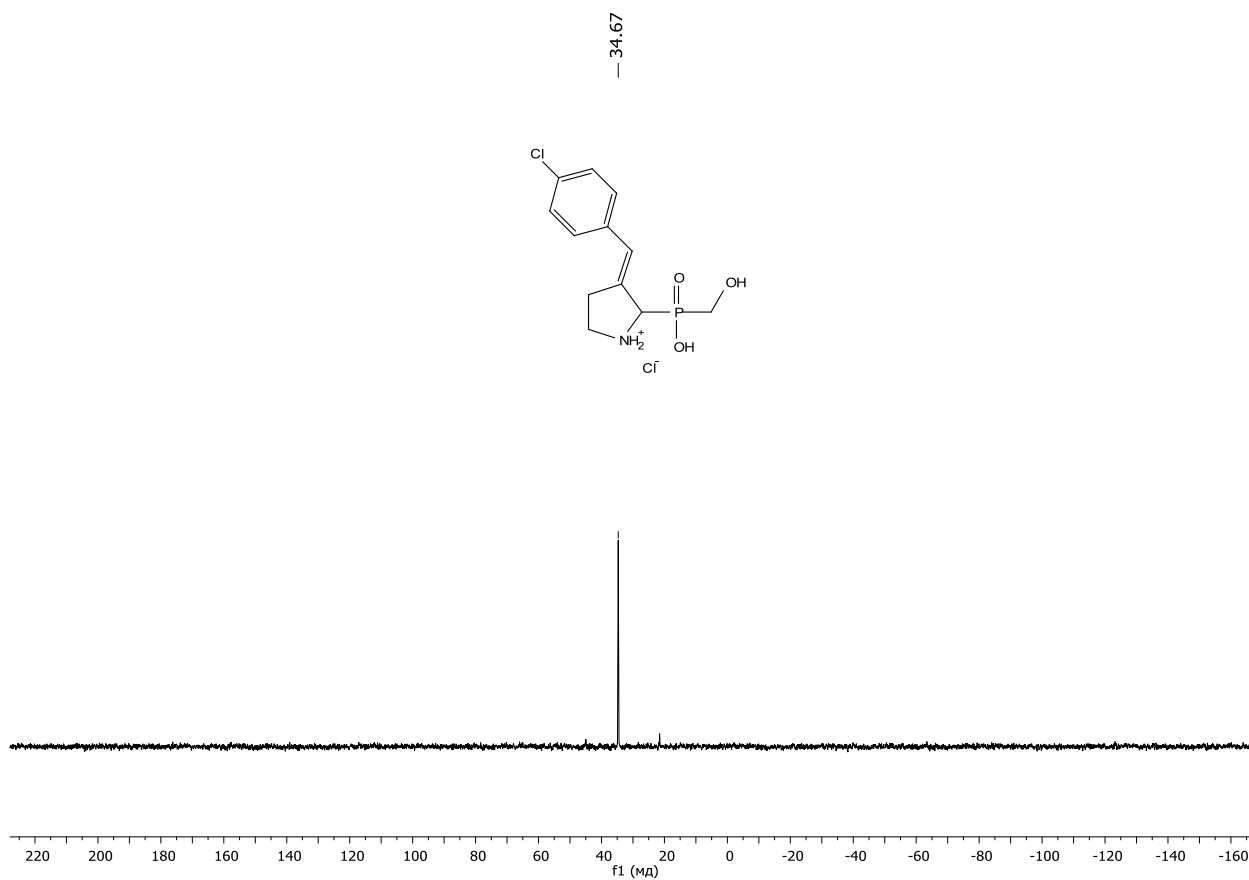


Figure S105. $^{31}\text{P}\{^1\text{H}\}$ NMR (DMSO- d_6 , 161 MHz) spectrum of the compound **3bh**

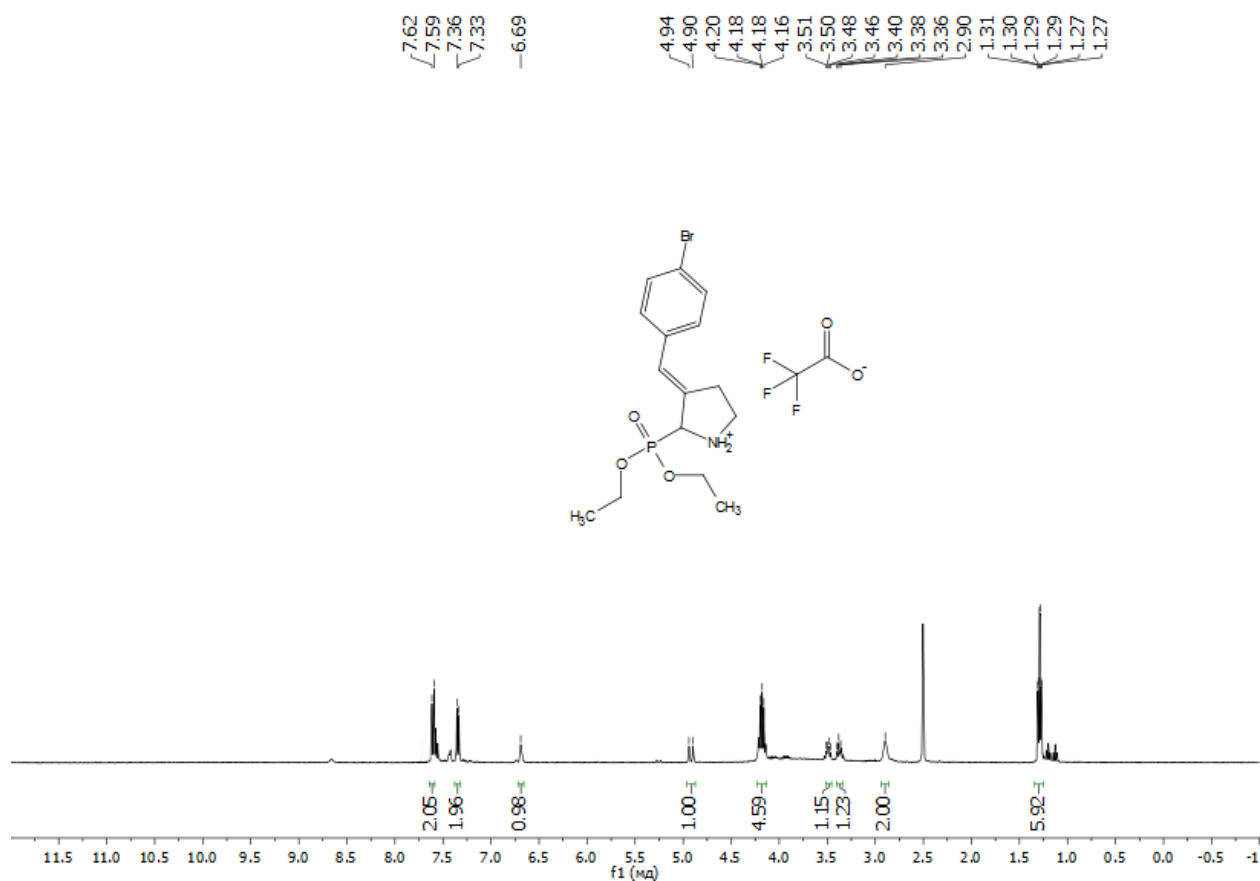


Figure S106. ¹H NMR (DMSO-*d*₆, 600 MHz) spectrum of the compound **3bi**

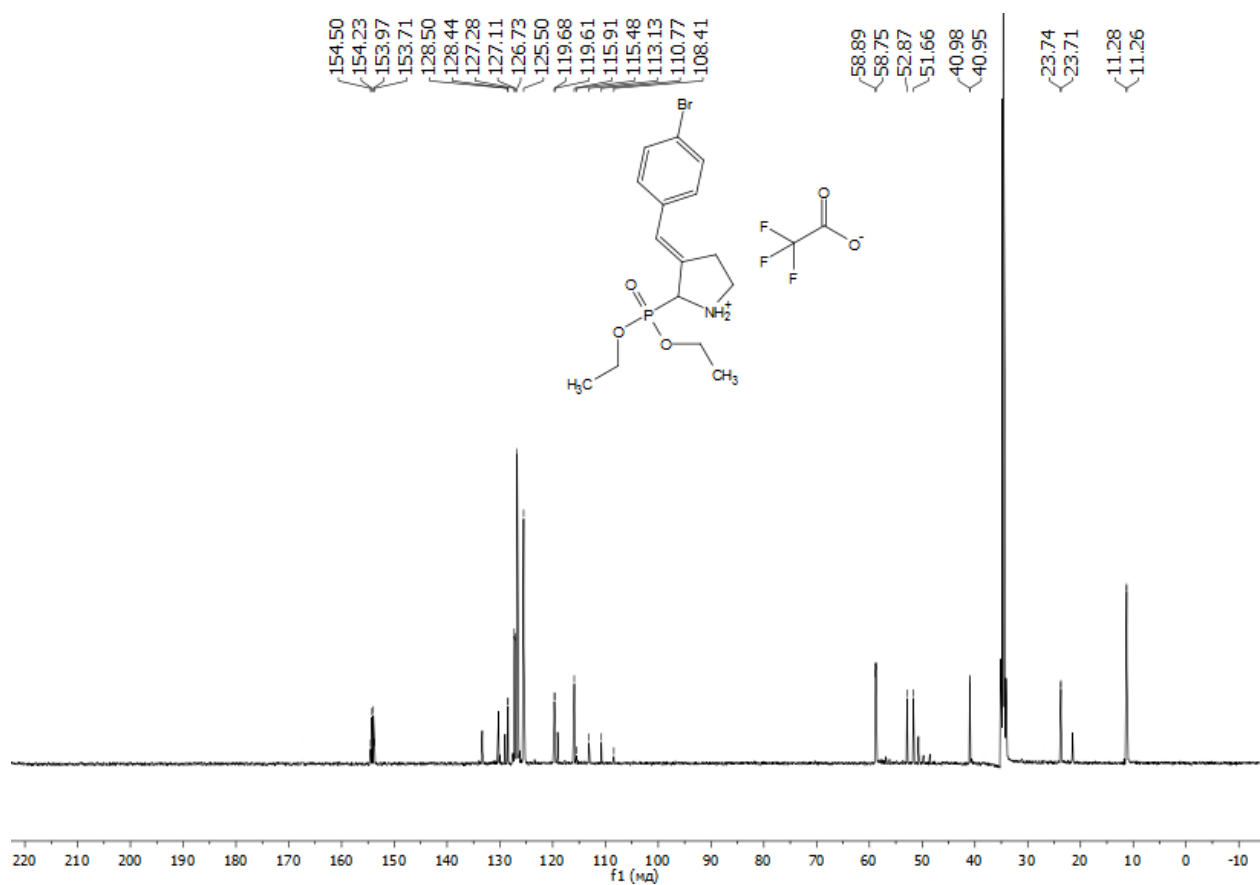


Figure S107. ¹³C{¹H} NMR (DMSO-*d*₆, 150 MHz) spectrum of the compound **3bi**

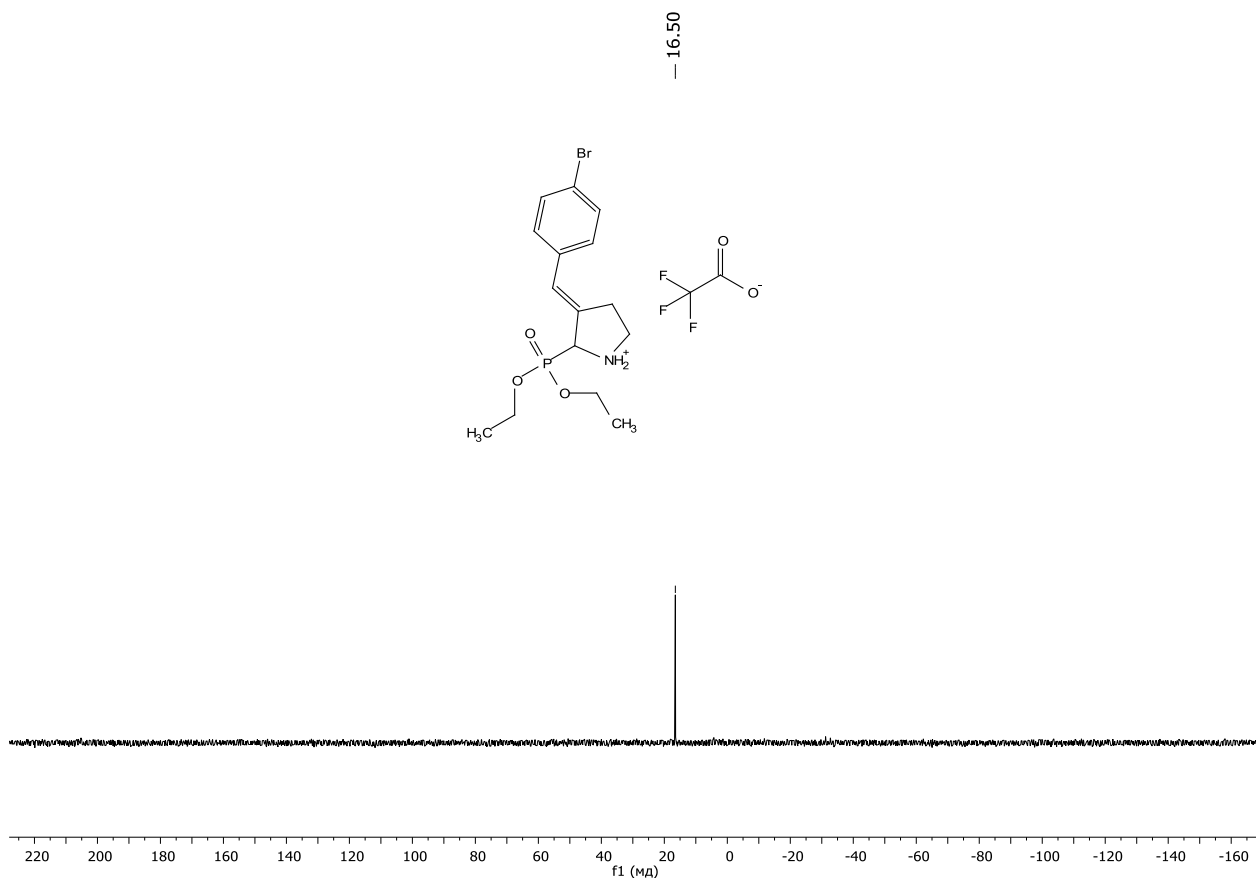


Figure S108. $^{31}\text{P}\{^1\text{H}\}$ NMR ($\text{DMSO-}d_6$, 161 MHz) spectrum of the compound **3bi**

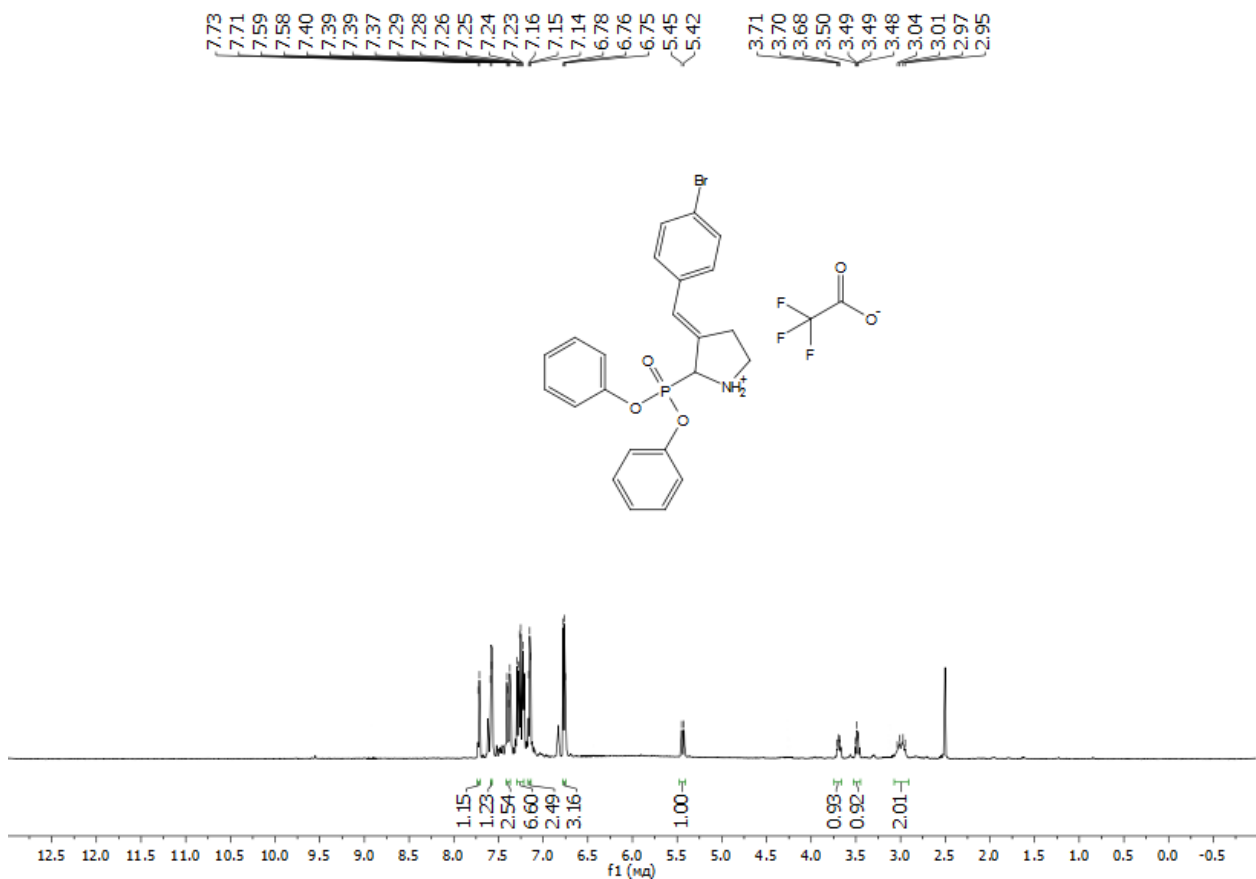


Figure S109. ^1H NMR ($\text{DMSO-}d_6$, 600 MHz) spectrum of the compound **3bj**

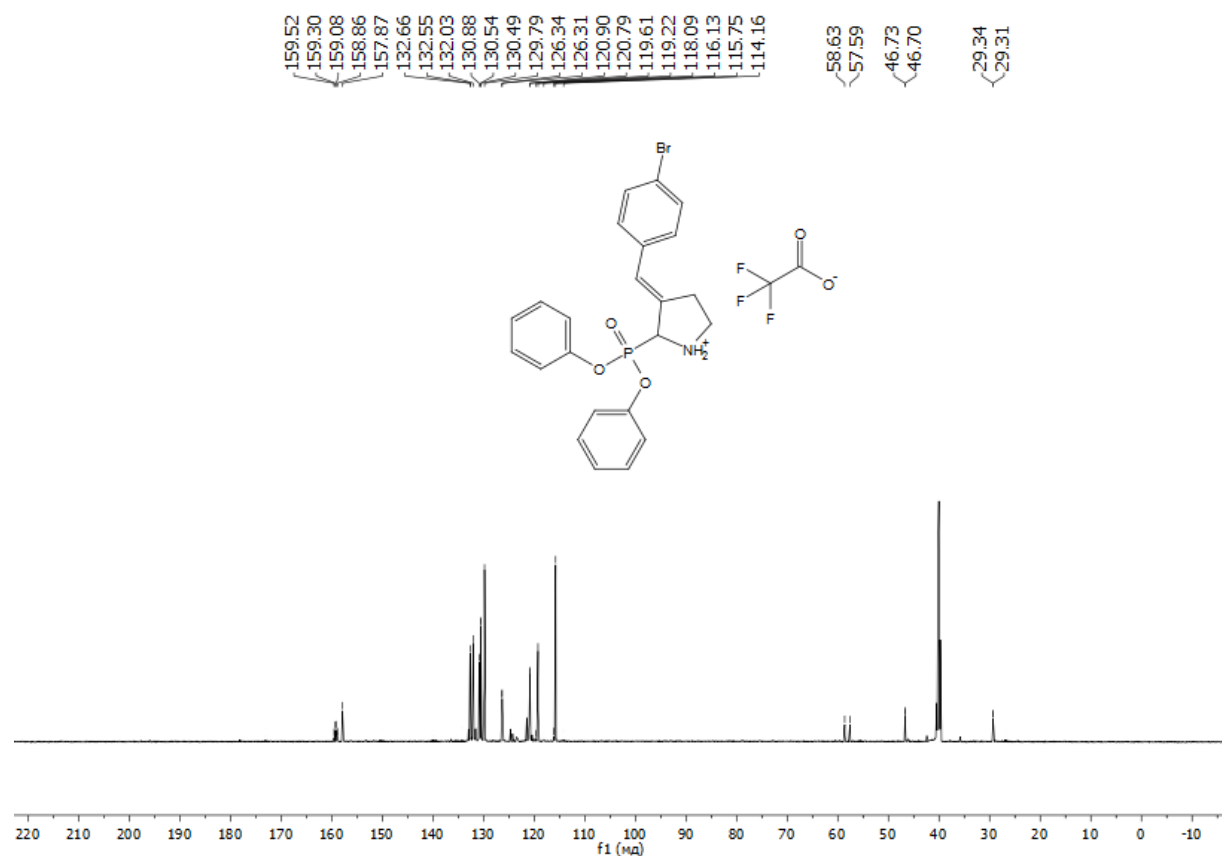


Figure S110. $^{13}\text{C}\{^1\text{H}\}$ NMR (DMSO- d_6 , 150 MHz) spectrum of the compound **3bj**

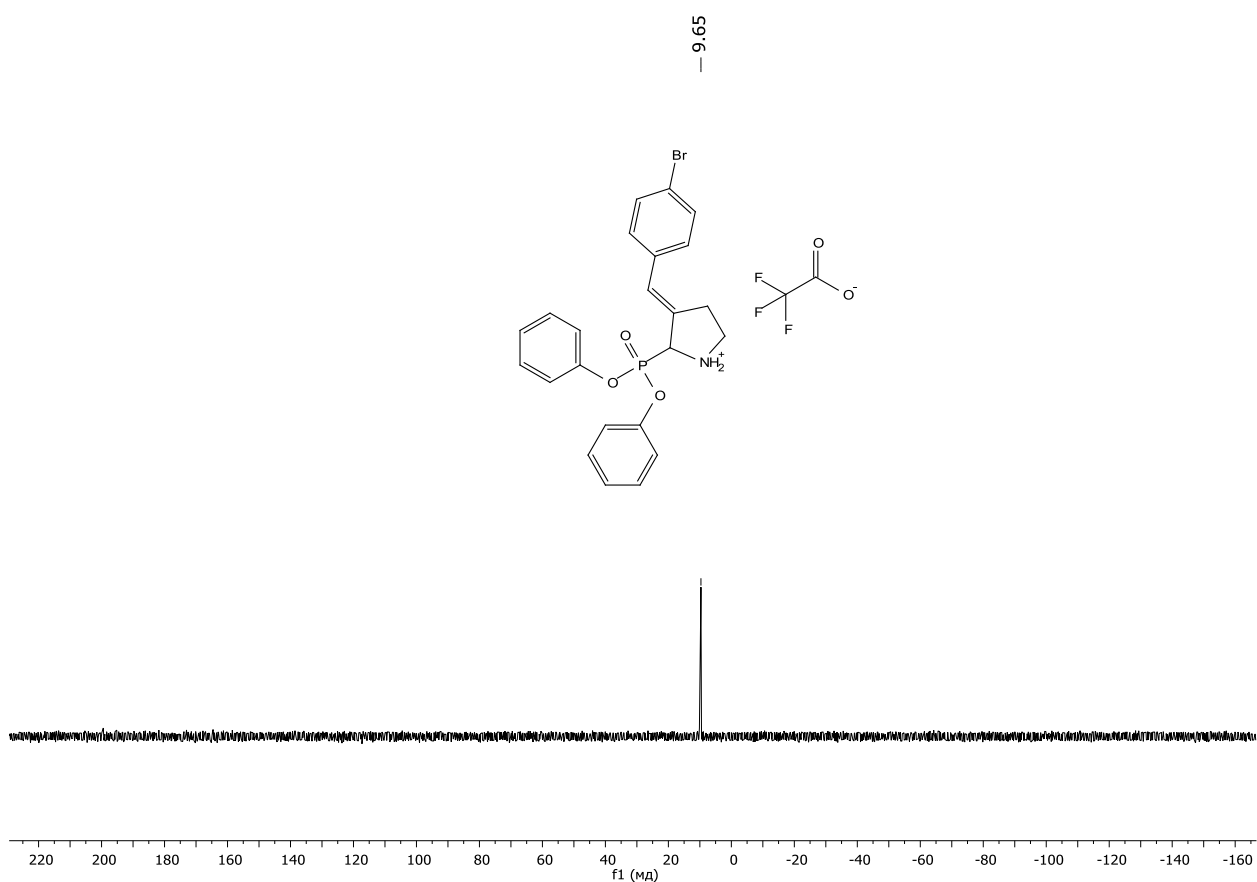
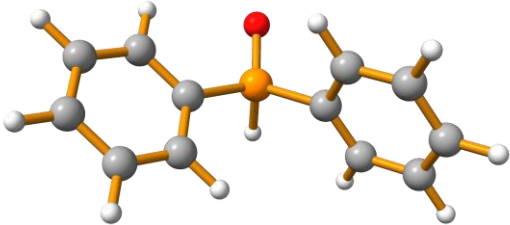
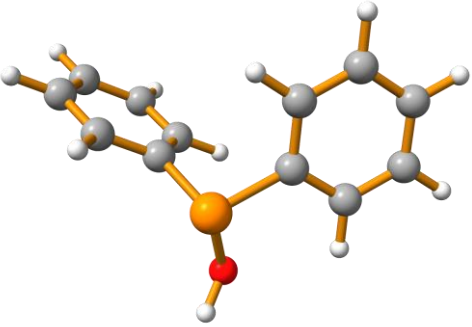
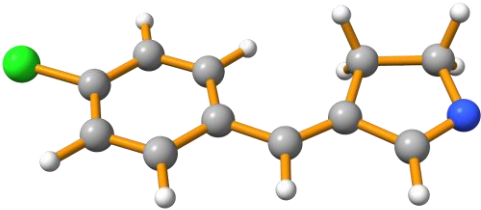
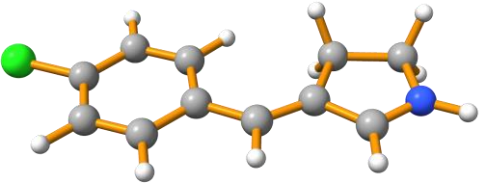
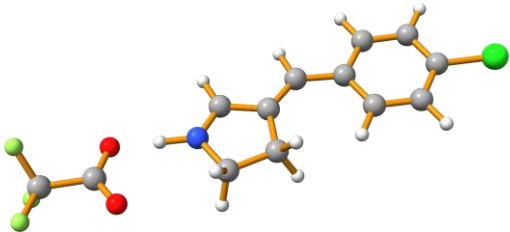
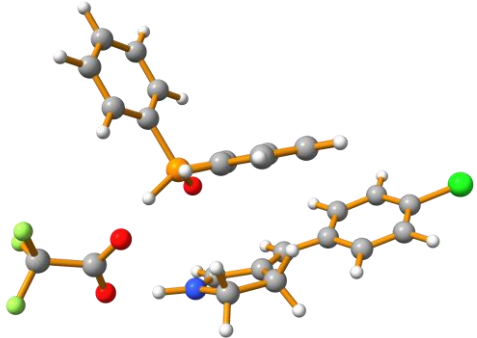


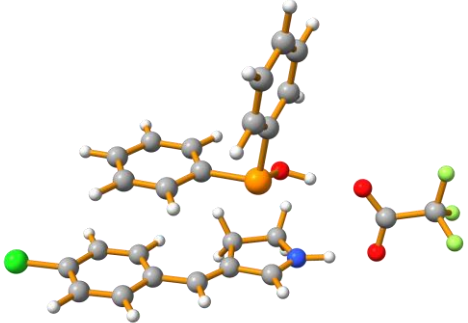
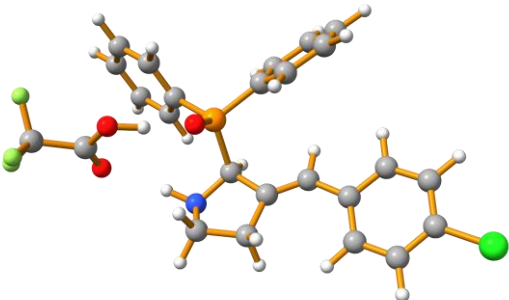
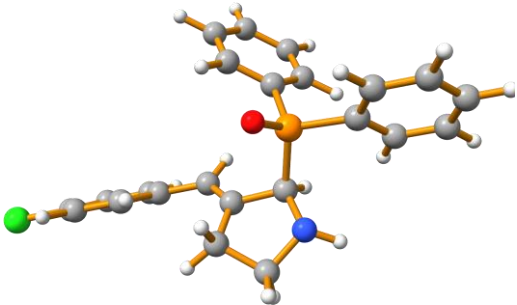
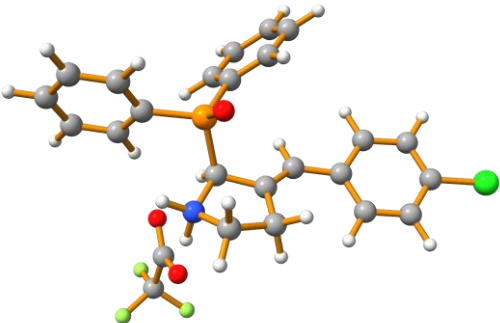
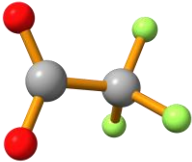
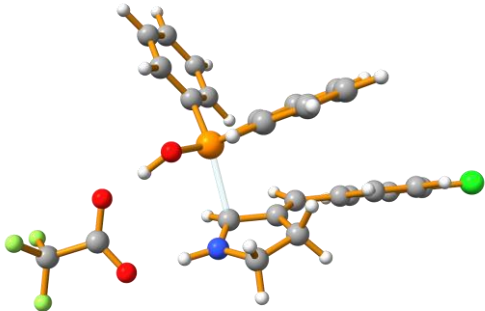
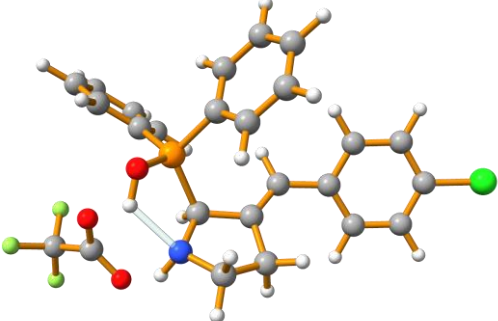
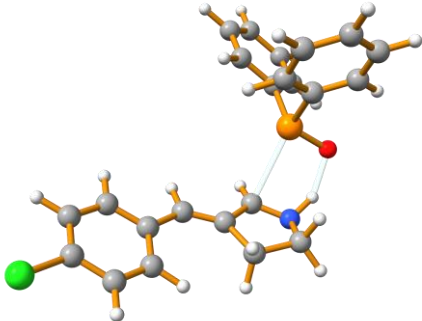
Figure S111. $^{31}\text{P}\{^1\text{H}\}$ NMR (DMSO- d_6 , 161 MHz) spectrum of the compound **3bj**

Quantum chemical calculations

All calculations were performed with the ORCA 6.0.0 package.^{1,2} Geometries were optimized using ω B97X-3c composite range-separated hybrid DFT method with a molecule-optimized polarized valence double- ζ basis set introduced by Grimme and coworkers.³ Geometry optimizations were followed by frequency calculations at the same level of theory. The structure was accepted if and only if only one imaginary frequency (transition states) or no imaginary frequencies (ground state compounds) were present. The solvent effects were accounted using implicit solvation model (C-PCM, benzene as a solvent).⁴ The IRC calculations were performed to verify that the obtained transition state really connects two minima. The images were prepared using ChimeraX software.⁵

Table 2. Absolute energies of starting compounds, intermediates and transition states as obtained from quantum chemical calculations

<p>Molecule: 2b_T1</p>  <p>Energy = -97.45526235 Hartree</p>	<p>Molecule: 2b_T2</p>  <p>Energy = -97.44826704 Hartree</p>
<p>Molecule: 4a</p>  <p>Energy = -93.48377878 Hartree</p>	<p>Molecule: 4a_H</p>  <p>Energy = -93.89394165 Hartree</p>
<p>Molecule: 4a_TFA</p>  <p>Energy = -210.59139028 Hartree</p>	<p>Molecule: CPLX_T1</p>  <p>Energy = -308.04263101 Hartree</p>

<p>Molecule: CPLX_T2</p>  <p>Energy = -308.03848295 Hartree</p>	<p>Molecule: INT1</p>  <p>Energy = -308.05504025 Hartree</p>
<p>Molecule: P</p>  <p>Energy = -190.94428404 Hartree</p>	<p>Molecule: P_TFA</p>  <p>Energy = -308.05773570 Hartree</p>
<p>Molecule: TFA_A</p>  <p>Energy = -116.63909593 Hartree</p>	<p>Molecule: TS1</p>  <p>Energy = -308.02613627 Hartree Imag. Freq. = -178.49 cm⁻¹</p>
<p>Molecule: TS2</p>  <p>Energy = -308.01016716 Hartree Imag. Freq. = -123.45 cm⁻¹</p>	<p>Molecule: TS3</p>  <p>Energy = -190.89164573 Hartree Imag. Freq. = -171.70 cm⁻¹</p>

References

- (1) Neese, F. Software update: The ORCA program system—Version 5.0 *WIREs Comput. Mol. Sci.* **2022**, *12* DOI: 10.1002/wcms.1606.
- (2) Neese, F.; Wennmohs, F.; Becker, U.; Riplinger, C. The ORCA quantum chemistry program package. *J. Chem. Phys.* **2020**, *152*, 224108 DOI: 10.1063/5.0004608.
- (3) Müller, M.; Hansen, A.; Grimme, S. ω B97X-3c: A composite range-separated hybrid DFT method with a molecule-optimized polarized valence double- ζ basis set. *J. Chem. Phys.* **2023**, *158* DOI: 10.1063/5.0133026.
- (4) Garcia-Ratés, M.; Neese, F. Effect of the Solute Cavity on the Solvation Energy and its Derivatives within the Framework of the Gaussian Charge Scheme. *J. Comput. Chem.* **2020**, *41*, 922–939 DOI: 10.1002/jcc.26139.
- (5) Meng, E. C.; Goddard, T. D.; Pettersen, E. F.; Couch, G. S.; Pearson, Z. J.; Morris, J. H.; Ferrin, T. E. UCSF ChimeraX: Tools for structure building and analysis. *Protein Sci.* **2023**, *32* DOI: 10.1002/pro.4792.